

**EVALUATION OF CONTACT PRESSURE MEASUREMENT SYSTEMS
FOR LOAD CARRIAGE APPLICATION**

by

Adam Joseph Ronald Thompson

A thesis submitted to the
Department of Mechanical & Materials Engineering
in conformity with the requirements for
the Degree of Master of Applied Science

Queen's University
Kingston, Ontario, Canada
(April 2024)

Copyright © Adam Joseph Ronald Thompson, 2024

Abstract

A load carriage system is routinely integrated into the lives of many around the world. These systems encompass backpacks, daypacks, or fanny packs and can be used by students, hikers, and soldiers. While a load carriage poses many benefits, it is also a source of discomfort and injury. As carried loads increase, there is a demand for load carriage improvement. An important and widely adopted biomechanical evaluation tool of load carriage systems is a skin contact pressure measurement system. These systems capture the distribution of pressure between individuals and their load carriage. Despite challenges identified while using the Tekscan F-Scan™ pressure measurement system, modern systems lack independent assessments to propose a new standard.

This thesis outlines the evaluation of three modern skin contact pressure measurement systems: Novel Pliance®, Tekscan I-Scan™, and XSENSOR™ X3. The first study evaluated the effect of system, surface geometry, and applied load on absolute error and measurement drift. An independent flat and semi-circular curved surface apparatus was developed to apply an equivalent theoretical pressure. The system of Novel Pliance® exhibited the greatest accuracy (4.51 ± 2.26 kPa), lowest drift (0.05 ± 0.06 kPa/min), and least time susceptibility. The second study evaluated the effect between systems on measurements of average pressure, peak pressure, and contact area, as well as the agreement between testing days per system. The systems of Novel Pliance® and XSENSOR™ X3 demonstrated more suitable performance on the Dynamic Load Carriage Simulator, while Tekscan I-Scan™ was application-challenged.

The present work advanced the understanding of modern skin contact pressure measurement systems and its implementation into load carriage applications. The novelty of the surface evaluation is that it independently compares three systems, two surfaces, and five loads at 30 minutes. The novelty of the simulator evaluation is that it established an advanced assessment methodology, applicable to future manikin commissioning and objective analysis of load carriage systems. Overall, the present work provides insight into measurement confidence, stability over time, and agreement between systems. Based on these findings, the Novel Pliance® pressure measurement system is recommended to capture skin contact pressure in future load carriage investigations.

Statement of Co-Authorship

- Chapter 1** Adam Thompson^a – manuscript composition
Qingguo Li^a – manuscript review
- Chapter 2** Adam Thompson^a – review of background and related work, and manuscript composition
Qingguo Li^a – manuscript review
- Chapter 3*** Adam Thompson^a – study design, data collection and analysis, and initial manuscript draft
Michael Shepertycky^a – study design, figure enhancement in results, and manuscript review
Jun-Tian Zhang^a – study design and manuscript review
Tim Bryant^a – study design and manuscript review
Evelyn Morin^a – study design and manuscript review
Adrienne Sy^b – study design and manuscript review
Linda Bossi^b – study design and manuscript review
Qingguo Li^a – project supervisor, study design, and manuscript review
- Chapter 4*** Adam Thompson^a – study design, data collection and analysis, and initial manuscript draft
Michael Shepertycky^a – study design, figure enhancement in results, and manuscript review
Jun-Tian Zhang^a – study design and manuscript review
Tim Bryant^a – study design and manuscript review
Evelyn Morin^a – study design and manuscript review
Adrienne Sy^b – study design and manuscript review
Linda Bossi^b – study design and manuscript review
Qingguo Li^a – project supervisor, study design, and manuscript review
- Chapter 5** Adam Thompson^a – manuscript composition
Qingguo Li^a – manuscript review

^a Ergonomic Research Team, Queen’s University, Kingston, ON, Canada, K7L 3N6

^b Defence Research and Development Canada, North York, ON, Canada, M3K 2C9

* Manuscript in preparation for journal submission

Acknowledgement

I am profoundly grateful for the invaluable guidance and support of numerous individuals in the completion of my thesis. My heartfelt appreciation extends to professional colleagues, friends, and family, all of whom have played a pivotal role in this journey.

Foremost, I extend my gratitude to the principal investigators of the Queen's University Ergonomic Research Team: Dr. Qingguo Li, Dr. Joan Stevenson, Dr. Tim Bryant, and Dr. Evelyn Morin. Their unwavering assistance and support have been integral to the success of this work. I am also thankful for the expertise and dedication of Dr. Jun-Tian Zhang and Dr. Michael Shepertycky, as well as undergraduate summer students Madeline Bond and Kaytlin Andrews.

A special acknowledgement is reserved for my direct supervisor, Dr. Qingguo Li, whose mentorship has been nothing short of inspirational. Dr. Li's guidance, encouragement, and consistent support have been indispensable throughout this entire process. I am grateful to have had such an excellent mentor, whom I am proud to share many great accomplishments with. I would also like to thank the members of my thesis examination committee: Dr. Qingguo Li (supervisor), Dr. Claire Davies (examiner), Dr. Heidi Ploeg (examiner), and Dr. Tim Bryant (chair). I appreciate their thoughtful questions and feedback.

I extend my gratitude to both the past and present members of the Bio-Mechatronics and Robotics Laboratory: Dr. Michael Shepertycky, Johann von Tiesenhausen, Karly Kudrinko, Samuel Brost, Paul Quinlan, Hannah Cooke, Will Bonin, Eric Godden, Claire Pooler, and Alex Pysklywec. Their diverse perspectives have enriched my understanding and provided invaluable friendships.

Furthermore, I wish to thank the load carriage team at Defence Research and Development Canada: Linda Bossi, Adrienne Sy, and Cerys McGuinness. My appreciation also extends to the McLaughlin Hall Technicians and the entire Machine Shop staff.

Finally, I express my deepest gratitude to my parents, Anneke and Ron Thompson, whose unwavering support and encouragement have fueled my passion for learning and pursuing my dreams. To my siblings, Caitlyn, Matt, and Curt, niece Evelyn, and my extended family, thank you for your unconditional support across my academics, athletics, and personal endeavours. Last but not least, I would like to express my genuine gratitude to Candice for her unwavering support, patience, and love.

Table of Contents

Abstract	ii
Statement of Co-Authorship	iii
Acknowledgement	iv
Table of Contents	v
List of Tables	ix
List of Figures	xi
List of Abbreviations	xii
Chapter 1 Introduction	1
1.1 Motivation.....	1
1.2 Objective	2
1.3 Contributions.....	3
1.4 Organization of Thesis	3
Chapter 2 Background and Related Work	5
2.1 Introduction.....	5
2.1.1 Load Carriage Task.....	5
2.2 Biomechanical Aspects of Load Carriage.....	6
2.3 Medical Issues of Load Carriage	6
2.4 Sustained Mechanical Loading	7
2.5 Advanced Load Carriage	8
2.6 Load Carriage Evaluation	9
2.7 Skin Contact Pressure Measurement Systems	10
2.8 Conclusion	14
Chapter 3 Under Pressure: The effect of system, surface geometry, and load on the measure of contact pressure	15

Highlights	16
Abstract.....	16
Keywords.....	16
3.1 Introduction.....	17
3.2 Materials and Methods.....	20
3.2.1 Experimental Setup.....	22
3.2.2 Experimental Protocol.....	25
3.2.3 Sensor Preparation	25
3.2.4 Data Analysis	26
3.2.5 Statistics	28
3.3 Results.....	30
3.3.1 Absolute Error.....	30
3.3.2 Measurement Drift	32
3.4 Discussion	39
3.4.1 Study Limitations.....	41
3.5 Conclusion	42
3.6 Funding	42
3.7 Declaration of Competing Interest.....	42
3.8 Supporting Information.....	42
Chapter 4 A comparative study of contact pressure measurement systems on the Dynamic Load Carriage Simulator.....	43
Highlights	44
Abstract.....	44
Keywords.....	44
4.1 Introduction.....	45
4.2 Methodology	48

4.2.1	Skin Contact Pressure Measurement Systems	48
4.2.2	Data Collection	49
4.2.2.1	Dynamic Load Carriage Simulator	50
4.2.2.2	Pressure Sensor Preparation and Placement	51
4.2.2.3	Load Carriage System Setup	51
4.2.3	Data Analysis	54
4.2.4	Statistical Analysis	55
4.3	Results	56
4.3.1	Between Day Agreement	58
4.4	Discussion	62
4.4.1	Limitations	64
4.5	Conclusion	65
4.6	Funding	66
4.7	Declaration of Competing Interest	66
4.8	Supporting Information	66
Chapter 5 Conclusions and Future Work		67
5.1	Effect of System, Surface Geometry, and Load on the Measure of Contact Pressure	68
5.2	Contact pressure on the Dynamic Load Carriage Simulator	69
5.3	Limitations and Outlook	70
5.4	Conclusion	72
References		73
Appendix A Data Sharing and Statistics		86
A.1	Surface Evaluation	86
A.1.1	Analysis of Absolute Error	86
A.1.2	Analysis of Measurement Drift	90
A.1.3	Analysis of Measurement Drift Over Time	98

A.2 Simulator Evaluation	104
A.2.1 Analysis Between Systems.....	104
A.2.2 Analysis Between Testing Days.....	108

List of Tables

Table 3.1 Characteristics of evaluated skin contact pressure measurement systems.....	22
Table 4.1 Evaluated pressure measurement system characteristics and specifications.	49
Table A.1 Absolute error of Novel.....	86
Table A.2 Absolute error of Tekscan.	87
Table A.3 Absolute error of XSENSOR™.	87
Table A.4 Descriptive statistics and assumption significance of absolute error.....	88
Table A.5 Main effect of measurement drift.	88
Table A.6 <i>Post hoc</i> of absolute error between systems	89
Table A.7 <i>Post hoc</i> of absolute error between load conditions per system and surface.	89
Table A.8 Measurement drift of Novel.....	90
Table A.9 Measurement drift of Tekscan.	91
Table A.10 Measurement drift of XSENSOR™.	92
Table A.11 Descriptive statistics and assumption significance of measurement drift.	93
Table A.12 Main effect of measurement drift.	94
Table A.13 <i>Post hoc</i> of measurement drift between systems.....	94
Table A.14 <i>Post hoc</i> of measurement drift by Novel between loads per surface.....	95
Table A.15 <i>Post hoc</i> of measurement drift by Tekscan between loads per surface.	96
Table A.16 <i>Post hoc</i> of measurement drift by XSENSOR™ between loads per surface.....	97
Table A.17 Descriptive statistics and assumption significance of measurement drift over time.....	98
Table A.18 Main effect of measurement drift over time.	99
Table A.19 <i>Post hoc</i> of measurement drift per system over time.	100
Table A.20 <i>Post hoc</i> of measurement drift over time per system and surface.....	100
Table A.21 <i>Post hoc</i> of measurement drift over time per surface and load for Novel.....	101
Table A.22 <i>Post hoc</i> of measurement drift over time per surface and load for Tekscan.....	102

Table A.23 <i>Post hoc</i> of measurement drift over time per surface and load for XSENSOR™.....	103
Table A.24 Average pressure, peak pressure, and contact area measured by Novel.	104
Table A.25 Average pressure, peak pressure, and contact area measured by Tekscan.	104
Table A.26 Average pressure, peak pressure, and contact area measured by XSENSOR™.	105
Table A.27 Descriptive statistics and assumption significance between systems.	105
Table A.28 Main effect between systems.	106
Table A.29 <i>Post hoc</i> between systems at 15 kg	106
Table A.30 <i>Post hoc</i> between systems at 25 kg	107
Table A.31 <i>Post hoc</i> between systems at 35 kg	107
Table A.32 Between testing day difference of average pressure, peak pressure, and contact area measured by Novel.....	108
Table A.33 Between testing day difference of average pressure, peak pressure, and contact area measured by Tekscan.	108
Table A.34 Between testing day difference of average pressure, peak pressure, and contact area measured by XSENSOR™.....	108
Table A.35 Descriptive statistics and normality significance between testing days per parameter and system.	109
Table A.36 Main effect between testing days per parameter and system.....	109
Table A.37 Descriptive statistics and normality significance between testing days per parameter, system and load.	110
Table A.38 Main effect between testing days per parameter and system.....	111

List of Figures

Figure 2.1 Dynamic Load Carriage Simulator – Generation I.....	10
Figure 2.2 F-Scan™ pressure sensors placed onto the Dynamic Load Carriage Simulator.....	11
Figure 2.3 Exploded cross-sectional view of a loaded Tekscan sensor.....	12
Figure 2.4 Exploded isometric view of a Tekscan sensor.....	12
Figure 3.1 Flat surface apparatus.....	23
Figure 3.2 Curved surface apparatus.....	24
Figure 3.3 Curved surface force analysis.....	27
Figure 3.4 Absolute error per system.....	30
Figure 3.5 Absolute error per system and surface.....	31
Figure 3.6 Absolute error per system, surface, and load.....	32
Figure 3.7 Drift per system.....	33
Figure 3.8 Drift rate per system and time interval.....	34
Figure 3.9 Drift rate per system and surface.....	35
Figure 3.10 Drift rate per system, surface, and time interval.....	36
Figure 3.11 Drift rate per system, surface, and load.....	37
Figure 3.12 Drift rate per system, surface, load, and time interval.....	38
Figure 4.1 Experimental setup of pressure sensors.....	51
Figure 4.2 Load distribution.....	52
Figure 4.3 Experimental setup control.....	53
Figure 4.4 Location and tension of strap force sensor.....	54
Figure 4.5 Measured average and peak pressure.....	57
Figure 4.6 Measured contact area.....	58
Figure 4.7 Between-Day Differences.....	60
Figure 4.8 Between day Bland-Altman.....	61

List of Abbreviations

ANOVA	Analysis of Variance
HSD	[Tukey's] Honest Significant Difference
LSD	[Fisher's] Least Significant Difference
S-W	Shapiro-Wilks
LoA	[Bland-Altman] Limits of Agreement

Chapter 1

Introduction

1.1 Motivation

In everyday life, there is a continual interface between the human skin and its surrounding environment. Whether the interface generates from the feet touching the ground, a leg crossing the other, or a hand grasping a cup, each point of contact produces a magnitude of skin contact pressure. These inconspicuous interactions are likely characterized by low magnitudes and brief durations of skin contact pressure. What may begin as a subtle inconvenience can gradually intensify into extraordinary discomfort and injury [1, 2]. Fortunately, skin contact pressure at these interfaces can be objectively captured using a pressure measurement system and can predict subjective discomfort [3, 4]. Measurement data obtained from these systems enable researchers and clinicians to objectively analyze and formulate strategies aimed at mitigating the unfavourable effects of mechanical loading.

Understanding and accurately capturing skin contact pressure cannot be overemphasized in the field of load carriage. Load carriage encompasses many applications, including backpacks, exoskeletons, and biomechanical energy harvesters [5-7], and impacts many user groups, including recreational hikers, military soldiers, and students [8-10]. Researchers have explored safe and efficient methods of load carriage for many years, with a predominate focus on military males [4, 9, 11, 12]. The knowledge gathered on males often lacks applicability to females, a demographic that can differ in age, anthropometrics, fitness, experience, load-carrying capacity, and injury mechanisms. With more females entering combat roles and shouldering heavier loads, their risk of experiencing a load carriage injury becomes increasingly prevalent [13, 14]. As technology continues to advance, the demand for precise and reliable measurements of skin contact pressure becomes increasingly relevant in determining safe and efficient methods of load carriage. Whether the pressure measurement systems are implemented in medical device development, performance

optimization, or equipment enhancement, skin contact pressure employs a profound influence on human well-being.

The previous evaluation of pressure measurement systems unfolds the intricacies of skin contact pressure [15-19]. Despite the importance of system evaluation, modern systems (Novel Pliance® [Novel GmbH, Munich, Germany], Tekscan I-Scan™ [Tekscan Inc., Norwood, MA, United States], and XSENSOR™ X3 [XSENSOR™ Technology Corp., Calgary, AB, Canada]) are infrequently evaluated under conditions experienced in load carriage applications. Without the evaluation of Tekscan F-Scan™ (Tekscan Inc., Norwood, MA, United States) as the previous standard in load carriage applications, researchers and clinicians would have been unaware of extreme hysteresis, high measurement drift, and poor accuracy [15-19]. Insights gained from modern system evaluation can therefore facilitate the selection of a new standard of skin contact pressure measurement system for the load carriage application. Thereby, this evaluation of contact pressure measurement systems may identify a direction for future research and development for load carriage applications.

1.2 Objective

The work in this thesis details the evaluation of three modern and commercially available skin contact pressure measurement systems: Novel Pliance®, Tekscan I-Scan™ and XSENSOR™ X3. These systems capture the distribution of contact pressure and were specifically promoted by their respective manufacturer for their potential efficacy in posterior-borne load carriage applications. The first objective evaluated the effect of system, surface, and load on absolute error and measurement drift. It further investigated the effect of time on measurement drift per system, surface, and load condition. The examined surfaces included flat and semi-circular curved, while the applied loads ranged between 30 to 90 kPa. Building upon simple conditions, the second objective extended into the mechanical simulation of the load carriage application. The second objective evaluated the between-system effect, as well as the between-testing day agreement, of pressure sensors placed onto the Dynamic Load Carriage Simulator. Utilizing the average male manikin as a baseline, this proposed assessment of pressure measurement systems draws on

historical load carriage evaluation. Most importantly, the methodology will provide essential groundwork for exploration with newly developed manikins of the female population.

1.3 Contributions

The major contributions of this thesis are as follows:

- The evaluation of three skin contact pressure measurement systems (Novel Pliance[®], Tekscan I-Scan[™], and XSENSOR[™] X3), on two surface geometries (flat and curved), and five loads (30, 45, 60, 75, and 90 kPa) to determine if absolute error at 30 minutes and measurement drift over 30 minutes were affected by the specific system, surface, and load conditions. The evaluation further evaluates the effect of time on measurement drift.
- The practical evaluation of three skin contact pressure measurement systems (Novel Pliance[®], Tekscan I-Scan[™], and XSENSOR[™] X3) to determine the effect between systems per backpack load (15, 25, and 35 kg), and the agreement between testing day (day #1 and 2).

1.4 Organization of Thesis

Chapter 2: Literature Review

Chapter 2 contains a scientific review of load carriage applications with respect to sustained mechanical loading and skin contact pressure. Next, it explores the approach of capturing skin contact pressure while using a pressure measurement system and reviews current system evaluations. Finally, this chapter identifies the lack of modern pressure measurement system evaluation in existing literature.

Chapter 3: Effect of System, Surface, and Load on Contact Pressure *(Planned Publication)*

Chapter 3 investigates the effect of absolute error and measurement drift on Novel Pliance[®], Tekscan I-Scan[™], and XSENSOR[™] X3. This evaluation considers the variation in surface (flat and curved) and load (30, 45, 60, 75, and 90 kPa), along with the impact of time on measurement drift. The insight gained from

this chapter identifies the importance of system selection to enhance confidence in measure, reduce experimentally controlled parameters, and provide measurement stability over time.

Chapter 4: Contact pressure on the Dynamic Load Carriage Simulator (*Planned Publication*)

Chapter 4 investigates the practical performance of the evaluated skin contact pressure measurement systems (Novel Pliance[®], Tekscan I-Scan[™], and XSENSOR[™] X3). The evaluation reports the between-system effect and agreement, as well as the individual between-testing day agreement. The insights gained from this chapter identify the importance of evaluation in practical application and highlight careful considerations in selecting a suitable skin contact pressure measurement system.

Chapter 5: Conclusions and Future Work

Chapter 5 consolidates the outcomes and implications of the research presented in this thesis. It provides a detailed overview of each study's scientific benefits, limitations, and direction of future research. The chapter concludes with an overall summary, offering a comprehensive perspective on the research conducted within this thesis.

Chapter 2

Background and Related Work

2.1 Introduction

A load carriage system can be identified and described using many names: a backpack, rucksack, day pack, fanny pack, book-bag, messenger bag, and camera bag. These systems can be worn on one or both shoulders and may include a hip belt. Load carriage systems serve as versatile tools for the storage and transportation of load, encompassing items of scholastic, recreation, and military [8-10]. Criteria such as ease of use, comfort, and aesthetics are typical considerations of load carriage design; however, these criteria can offer varying influences of subjectiveness that can differ from one user to another. Some examples of subjectiveness include an individual's experience, tolerance to pain, and personal preferences (e.g., load carriage system colour and price). Alternatively, biomechanical measures can objectively evaluate a load carriage design and performance [20]. Among biomechanical measures, the capture of skin contact pressure is a widely adopted tool, particularly as the load carriage directly interfaces with the trunk and the information gathered can be correlated with the limits of human tolerances [4, 21, 22].

2.1.1 Load Carriage Task

A load carriage is routinely donned by many individuals, including students [23], hikers [8], military soldiers [1, 9], mountain rescuers [24], firefighters [25], and law enforcement [26, 27]. Each load carriage individual possesses different scopes and goals that can differ beyond application considerations. While some load carriage individuals may carry a few items to achieve success, others may carry a lot. More often, load carriage individuals carry too many items that cumulatively elevate their carried weight.

According to Negrini et al. [23], 34.8% of schoolchildren carry more than 30% of their body weight at least once a week, equivalent to 11.5 kg. Alternatively, recreational hikers can bear up to 40% of their body weight, amounting to 24.5 kg [8]. Lastly, trained military soldiers can support loads as high as 75%

of their body weight, reaching 60 kg [28]. While certain individuals are required to endure heavy loads in their occupational role, it is important to understand the substantial loading of tissue beneath load-bearing sites [11, 29]. Tissue loading is especially apparent for female load carriage individuals who experience a greater rate of injury due to gender-related differences (e.g., stature, absolute aerobic capacity, muscle strength, and equipment fit) [13]. Although weight limits are suggested (children: 10% body weight [30]; hikers: 30% body weight [8]; military soldiers: 45% body weight [31]), carried loads have continued to increase [9].

2.2 Biomechanical Aspects of Load Carriage

Biomechanics is an important aspect of load carriage design given that suboptimal metrics can lead to injury and diminish application performance [32]. Some biomechanical considerations include spinal alignment, centre of mass and stability, gait and stride length, muscle activation, skin contact pressure, and energy expenditure [33]. The weight of the carried load inherently impacts load carriage biomechanics; however, load placement within the load carriage is equally as important [9]. Regarding the vertical position of the load centre of mass, a higher placement with respect to the individual was shown to be most preferred [9]. In return, load carriage individuals whose load carriage contains a higher center of mass placement exhibit less forward lean to align the load carriage centre of mass with the individual's neutral centre of mass [34]. Although increased lean can be beneficial in terms of gait, greater lean angles may also contribute to discomfort and injury [35, 36].

2.3 Medical Issues of Load Carriage

The positive health benefits of load carriage activities, such as recreational backpacking [37], can be negated by the presence of discomfort and injury [1, 9]. In the military, load carriage injuries can be termed a hidden epidemic as they can reduce the effectiveness of an entire military unit [9]. Despite

advancements in load carriage design over the past few decades, the loads carried by individuals impose substantial physiological strain [9, 36], especially while carried loads continue to increase [9].

A primary factor limiting load carriage design and functionality appears to be the tolerance of shoulder tissue to mechanical loading, as indicated by the collection of subjective discomfort and pain ratings and studies on skin contact pressure [1, 9]. In contrast to other load-bearing sites (e.g., the neck, hands, arms, and upper back), the shoulders were identified as more susceptible to skin and subcutaneous soft tissue damage while sustaining mechanical loading [1, 38, 39]. The compression of the underlying skin and soft tissue by load carriage shoulder straps often results in sensory deficits, numbness, increased pain, discomfort, and reduced performance due to the majority of load placed onto the shoulders [1, 40].

While short-term discomfort can be alleviated with time and rest from load carriage activities [1], a severe and prolonged effect of sustained mechanical loading onto the shoulders is called brachial plexus palsy or rucksack palsy [9]. The mechanism behind brachial plexus palsy has been postulated by either the traction (e.g., stretching) or compression of the fifth or sixth cervical nerve routes due to the heavy downward force exerted by the load carriage in the region of the brachial plexus [9]. Symptoms of brachial plexus palsy include numbness, paralysis, pain, and weakness in upper limb musculature [9]. Although sensorimotor defects from brachial plexus palsy are typically transient, certain cases may lead to chronic conditions [9]. Therefore, the monitoring of skin contact pressure beneath the shoulder strap may alleviate some medical complications in the load carriage application.

2.4 Sustained Mechanical Loading

The impact of sustained mechanical loading has been extensively explored in the context of skin contact pressure [21, 22, 41, 42]. The shoulder strap of a load carriage system commonly exerts compression onto the anterior portion of the shoulder, potentially leading to the restriction of blood flow in axillary arteries and veins [43]. Previous investigations with children in load carriage studies measured skin contact pressure beneath the shoulder strap ranging from 9.3 to 14.7 kPa [21, 22]. Similarly, military load carriage

studies measured contact pressure ranging from 20 to 55 kPa [40, 44]. In these cases, the measured contact pressures exceeded ischemic thresholds, contributing to perceived discomfort and injury [1, 21].

Classical investigations of ischemic thresholds have identified that skin contact pressure of more than 14 kPa can lead to irritation and redness [45]. Prolonged exposure to these pressures (e.g., over 2 hours) has been linked to swelling and inflammation of the dermis in underlying tissue [45]. Other investigations reported almost zero blood flow at 16 kPa [46], and pressure below 10 kPa applied over muscle has been shown to reduce the partial pressure of oxygen to zero [47]. To prevent sensory loss, pain, and nerve damage [38, 39], skin contact pressure beneath the shoulder strap is recommended to remain below the critical threshold of 10 kPa [11].

More recent studies have evaluated micro- and macro-hemodynamical performance while wearing a load carriage system. An earlier investigation revealed that healthy adults wearing a moderately-weighted backpack of 12 kg for 10 minutes decreased upper extremity sensation, as well as macrovascular and microvascular hemodynamic changes (e.g., a 43% decrease in brachial plexus artery blood flow to baseline) [41]. A subsequent study found that healthy adults wearing a 10 kg backpack for 5 minutes significantly reduced shoulder muscle oxygenation by 22% and decreased skin microvascular flow by 82%, compared to an empty backpack control condition [42]. Prolonged contact pressure from load carriage systems can reduce hemodynamic parameters (e.g., blood flow), and result in neurologic dysfunction and the inability to conduct fine motor skills [41], thereby emphasizing the need for load carriage system designs to distribute and minimize pressure effectively [11].

2.5 Advanced Load Carriage

Researchers have proposed the strategic redistribution of carried load from the shoulders to the hips as a measure to alleviate adverse health effects in load carriage individuals [48]. The hip region exhibits three times less sensitivity to loading and provides a greater area of contact compared to the shoulders [11, 49]. While maintaining the total magnitude of the carried load, the integration of a hip belt was shown to

shift up to 30% of the carried load away from the shoulders and upper back [48]. This redistribution has been associated with a decrease in contact pressure at the shoulders [4, 11, 12], along with a reduction in perceived exertion [2].

Despite these favourable outcomes, up to 70% of the vertical forces remain concentrated on the shoulders and upper back [48]. With the continued escalation of total carried load [9], reports of ischemic symptoms (e.g., numbness in the hands and fingers), cases of rucksack palsy, and a decline in task performance persist [1, 43]. This emphasizes the necessity to biomechanically evaluate load carriage system designs, with a specific focus on understanding and properly distributing skin contact pressure in the shoulder region. Such evaluations enable the objective quantification of discomfort and potential risk of injury associated with the varying load carriage configurations [4].

2.6 Load Carriage Evaluation

The biomechanical evaluation of load carriage systems includes both human participants and mechanical simulation studies [4, 20, 50]. While participant-based studies offer quick face and content validity, they present challenges related to their reliability and logistics (e.g., time-consuming and participant-subjective) [20]. To address these challenges, a standardized and efficient methodology of load carriage system evaluation was developed using the Dynamic Load Carriage Simulator (Figure 2.1) [20, 51, 52]. The simulator provides an objective, reliable, and efficient assessment of alternative torso-borne load carriage for its impact on the individual's comfort and safety. Of the many outcome measures (e.g., relative motion, forces, and moments), skin contact pressure captured by a pressure measurement system on the Dynamic Load Carriage Simulator offers valuable insight into the measure of tissue tolerance and enables the differentiation between various load carriage system designs [11, 53].

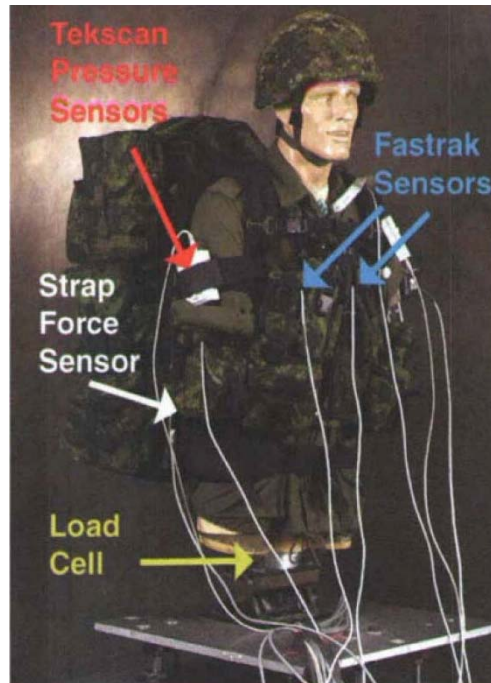


Figure 2.1 Dynamic Load Carriage Simulator – Generation I. [52]

2.7 Skin Contact Pressure Measurement Systems

Skin contact pressure measurement systems are commonly employed in load carriage research and development to biomechanically assess the interaction between the load carriage and its user [4, 20]. These systems facilitate the measurement and comparison of contact pressure to provide a measure of tissue tolerance and evaluation of load carriage system design [4, 20-22, 52]. Several international manufacturers market skin contact pressure measurement systems, where their system specifications differ in terms of sensor size, element number, and sensor type. The appropriateness of a system can be further categorized based on its strengths and weaknesses.

In previous load carriage studies, the Tekscan F-Scan™ skin contact pressure measurement system was used (Figure 2.2) [4, 20, 52]. The thin and flexible force-based sensors of Tekscan F-Scan™ provided high resolution and facilitated straightforward data acquisition. With the ability to capture real-time dynamic feedback, the positive characteristics of the Tekscan system exceeded the static frames of Fuji Film Prescale (Fuji Photo Film Co. Ltd., Tokyo, Japan) [54].



Figure 2.2 F-Scan™ pressure sensors placed onto the Dynamic Load Carriage Simulator. [52]

Tekscan Inc. developed a force-based sensor with the capacity to display contact pressure within its operating software. The construction of Tekscan F-Scan™ sensors involves imprinting conductive pathways onto an upper and low polyester substrate, followed by the deposition of pressure-sensing ink (Figure 2.3 and Figure 2.4). An electrically isolated connection is established at each pathway intersection. The pathway intersections are strategically arranged in a Cartesian format to form rows and columns of force-sensing elements. By dividing the area between each force-sensing element, a pressure profile can be created through the calculation of force divided by area. Calibration of Tekscan sensors is achieved by associating a known force with a change in electrical resistance per element. Although sensor preparation is commonly performed in a calibration device containing a rigid and flat base, there are many applications where the lower polyester substrate is in contact with a curved and compliant surface. [17, 19, 55]

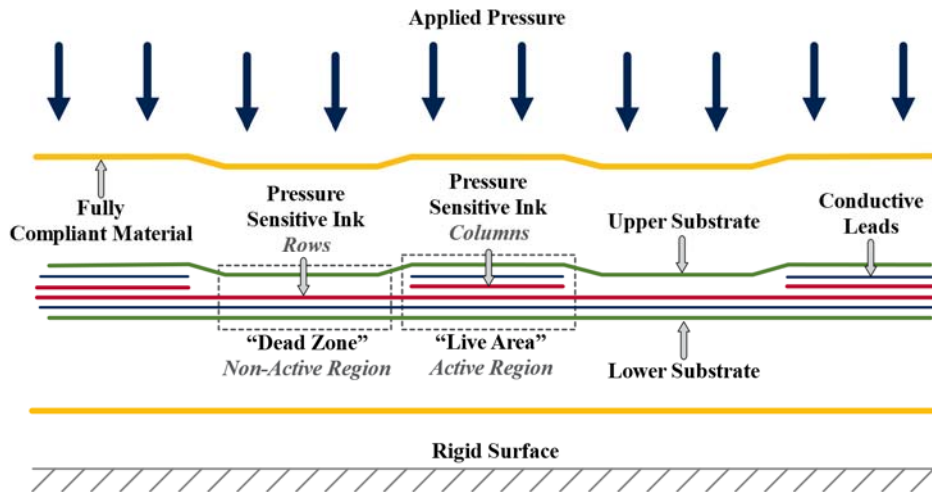


Figure 2.3 Exploded cross-sectional view of a loaded Tekscan sensor. An even pressure distribution applied across an exploded cross-sectional view of a Tekscan sensor. Image adapted from a Tekscan guide on calibration and equilibration. [56]

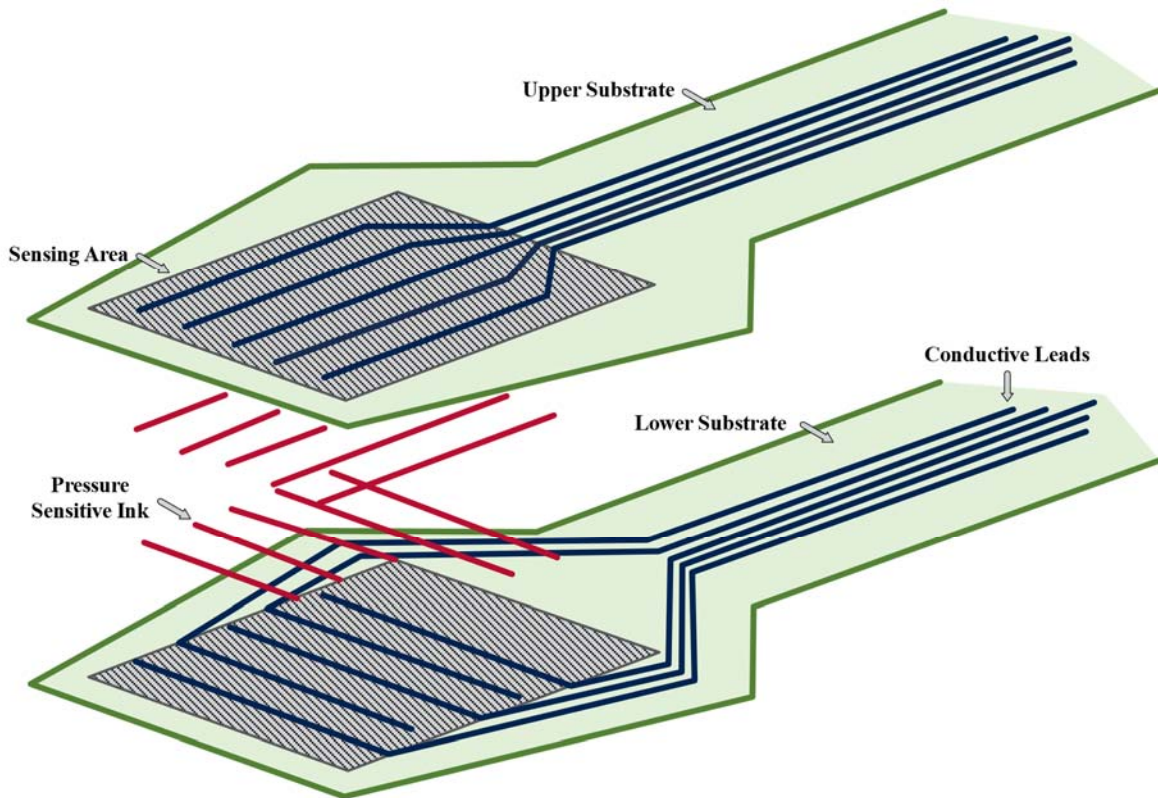


Figure 2.4 Exploded isometric view of a Tekscan sensor. An exploded isometric view of a Tekscan sensor. Image adapted from a Tekscan guide on calibration and equilibration. [56]

The Tekscan F-ScanTM skin contact pressure measurement system offers a convenient method of measuring contact pressure between two opposing surfaces; however, the system faces validity and reliability challenges [19, 57]. There are several factors known to affect the output (accuracy) of Tekscan F-ScanTM. These include measurement creep under constant applied pressure over time, hysteresis in dynamic response, operating temperature and environmental humidity, compliance with surface contact, and variation in element sensitivity [16-18, 58]. These factors have led to measurement errors as great as 34% when evaluated in simplistic geometric conditions [16, 17, 19].

The challenges of Tekscan F-ScanTM were addressed in the development of newer skin contact pressure measurement systems: Novel Pliance[®], Tekscan I-ScanTM, and XSENSORTM X3. Each of these systems was marketed and recommended by the manufacturers for load carriage research. Without system evaluation, these systems initially differ in terms of sensing technology. While Tekscan I-ScanTM continues to implement resistive technology (like Tekscan F-ScanTM), both Novel Pliance[®] and XSENSORTM X3 utilize capacitive transducers. Capacitive pressure sensors store energy in the form of an electrical field, where a change in electrical characteristics can be translated into levels of known external load (e.g., applied pressure). Another difference co-aligns with the sensing technology, where both Novel Pliance[®] and XSENSORTM X3 employ pressure as an input parameter of sensor calibration (measured in kilopascals), while Tekscan I-ScanTM relies on force (measured in Newtons).

Although extensive evaluation was conducted on the Tekscan F-ScanTM system [17, 19, 55, 58], research on the evaluation of the newer skin contact pressure measurement systems is limited. Of the available research, evaluations were commonly conducted individually and under simplified bench-top conditions [57, 59-61]. Moreover, diverse assessment methodologies (e.g., loading and environmental conditions) challenge the effectiveness of comparing performance between systems. Available research is further conducted under excessively high- or low-pressure conditions to be relevant in the load carriage application [60-63]. With load carriage pressures ranging up to 90 kPa [40, 44, 64], the review of pressure

garment (excessively low pressures) and plantar pressures (excessively high pressures) evaluations possess difficulty in extending their findings to load carriage applications.

2.8 Conclusion

Many individuals incorporate load carriage into their daily lives. With individuals often bearing substantial weight, complications including discomfort, sensory loss, and tissue damage have emerged. Biomechanical measures, particularly skin contact pressure, serve as a valuable tool for the assessment of load carriage design and performance. Given the direct interface between the carried load and the individual, the measure of skin contact pressure is widely adopted for its objective application within the limits of human tolerance. Despite the longstanding implementation of the Tekscan F-Scan™ skin contact pressure measurement system as a standard in load carriage applications, the dated system has become validity and reliability challenged. While new systems have emerged, limited literature exists to target the application of load carriage. Consequently, there is a necessity to thoroughly evaluate the technical specifications of these newer skin contact pressure measurement systems prior to selecting a system for its use in subsequent load carriage applications. Furthermore, there is a need to develop a testing protocol that can identify key performance characteristics, such as absolute error and measurement drift with response to time.

Chapter 3

Under Pressure: The effect of system, surface geometry, and load on the measure of contact pressure

Adam Thompson^{a,*}, Michael Shepertycky^a, Jun-Tian Zhang^a, Tim Bryant^a, Evelyn Morin^a,
Adrienne Sy^b, Linda Bossi^b, and Qingguo Li^a

^a **Ergonomic Research Team, Queen's University**, Kingston, ON, Canada, K7L 3N6

^b **Defence Research and Development Canada**, North York, ON, Canada, M3K 2C9

* Corresponding author. Email: adam.thompson@queensu.ca (A.T.)

Manuscript in preparation for the journal of
Measurement Science and Technology
(IOP Publishing, Bristol, United Kingdom)

Highlights

- Comparison of three commercially available pressure measurement systems.
- The effect of system, surface, load, and time was evaluated.
- Novel Pliance[®] exhibited the lowest absolute error and rate of measurement drift.
- Time affected nearly all system, surface, and load conditions for drift rate.

Abstract

Three pressure measurement systems were evaluated for absolute error and drift rate. The Novel Pliance[®], Tekscan I-Scan[™], and XSENSOR[™] X3 systems were calibrated according to the manufacturer's protocol and tested on a flat and curved surface for pressures between 30–90 kPa. Ten independent trials were collected per system, surface, and load at 30 minutes of static pressure. Novel Pliance[®] exhibited the lowest absolute error (4.51 ± 2.26 kPa) and drift rate (0.05 ± 0.06 kPa/min), which significantly differed from Tekscan I-Scan[™] (absolute error: 7.16 ± 4.70 kPa; drift rate: 0.15 ± 0.11 kPa/min) and XSENSOR[™] X3 (9.29 ± 4.90 kPa; 0.08 ± 0.07 kPa/min). Moreover, Novel Pliance[®] exhibited no absolute error difference per surface and load, and drift significantly lessened over time for nearly all conditions of system, surface, and load. This study presents the importance of system selection in biomechanical and clinical applications to enhance confidence in measures, reduce controlled parameters, and provide measure stability.

Keywords

Skin contact pressure, load carriage, and pressure measurement

3.1 Introduction

Skin contact pressure is inevitably experienced between all mechanical contacts with the human body. Daily activities (e.g., walking, sitting, and sleeping) can result in skin contact pressures that extend beyond the safe operating limits [46, 47], and induce discomfort, pain, and injury [1, 2]. Moreover, skin contact pressure is the primary predictor of discomfort during load carriage [3, 4] and, therefore, is an essential measure when assessing applications where the load is borne onto the large posterior area of the human torso (e.g., backpacks [5], exoskeletons [6], and biomechanical energy harvesters [7]).

Over the past century, humans have become increasingly dependent on carrying a load, particularly in applications such as hiking [8], military [9], and scholastic [10]. Human adolescents incorporate load carriage into their daily activities, where they are frequently loaded up to 30% of their body weight [10, 30]. These weights have led to biomechanical and physiological adaptations, which have increased the user's susceptibility to musculoskeletal injuries, fatigue, redness, swelling, and discomfort [10, 22, 30]. Adolescent backpacks are commonly designed in the absence of a waist belt, and therefore, distribute the majority of borne load onto the shoulders [21]. Furthermore, heavy loads are carried in professional occupations, such as the military [9], firefighting [65], and mountain rescue [66]. These personnel routinely bear posterior-borne loads greater than 60% of their total body weight (greater than 40 kg) while performing maneuvers in extreme and hostile environments [1, 9, 28]. Many human complications, such as discomfort, sensory loss, tissue damage, pain, and injury [1, 2], have been associated with the continual increase of borne load [9].

Various psychophysical (perceived exertion), physiological (energy expenditure), and biomechanical (gait patterns) measures are implemented in load carriage performance and design evaluation [20, 33]. The objective measure of skin contact pressure has become widely adopted for its association with the limits of human tolerance [4, 20, 21]. Although a load bearer may overcome a degree of perceived pain and discomfort, elevated skin contact pressure reduces the blood flow beneath its applicator. Many studies suggest that the threshold of ischemia is below 16 kPa [45-47], while others

provide recommendations for average and peak pressures in the load carriage application [20]. To demonstrate the severity of skin contact pressure in application, a moderately weighted backpack of 12 kg accompanied a decrease in upper extremity sensation and a microvascular and macrovascular hemodynamic decline in healthy adults after only 10 minutes [41].

Established by the subjective perception of discomfort and pain and the objective measure of skin contact pressure, the upper limb tolerance was found to be more susceptible to load carriage complications than the lower and is a major limiter of load carriage performance [1, 11]. Approximately 70% of load carriage load was found to be supported by the upper torso [48], which has led to significant shoulder discomfort over other regions [1]. Supporting the load carriage on the anterior shoulder can compress essential nerves and vasculature [43], thus leading to sensory loss in the hands and arms, as well as the impairment of commonly executed tasks (e.g., abducting the arm) [1, 21]. Although complications are predominately short-term, and dissipate following borne load removal, long-term effects, such as rucksack palsy, can become disabling [1]. Rucksack palsy occurs when the shoulder strap entraps the brachial plexus nerve, where symptoms include numbness, paralysis, and cramping of the arm [9]. Since the hips are more tolerable to peak pressures [4], advanced load carriage designs distribute the load from the shoulders using rigid frames and waist belts [67, 68]. In one case, utilizing a rigid frame decreased the rate of injury by 7.4 times over that without a frame, and sustained injuries were considered more benign [67]. Despite load carriage modernization, skin contact pressure generated in the shoulder region is observed to peak at 90 kPa [12, 29], which greatly surpasses thresholds of ischemia.

The distribution of pressure during load carriage has been extensively measured with human participants [4, 22, 58] and load carriage simulators [20, 50, 69] while using the Tekscan F-Scan™ (Tekscan Inc., Norwood, MA, United States) sensors. The resistive-based sensors appealed to biomechanical research as they were thin and flexible, thus allowing them to conform to concave and convex surfaces with ease. Although initially advanced, the sensors were susceptible to measurement drift and hysteresis, which cautioned the use of absolute measurements [15, 16]. Subsequently, they were identified to be sensitive to

surface hardness, loading speed, and temperatures surpassing 30° C [17, 18], which required a careful calibration process to capture the unique sensor characteristics [55, 70]. Ultimately, measurement errors of the Tekscan F-Scan™ system were as high as 34% when evaluated in the simplest geometric condition [15, 16, 19]. Newer skin contact pressure measurement systems, such as Novel Pliance® (Novel GmbH, Munich, Germany), Tekscan I-Scan™ (Tekscan Inc., Norwood, MA, United States), and XSENSOR™ X3 (XSENSOR™ Technology Corp., Calgary, AB, Canada), have evolved to address the challenges encountered in practical application. While Tekscan I-Scan™ followed the resistive technology of Tekscan F-Scan™, Novel and XSENSOR™ developed capacitive pressure sensing technology, where a change in stored energy is associated with a known applied load to the sensor.

Before understanding the distribution of pressure between a load carriage system and its bearer, the measurement system must be validated under the anticipated conditions of load and geometry. Historical determination of system performance has supplied a baseline, where systems were evaluated individually and in a flat geometric orientation [17, 59, 62]. A primary limitation of these studies is the ability to confidently extend the performance results of the system into application [57], where systems are customarily applied in concave-convex geometries (e.g., shoulder region). While preliminary curved surface evaluations exist, pneumatic load applicators, such as a sphygmomanometer, are prone to air leaks, binary pressure distributions, and low applied magnitudes of pressure [59]. Beyond the geometric condition, more recent evaluation efforts have been commonly conducted at low (e.g., pressure garments [60, 61, 71]) and high (e.g., plantar pressures [62, 63]) magnitudes of applied pressure, which only exist in extreme instances of load carriage.

Since comprehensive studies investigating multi-system, -surface, and -load are not widely reported, this study aims to first compare three systems over two surfaces and five applied loads to determine if the absolute error at 30 minutes of static pressure depends on the evaluated conditions. The second aim is to compare the system, surface, and load to determine if the rate of measurement drift over 30 minutes of static pressure depends on the evaluated conditions. The third aim is to compare the system, surface, and

load to determine if time affects the rate of measurement drift. Because each system has different characteristics, an inherent difference in absolute error and drift rate between each system is hypothesized. Likewise, because Novel Pliance[®] sensors are unloaded on the experimental surface before data acquisition, no difference in absolute error or drift rate between surface conditions per system is hypothesized. Thirdly, because the literature demonstrates a load dependency on system performance [60], a significant effect of load on absolute error and rate of measurement drift is hypothesized. Finally, because system evaluation in literature exhibits a measurement drift that lessens over time [16], a significant difference for each time interval is hypothesized.

3.2 Materials and Methods

Three skin contact pressure measurement systems (Novel Pliance[®], Tekscan I-Scan[™], and XSENSOR[™] X3; Table 3.1) were evaluated to determine the effect of system, surface geometry, and applied load on absolute measurement error and rate of measurement drift. The five applied loads were 30, 45, 60, 75 and 90 kPa and the two surface geometries were flat and semi-circular curved¹. These applied loads were selected to represent skin contact pressures caused by posterior-borne load carriage [4, 29, 58]. These two geometric conditions were selected because a flat surface represents the standard sensor configuration under which pressure systems are commonly calibrated, and a curved surface represents a more complex geometry that is commonly observed in ergonomic applications (e.g., shoulders during load carriage, lower and upper limb segments during exoskeleton applications).

All three systems were publicized by the manufacturer to be designed for posterior-borne load carriage and were purchased through normal procurement channels. At the centre of each pressure measurement system were the Novel Pliance[®] box, Tekscan VersaTek[™] hub, and XSENSOR[™] X3 Pro electronic unit. The system centre receives measurements from the pressure sensor and relays the digital

¹ The authors recognize that load typically refers to a force and that pressure is equivalent to force divided by area. For written simplification, five ‘loads’ were applied to the surface conditions instead of specifying applied pressure.

information to the computer software. Of the available system capacities, the Novel Pliance[®] xf-32, Tekscan I-Scan[™] VersaTek[™] high-speed USB, and XSENSOR[™] X3 professional version were used.

Pressure sensors capture the distribution of skin contact pressure while utilizing capacitive technology for Novel Pliance[®] and XSENSOR[™] X3, and resistive technology for Tekscan I-Scan[™]. A variety of pressure sensors were listed by each manufacturer for the application of posterior-borne load carriage. Two criteria were used to select the evaluated sensors. First, the length and width of an individual pressure-sensing element were similar. The pressure sensing elements were square-shaped for Novel Pliance[®] (1.41 x 1.41 cm) and XSENSOR[™] X3 (1.27 x 1.27 cm), while rectangular-shaped for Tekscan I-Scan[™] (1.27 x 1.71 cm). Although the width of the Tekscan I-Scan[™] sensor is greater than Novel Pliance[®] and XSENSOR[™] X3, the majority of the width dimension is located in an ‘inactive zone’, where the Tekscan I-Scan[™] computer software assumes constantly applied pressure, as measured by the ‘active zone’ of each pressure sensing element.

The second criterion is that the measurable range of the pressure sensor was adequate for the anticipated skin contact pressure caused by posterior-borne load carriage [4, 29, 58]. The measurable range of pressure spans from an activation threshold to a maximum value. Pressure beyond the measurable range would be inaccurate [57], or the sensor itself would be insensitive [17]. Unique to the Tekscan I-Scan[™] VersaTek sensor handles, is the adjustment of sensitivity (5x up to 3x down) to meet application needs. Both Novel and XSENSOR[™] predefined the measurable pressure range.

Sensor calibration is a critical process that ensures the accuracy and precision of pressure sensing systems. Yearly sensor calibration is recommended by Novel and XSENSOR[™], while Tekscan recommends re-preparation for sensors left idle for more than 3 hours. Sensors are inserted into a pneumatic calibration device, where a bladder is inflated to apply an even and known applied load distribution. Purchased with the Novel Pliance[®] and Tekscan I-Scan[™] systems were the recommended trublu[®] and PB100C calibration devices, respectively. XSENSOR[™] markets a calibration device; however, it is limited

to a 100 kPa capacity. Characteristics of the systems and their calibration are given in Table 3.1. Further sensor preparation discussion is in Section 3.2.3.

Table 3.1 Characteristics of evaluated skin contact pressure measurement systems.

Characteristic	Skin Contact Pressure Measurement System		
	Novel Pliance®	Tekscan I-Scan™	XSENSOR™ X3
System Hub	Pliance® Box	High-Speed VersaTek™	X3 Pro
Sensor Technology	Capacitive	Resistive	Capacitive
Sensor Model	S2158	9830	LX210
Element Size [cm]	1.41 x 1.41	1.71 x 1.27	1.27 x 1.27
Number of Elements	30 x 8 <i>240 total</i>	11 x 16 <i>176 total</i>	10 x 14 <i>140 total</i>
Measurable Range [kPa]	5–240	1–~190	1–221
Calibration Device	trublu®	PB100C	N/A
Calibration Period	Yearly	Prior to data collection	Yearly

3.2.1 Experimental Setup

Experimental apparatuses were developed to evaluate pressure sensors on a flat and curved surface. The flat apparatus consisted of a standard contact and interchanging block (Figure 3.1). The blocks were manufactured of mild steel and prearranged in desired configurations. Force was applied perpendicularly to the sensor via two 4 mm thick BockLite™ (#617S1=H4, Ottobock, Duderstadt, Germany) strips (dimensions provided in Section 2.4), made of polyethylene closed cell foam (~35° Shore A hardness). These strips were consistent for all experimental trials for the flat surface condition and were attached in parallel to the bottom of the standard contact block. Placed onto the sensor was the standard contact block, where the two BockLite™ strips interface. Exchanging the mass configuration above the standard contact

block achieved the five desired magnitudes of load (30, 45, 60, 75, and 90 kPa). Surface preparation for the flat condition entailed the establishment of a level plane ($0^\circ \pm 0.2^\circ$) and the placement of 3 mm thick polyethylene closed cell foam upon it [17]. White tape was applied to the sensor to define the loaded elements per system.

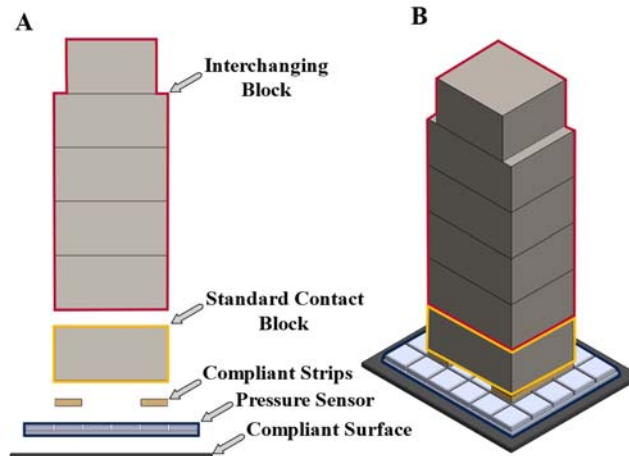


Figure 3.1 Flat surface apparatus. Exploded (A) and isometric (B) views of a load configuration for the flat surface condition.

The curved surface experimental apparatus consisted of a small and large T-slot frame, a force plate (#ACG-O, AMTI Inc., Watertown, MA, United States), a semi-circular hard-foamed cylinder (6 PCF solid polyurethane foam), a standard posterior-borne load carriage strap, a small scissor lift, and freely hung loads (Figure 3.2). The large T-slot assembly was designed to support the force plate and four steel rollers. Placed onto the force plate was the small T-slot frame assembly. On top of the small frame, a semi-circular hard-foamed cylinder with a radius of 6.54 ± 0.002 cm, was attached. Wrapped around the semi-circular surface was 4 mm BockLite™, which provided surface compliance for a more even distribution of applied pressure [17]. Pressure sensors were individually attached to the semi-circular surface, where the interface was marked with tape for a consistent position of load. An analogous 2.60 ± 0.002 cm wide strap for posterior-borne load carriage was placed across the semi-circular curved surface and steel rollers of the

large T-slot frame assembly. Beneath the large T-slot frame assembly was a scissor lift. Placed on the scissor lift were two equivalent masses, which were attached to both ends of the strap. The strap was laid perpendicularly across the curved surface and steel rollers, where marks on the steel roller allowed repeatable strap placement. A scissor lift was used to symmetrically tension the strap to minimize shear loading onto the evaluated sensor [57]. Once the scissor lift was lowered, the strap created contact pressure on the sensor. Preparation for loading the curved surface entailed the establishment of a level plane ($0^\circ \pm 0.2^\circ$) on the surface of the force plate and the top of the small T-slot frame assembly.

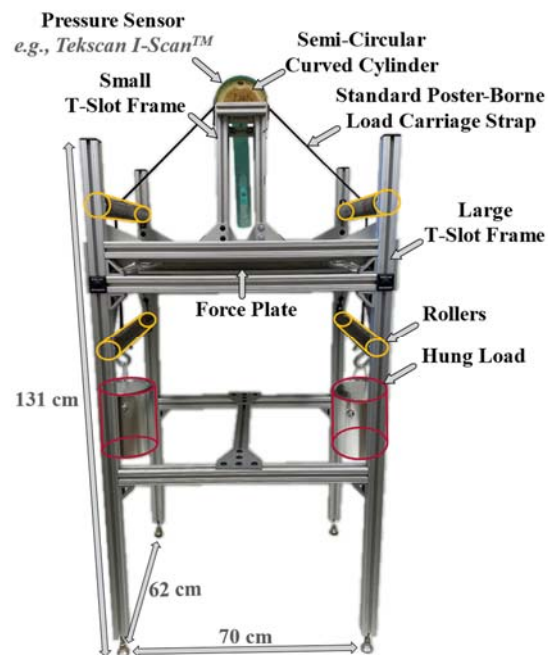


Figure 3.2 Curved surface apparatus. Supported on the large T-slot frame assembly was a force plate and a small T-slot frame assembly. A pressure sensor was attached to the semi-circular hard-foamed cylinder covered with BockLite™. A standard posterior-borne load carriage strap was tensioned across the sensor and rollers and symmetrically loaded via hung load.

3.2.2 Experimental Protocol

Ten independent trials were performed per system (Novel Pliance[®], Tekscan I-Scan[™], and XSENSOR[™] X3), surface (flat and curved), and load (30, 45, 60, 75, and 95 kPa)², for a total of 300 trials. Data collection was first randomized for system order, arbitrarily collected in the flat condition before curved, and followed a balanced applied load order. The balanced order consisted of an applied load sequence, which allowed each load to be ordered in numerical sequence from the first to the fifth position twice per system and surface condition. All ten trials per system and surface condition were collected prior to changing conditions. Each trial lasted 30 minutes from the first point of the measured load and data was collected at 50 Hz.

3.2.3 Sensor Preparation

A single investigator prepared the Novel Pliance[®] and Tekscan I-Scan[™] pressure sensors in the laboratory following guidelines outlined in the respective manufacturer's user manual [72, 73]. Novel Pliance[®] preparation entailed two-point amplification and multi-point recalibration within the trublu[®] pneumatic calibration device. Factory settings (e.g., applied pressures), provided by the manufacturer, were utilized. Tekscan I-Scan[™] preparation entailed conditioning (130 kPa), sensitivity adjustment, equilibration (25, 50, 75, 100, and 125 kPa), and calibration (25, 50, 75, 100, and 125 kPa). Equilibration was excluded when preparing the flat surface sensor due to identical geometric complexity between calibration and evaluation. A new Tekscan I-Scan[™] sensor was prepared for each surface condition to account for signal degradation caused by use [17, 57]. Points of calibration and equilibration were self-selected to encompass the various loads of evaluation [57]. As recommended, the XSENSOR[™] X3 pressure sensor was calibrated by the manufacturer within the recommended calibration period. All sensor

² The exact applied pressures of 29.7, 46.7, 62.7, 78.8, and 94.6 kPa were rounded for ease of communication. All calculations conducted use exact applied pressures.

preparation and evaluation were conducted in the same laboratory that maintained a consistent temperature and humidity.

3.2.4 Data Analysis

Simplified models were used to apply an equivalent theoretical pressure (30, 45, 60, 75, and 90 kPa) to each surface (flat and curved), where the applied pressure was equivalent to the force divided by area. For the flat condition, force was generated by the summation of the weight of the standard contact and interchanging block. The weight and contact area of the standard contact block remained identical for all flat surface trials. The area of contact, of the two BockLite™ strips, was measured using standard callipers (TOL-10997, SparkFun Electronics, United States) and was calculated to be $14 \pm 0.01 \text{ cm}^2$. The BockLite™ strip dimensions were $(1.43 \times 5.05) \pm 0.01 \text{ mm}$ and $(1.40 \times 5.16) \pm 0.01 \text{ mm}$. For the curved condition (Figure 3.3), the force was applied to the surface using a tensioned strap. Attached at either end of the strap were freely hung loads of equivalent weight. Using steel rollers, that were equidistant from the curved surface, the direction of the tension vector was directed towards the surface and contacted it at an angle of $43.5 \pm 0.2^\circ$ from the horizontal, as measured using a digital inclinometer (WR300-TY2, Barry Wixey Development, United States). Using the known dimensions of pressure sensing elements per manufacturer and the curved surface geometric relationship, the vertical force component of the applied force was resolved per element. The curved surface contact area was $26 \pm 0.08 \text{ cm}^2$.

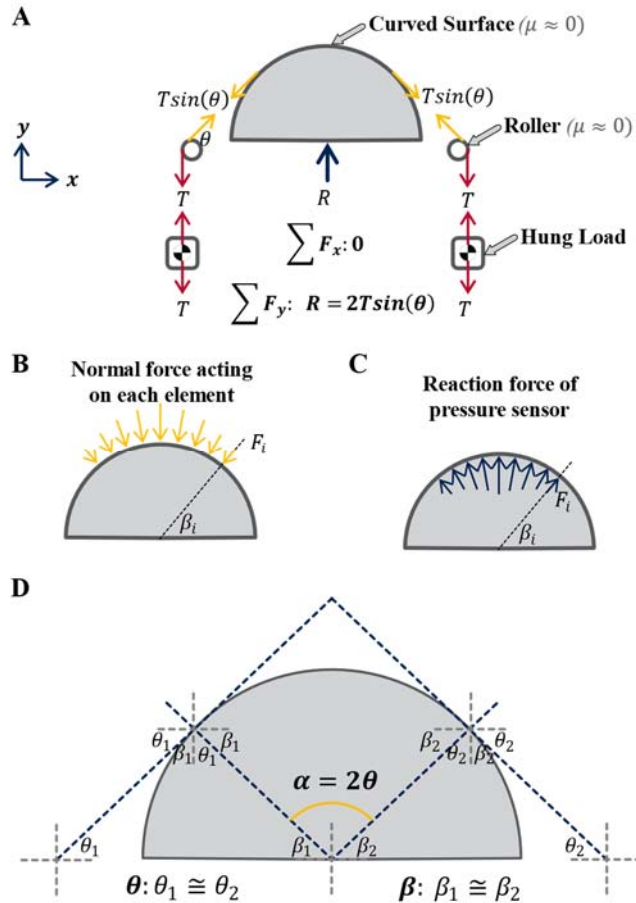


Figure 3.3 Curved surface force analysis. A free-body diagram of the curved surface apparatus (A). An example of normal forces acting on each pressure sensing element (B). The reaction forces are measured by the pressure sensor (C). Angle determination of acting forces (D).

Pre-data analysis was conducted to visually inspect the active elements of each trial. Specifically, the inspection searched for the bleeding of pressure, where pressure was numerically captured despite a physically unloaded sensing element. Since load placement was defined per system and surface condition, particular rows and columns of pressure-sensing elements were anticipated to record pressure above its activation threshold. Because pressure bleeding was common to higher load magnitudes and resulted in low measured pressure, the impact of pressure bleeding was pronounced in average pressure calculations prior to pre-data analysis.

Static pressure measurements were analyzed using a custom MATLAB (R2020B, MathWorks[®], United States) script. The script first calculated the average pressure of active elements per collected frame. Next, an initial point of loading for each trial was sought, based on when the average calculated pressure surpassed 5 kPa. Because each system had different activation pressures, the highest threshold was selected (Table 3.1). From the first point of loading, 30 minutes (e.g., 90,000 frames) of static loading was extracted. An overall average pressure was calculated at 3, 12, 21, and 30 minutes per trial using a full second (e.g., 50 frames) of collected data. For the analysis of absolute measurement error (measured minus applied load), only pressure measurement data at 30 minutes was considered. This was because pressure sensors can be loaded for extended periods in application, prior to the actual collection of data. For the analysis of drift, the rate of pressure change was calculated between 3–12, 12–21, and 21–30 minutes. The first three minutes of pressure data were discarded while the sensor was acclimatized to loading. Each time interval spanned 9 minutes to provide a general understanding of drift over 30 minutes of static pressure.

3.2.5 Statistics

Mean and standard deviation were calculated for each system (Novel Pliance[®], Tekscan I-Scan[™], and XSENSOR[™] X3), surface (flat and curved), and load (30, 45, 60, 75, and 90 kPa) for absolute measurement error (experimental minus theoretical) and rate of measurement drift (3–12, 12–21, and 21–30 minutes). The absolute error was analyzed using a series of statistical analyses to determine differences attributed to system, surface, and load. First, a one-way analysis of variance (ANOVA; significance level $\alpha = 0.05$) determined the effect of the system, without considering surface or load. Second, an independent sample t-test (significance level $\alpha = 0.05$) determined the difference of surface per system, without considering load. Third, a one-way ANOVA determined the effect of load per system and surface condition. If the omnibus ANOVA revealed a significant effect, the difference between conditions was compared using Tukey's Honest Significant Difference (HSD) or Games-Holwell as *post hoc* tests. The Shapiro-Wilk test verified the assumption of normality, where violations are present in some comparisons of system, surface, and load. Non-normality remained uncorrected because ANOVAs are robust to this violation,

mainly when sample sizes are equal [74]. Levene's test verified the assumption of homogeneity of variance, where violations were corrected using the Satterthwaite adjustment for degrees of freedom [75], and the Cochran-Cox adjustment for the standard error estimate [76], as Welch's correction.

The effect of measurement drift over 3–12, 12–21, and 21–30 minutes was analyzed using a series of statistical analyses to determine differences attributed to system, surface, and load. The equivalent technique of absolute error was applied to measurement drift, where a one-way ANOVA determined the effect of system and load, and a two-tail independent sample t-test determined differences attributed to surface. If the omnibus ANOVA revealed a significant effect, the difference between conditions was compared using Tukey's HSD or Games-Holwell as *post hoc* tests. Normality and homogeneity of variance were verified as previously outlined.

Furthermore, the effect of time on measurement drift was analyzed using repeated measures ANOVA (significance level $\alpha = 0.05$) to determine differences attributed to time of measurement. The applicable Greenhouse-Geisser ($\epsilon < 0.75$) and Huynh-Feldt ($\epsilon > 0.75$) corrections were applied where Mauchly's Test of Sphericity was significant [77]. The assumption of normality was verified as aforementioned. If the omnibus ANOVA revealed a significant effect, the difference between conditions was compared using Fisher's Least Significant difference (LSD) *post hoc* test. This *post hoc* method differed from the previous *post hoc* analysis since Fisher's LSD holds the rate of family-wise error at 0.05 when three groups are compared [78]. All statistical analyses were performed using SPSS version 27 (IBM Corp., NY, USA).

3.3 Results

3.3.1 Absolute Error

Figure 3.4 illustrates the absolute error per system (mean \pm standard deviation). The one-way ANOVA revealed a significant effect on absolute error (*Welch's* $F_{2,00,172.98} = 45.148, p < 0.001, est. \omega^2 = 0.227$). Games-Howell *post hoc* test revealed that Novel Pliance[®] (4.51 ± 2.26 kPa) measured significantly less absolute error than both Tekscan I-Scan[™] (7.16 ± 4.70 kPa, $p < 0.001$) and XSENSOR[™] X3 (9.29 ± 4.90 kPa, $p < 0.001$). Similarly, Tekscan I-Scan[™] measured significantly less absolute error than XSENSOR[™] X3 ($p = 0.006$).

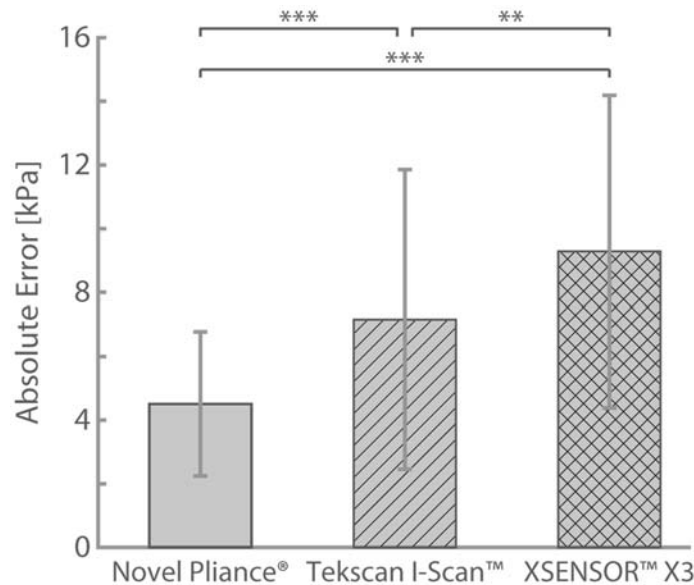


Figure 3.4 Absolute error per system. Mean and standard deviation of absolute error per system (Novel Pliance[®], Tekscan I-Scan[™], and XSENSOR[™] X3). ** $p < 0.01$, *** $p < 0.001$.

Because absolute error per system differed significantly, surface condition per system was analyzed, as illustrated in Figure 3.5. The two-tailed independent sample t-test revealed a significant difference in absolute error between surface conditions of both Tekscan I-Scan[™] ($t_{98,00} = -2.717, p = 0.008, \eta^2 = 0.070$) and XSENSOR[™] X3 (*Welch's* $t_{90,91} = -5.532, p < 0.001, est. \omega^2 = 0.228$). Therefore, indicating significantly less absolute error was measured on a flat than curved surface for both Tekscan I-Scan[™]

(mean difference \pm standard error difference: 2.47 ± 0.91 kPa) and XSENSOR™ X3 (4.76 ± 0.86 kPa). Despite similar performance characteristics by Novel Pliance® (0.85 ± 0.45 kPa), no difference in absolute error between surfaces was statistically supported ($t_{98,00} = -1.913, p = 0.059, \eta^2 = 0.036$).

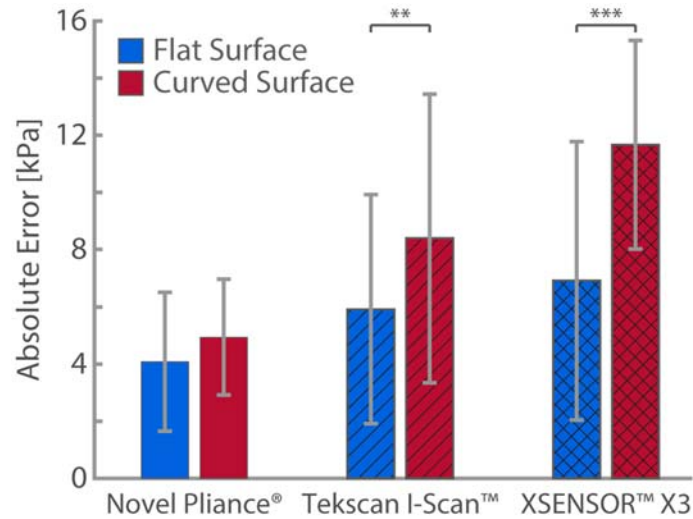


Figure 3.5 Absolute error per system and surface. Mean and standard deviation of absolute error per system (Novel Pliance®, Tekscan I-Scan™, and XSENSOR™ X3) and surface (flat and curved). ** $p < 0.01$, *** $p < 0.001$.

Because absolute error differed significantly for Tekscan I-Scan™ and XSENSOR™ X3 per surface, load per system and surface condition were analyzed, as illustrated in Figure 3.6. The one-way ANOVA revealed a significant effect on load for Tekscan I-Scan™ flat ($F_{4,00,45,00} = 90.165, p < 0.001, \eta^2 = 0.890$) and curved (Welch's $F_{4,00,21,23} = 64.319, p < 0.001, est. \omega^2 = 0.840$) and XSENSOR™ X3 curved ($F_{4,00,45,00} = 45.393, p < 0.001, \eta^2 = 0.800$). No effect on load was revealed for XSENSOR™ X3 ($F_{4,00,45,00} = 1.788, p = 0.148$). Tukey's HSD and Games-Howell *post hoc* tests revealed many significant pairwise conditions (*all p-values* < 0.047), as illustrated in Figure 3.6. Tekscan I-Scan™ exhibited a greater error dependency on load than XSENSOR™ X3.

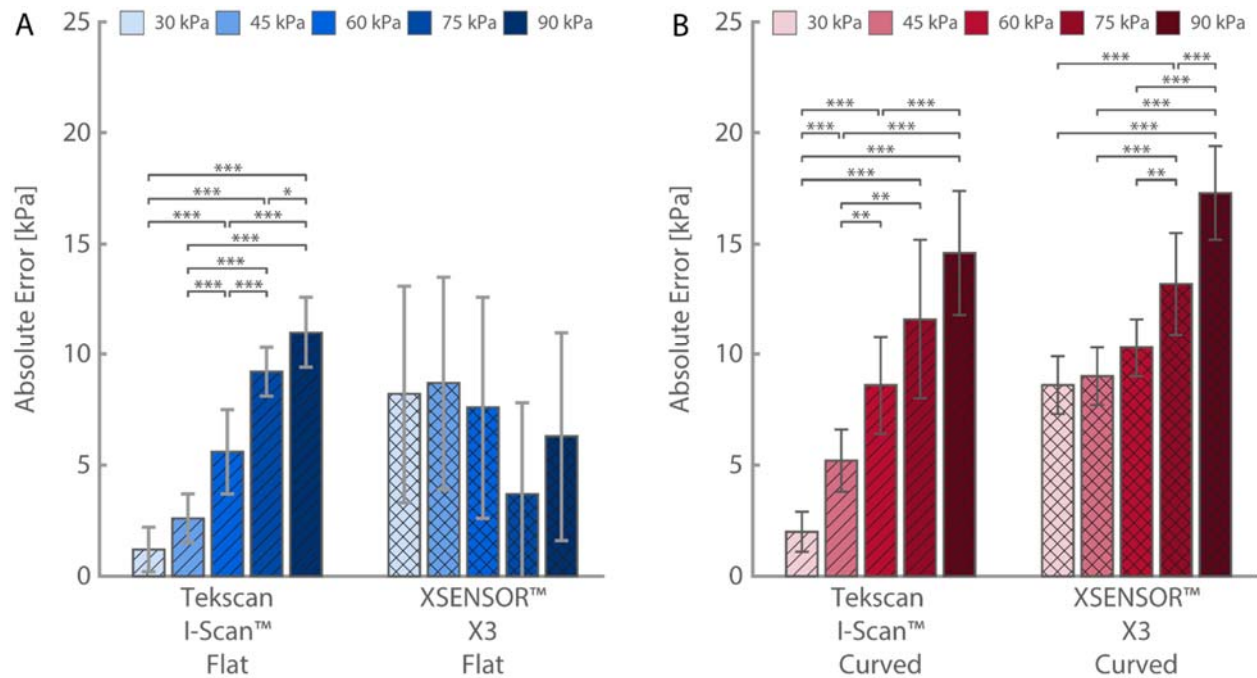


Figure 3.6 Absolute error per system, surface, and load. Mean and standard deviation of absolute error per system (Tekscan I-Scan™ and XSENSOR™ X3), surface (flat: A; curved: B), and load (30, 45, 60, 75, and 90 kPa). * $p < 0.05$, ** $p < 0.01$, *** $p < 0.001$.

3.3.2 Measurement Drift

Figure 3.7 illustrates the rate of measurement drift per system (mean \pm standard deviation). The one-way ANOVA revealed a significant effect on the rate of measurement drift per system (*Welch's* $F_{2,00, 572.31} = 107.565$, $p < 0.001$, *est. $\omega^2 = 0.191$*). Games-Howell *post hoc* test revealed that Novel Pliance® (0.05 ± 0.06 kPa/min) drifted significantly less than Tekscan I-Scan™ (0.15 ± 0.11 kPa/min, $p < 0.001$) and XSENSOR™ X3 (0.08 ± 0.07 kPa/min, $p < 0.001$). Similarly, XSENSOR™ X3 drifted significantly less than Tekscan I-Scan™ ($p < 0.001$).

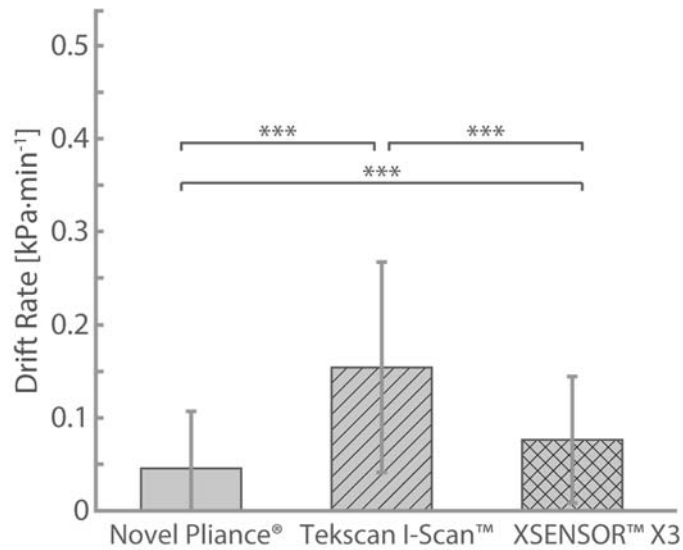


Figure 3.7 Drift per system. Mean and standard deviation for the rate of measurement drift per system (Novel Pliance®, Tekscan I-Scan™, and XSENSOR™ X3). *** $p < 0.001$.

Because the rate of measurement drift per system differed significantly, time intervals per system were analyzed, as illustrated in Figure 3.8 (mean \pm standard deviation). The one-way repeated measures ANOVA, with Greenhouse-Geisser correction, revealed a significant effect on time for each system (*all F-values* > 156.847 , *all p-values* < 0.001). *Post hoc* tests, using Fisher's LSD, revealed significant differences between time intervals for each system (*all p-values* < 0.001). Therefore, indicating that the magnitude of measurement drift significantly lessened over time for all systems.

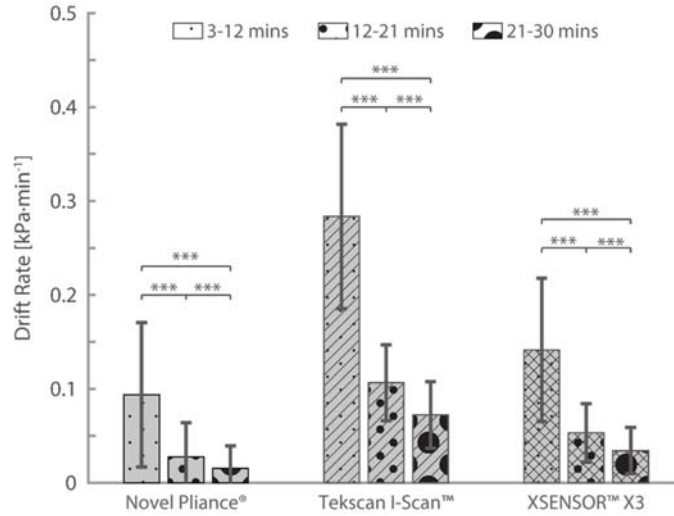


Figure 3.8 Drift rate per system and time interval. Mean and standard deviation for the rate of measurement drift per system (Novel Pliance®, Tekscan I-Scan™, and XSENSOR™ X3) and time interval (3–12, 12–21, and 21–30 minutes). *** $p < 0.001$.

Because the rate of measurement drift per system differed significantly, surface conditions per system were analyzed, as illustrated in Figure 3.9. The two-tailed independent sample t-test revealed a significant difference in drift rate for all systems (*all t-values* < -2.289, *all p-values* < 0.023). Therefore, indicating that the magnitude of measurement drift was significantly less on the flat surface than curved surface for Novel Pliance (mean difference \pm standard error difference: 0.02 ± 0.01 kPa), Tekscan I-Scan (0.03 ± 0.01 kPa), and XSENSOR™ X3 (0.02 ± 0.01 kPa).

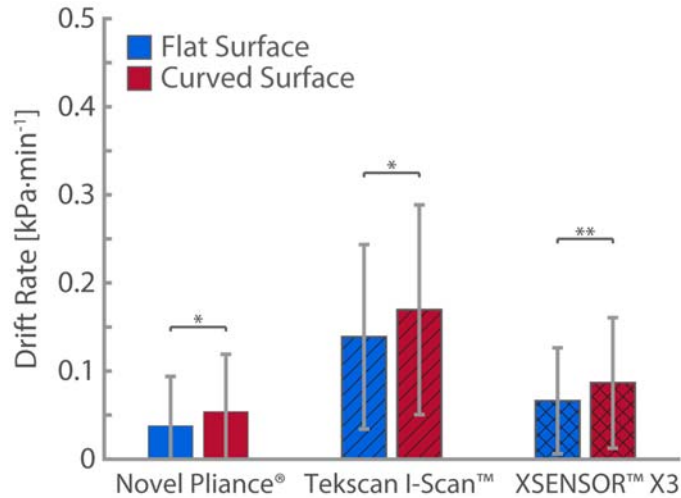


Figure 3.9 Drift rate per system and surface. Mean and standard deviation for the rate of measurement drift per system (Novel Pliance®, Tekscan I-Scan™, and XSENSOR™ X3) and surface (flat and curved). * $p < 0.05$, ** $p < 0.01$.

Because the rate of measurement drift differed significantly per system and surface condition, time intervals per system and surface were analyzed, as illustrated in Figure 3.10. The one-way repeated measures ANOVA, with applicable Greenhouse-Geisser and Huynh-Feldt corrections, revealed a significant effect on time for drift rate per system and surface condition (*all F-values* > 69.975, *all p-values* < 0.001). Fisher's LSD *post hoc* tests revealed significant differences between the evaluated time intervals of each system and surface condition (*all p-values* < 0.004). In agreement with the previous study outcome, the magnitude of measurement drift significantly lessened over time for each system and surface condition.

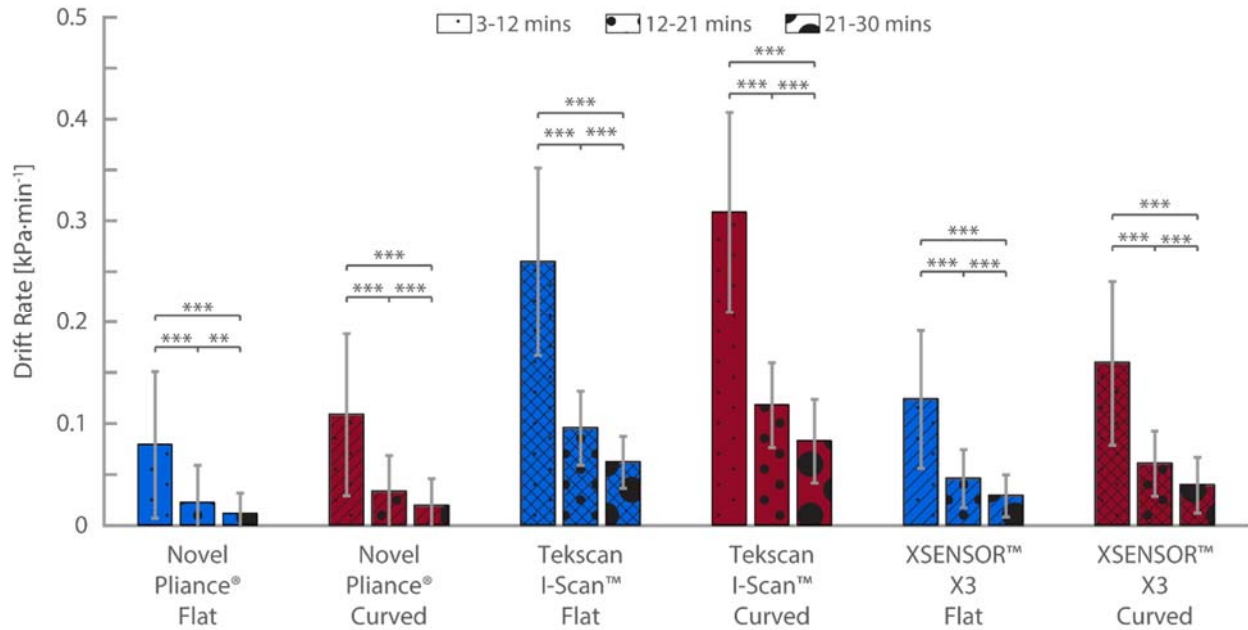


Figure 3.10 Drift rate per system, surface, and time interval. Mean and standard deviation for the rate of measurement drift per system (Novel Pliance[®], Tekscan I-Scan[™], and XSENSOR[™] X3), surface (flat and curved), and time interval (3–12, 12–21, and 21–30 minutes). ** $p < 0.01$, *** $p < 0.001$.

Because the rate of measurement drift per system and surface differed significantly, load per system and surface condition were analyzed, as illustrated in Figure 3.11. The one-way ANOVA revealed a significant effect on load per system and surface condition for drift rate (*Welch's F-values* > 6.001, all *p-values* < 0.001). Games-Howell *post hoc* tests revealed numerous significant differences in load (all *p-values* < 0.047), as illustrated in Figure 3.11. All evaluated conditions, but Tekscan I-Scan[™] curved at 60 kPa, exhibited at least one significant difference in load. Furthermore, the 30 kPa condition displayed the majority of significant comparisons for each system and surface condition. At 30 kPa, Novel Pliance[®] exhibited significant negative drift.

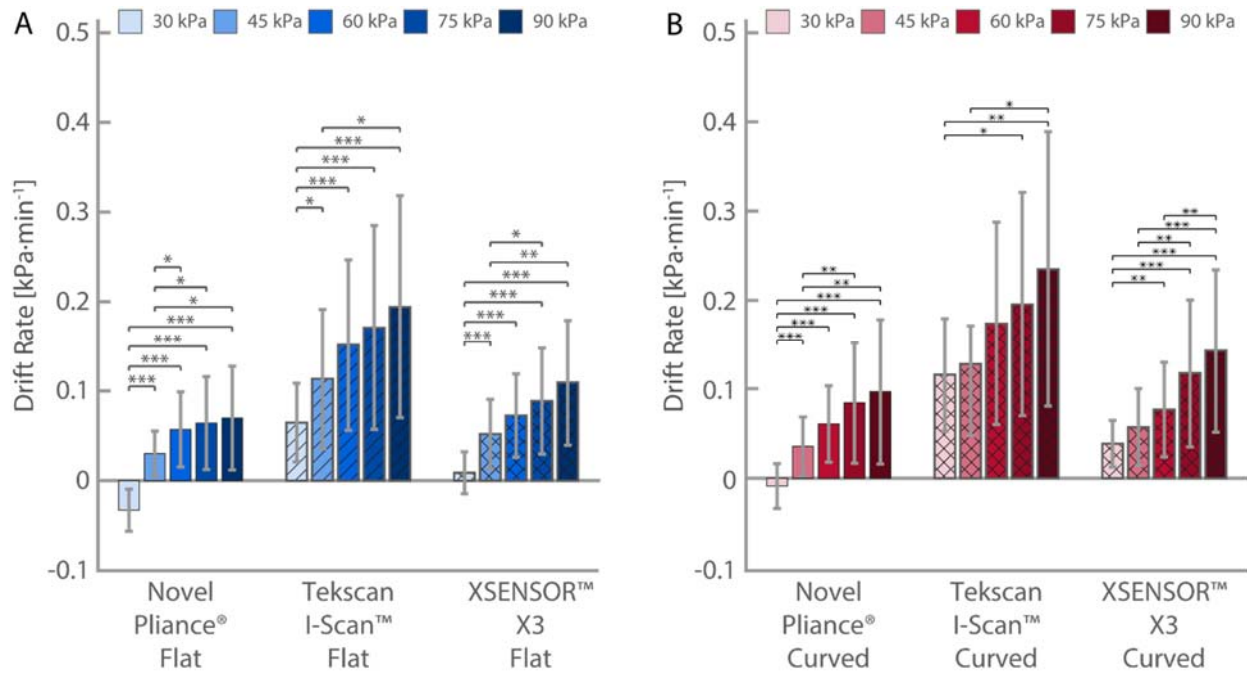


Figure 3.11 Drift rate per system, surface, and load. Mean and standard deviation for the rate of measurement drift per system (Novel Pliance[®], Tekscan I-Scan[™], and XSENSOR[™] X3), surface (flat: A; curved: B), and load (30, 45, 60, 75, and 90 kPa). * $p < 0.05$, ** $p < 0.01$, *** $p < 0.001$.

Because the rate of measurement drift differed significantly per system, surface, and load, time intervals per system, surface, and load were analyzed, as illustrated in Figure 3.12. The one-way repeated measures ANOVA, with applicable Greenhouse-Geisser correction, revealed many significant effects on time per system, surface, and load for drift rate (*all Welch's F-values* > 4.893, *all p-values* < 0.019). No effect on time was revealed for both Novel Pliance[®] curved ($F_{2.00, 18.00} = 2.359$, $p = 0.123$, $\eta_p^2 = 0.208$) and XSENSOR[™] X3 flat ($F_{1.12, 10.03} = 4.501$, $p = 0.057$, $\eta_p^2 = 0.333$) at 30 kPa. Fisher's LSD *post hoc* tests revealed numerous significant differences in time (*all p-values* < 0.047), as illustrated in Figure 3.12. All time comparisons for XSENSOR[™] X3 flat (except 30 kPa load) and curved, as well as Tekscan I-Scan[™] flat, were significant. The most frequent comparator exhibiting no difference in measure on time was Novel Pliance[®].

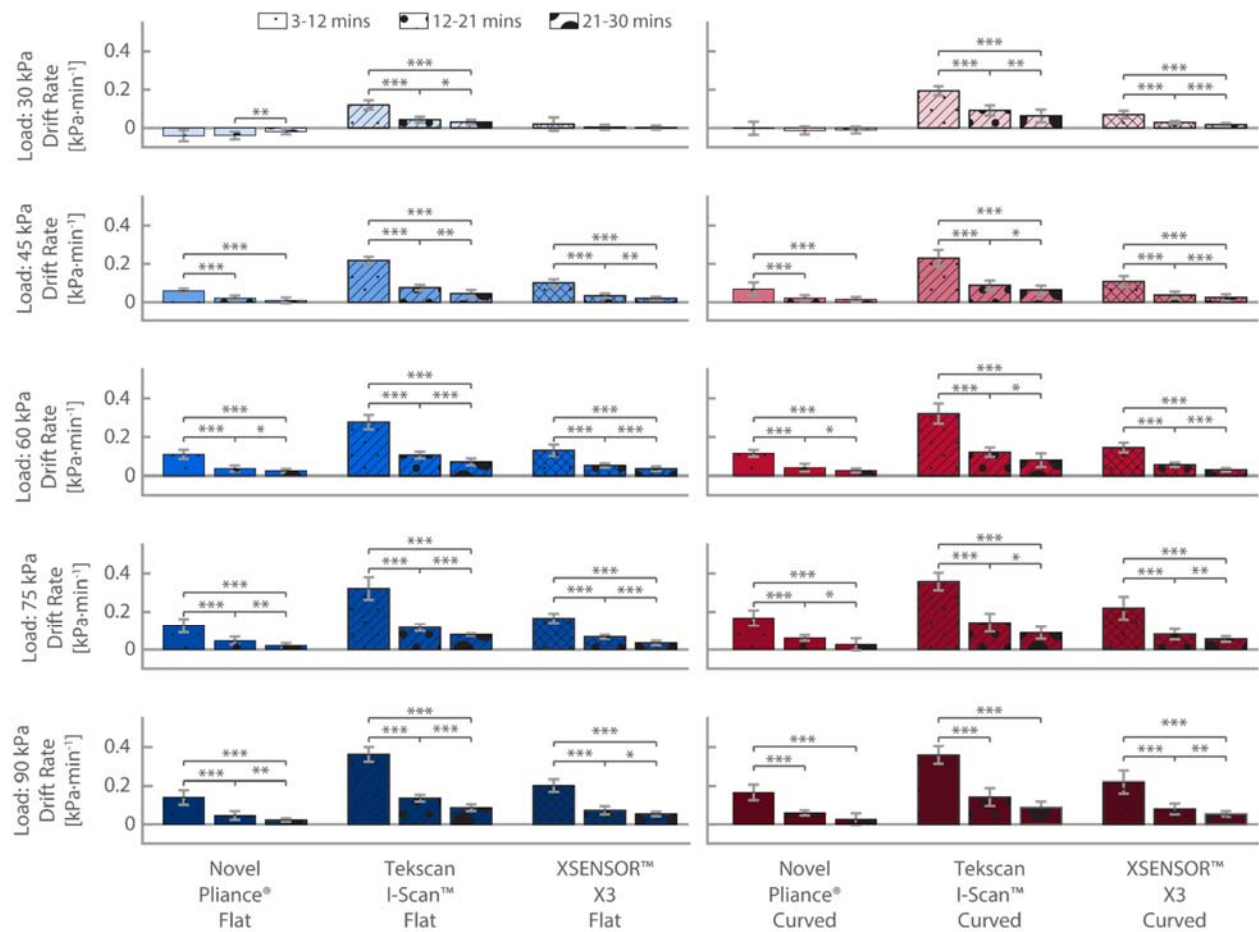


Figure 3.12 Drift rate per system, surface, load, and time interval. Mean and standard deviation for the rate of measurement drift per system (Novel Pliance[®], Tekscan I-Scan[™], and XSENSOR[™] X3), surface (flat and curved), load (30, 45, 60, 75, and 90 kPa) and time interval (3–12, 12–21, and 21–30 minutes). * $p < 0.05$, ** $p < 0.01$, *** $p < 0.001$.

3.4 Discussion

This study quantified the effect of system (Novel Pliance[®], Tekscan I-Scan[™], and XSENSOR[™] X3), surface (flat and curved), and load (30, 45, 60, 75, and 90 kPa) on the absolute error at 30 minutes of static pressure. Furthermore, this study assessed the effect of system, surface, and load on the rate of measurement drift over 30 minutes of static pressure. Lastly, this study quantified the effect of system, surface, and load on drift rate over 3–12, 12–21, and 21–30 minutes. This comparison acts to inform researchers and clinicians of skin contact pressure measurement system performance regarding their respective absolute error and rate of measurement drift while examined under various surface, load, and time conditions.

For the evaluation of absolute error, Novel Pliance[®] yielded the lowest, followed by Tekscan I-Scan[™] and XSENSOR[™] X3. These results agreed with the literature, where a Novel system yielded lower errors than Tekscan and XSENSOR[™] [62, 63]. Since the absolute error of each system differed significantly, it can be said that Novel Pliance[®] had greater accuracy than Tekscan I-Scan[™] and XSENSOR[™] X3 under the evaluated conditions. Similarly, Novel Pliance[®] exhibited the lowest measurement drift, followed by XSENSOR[™] X3 and Tekscan I-Scan[™]. Interestingly, the two capacitive-based systems (Novel Pliance[®] and XSENSOR[™] X3) drifted significantly less than the resistive (Tekscan I-Scan[™]). Although resistive-based systems were characterized by measurement drift decades ago [16], measurement drift continues to weaken system performance in comparison to other systems available. Since measurement drift differed significantly between systems, it can be said that Novel Pliance[®] drifted less than XSENSOR[™] X3 and Tekscan I-Scan[™] under the evaluated conditions. Ultimately, stability of measure over time benefits many applications (e.g., the design of backpacks [5], exoskeletons [6], and biomechanical energy harvesters [7]); however, all systems experienced significant effects of measurement drift on time. This significant outcome was desirable since measurement drift decreased with time, thereby leading to a more stable measurement.

Despite previous assessments of skin contact pressure measurement systems on a curved surface [59], this evaluation uniquely compared captured pressures between surface conditions. No difference of

absolute error on the surface was exhibited by Novel Pliance[®], while both Tekscan I-Scan[™] and XSENSOR[™] X3 were surface susceptible. Of the two surface-significant systems, XSENSOR[™] X3 showed more surface susceptibility based on a greater mean difference between conditions ($2.47 \pm 0.91 < 4.76 \pm 0.86$ kPa). No difference of surface absolute error by Novel Pliance[®] was a key study outcome as it suggests their sensors may be placed on contouring surfaces without significant performance degradation. A non-significant difference in surface absolute error reduces the deliberately controlled variables in an application (e.g., pressure garments [60, 61]). Likewise, all three systems exhibited significantly different measurement drift between evaluated surfaces. Under the evaluated conditions, Novel Pliance[®] showed significance between surfaces but was the least surface susceptible based on their mean differences. Furthermore, Novel Pliance[®] was less susceptible to drift over time based on their mean differences.

Absolute error per load was evaluated for Tekscan I-Scan[™] and XSENSOR[™] X3, since Novel Pliance[®] revealed no difference in surface measure. Of the load-evaluated systems, XSENSOR[™] X3 exhibited no effect on absolute error, therefore demonstrating measurement stability. Moreover, Tekscan I-Scan[™] flat and curved and XSENSOR[™] X3 curved exhibited significant load effects, as well as many load differences (illustrated in Figure 3.6). Although many significant load conditions were found, a complete load dependency cannot be drawn. It can be said that XSENSOR[™] X3 was the least load-susceptible based on the magnitudes of mean differences. Furthermore, each system revealed a significant effect on measurement drift, where Tekscan I-Scan[™] exhibited the least susceptibility based on the magnitudes of mean differences, especially for 60 kPa (the middle load condition). Since Novel Pliance[®] flat at 30 kPa exhibited negative drift (meaning the measure decreased over time), all comparisons to 30 kPa were inherently significant. Finally, both Novel Pliance[®] curved and XSENSOR[™] X3 flat at 30 kPa exhibited no effect on time, therefore, indicating that the initial pressure measured remained relatively stable across 30 minutes. All time intervals, except one condition of Tekscan I-Scan[™], revealed significantly different drift rates. Although Novel Pliance[®] exhibited many significant differences, it was the system that was found to be the least load-susceptible based on mean differences.

Three hypotheses were developed and statistically evaluated: 1) the absolute error and drift rate will differ significantly between systems, 2) there will be no absolute error and drift rate difference between surfaces for Novel Pliance[®] only, 3) the absolute error and drift rate will have a significant effect per system, surface, and load and 4) the rate of drift will differ significantly over time. The first tested hypothesis agreed with the study results; a difference in both absolute error and drift rate per system was anticipated and found. The second tested hypothesis agreed with the results of absolute error, where no difference on the surface was expected and observed (Novel Pliance[®] only); however, Novel Pliance[®] exhibited significantly different drift rates over time. Next, a significant effect on load per system and surface agreed with the third tested hypothesis. Finally, the results comparing time per system, surface, and load agreed with the fourth hypothesis, except for Novel Pliance[®] curved and XSENSOR[™] X3 flat at 30 kPa.

3.4.1 Study Limitations

The unequal area between the flat and curved surface is the first study limitation. A smaller flat than curved surface contact area improved the loading process with less mass required to reach the theoretical pressures. Furthermore, an arbitrary curved surface radius was evaluated. Future studies may evaluate additional radii to extend the understanding of system and surface performance to commonly found curvatures of the human body. Moreover, the experiment evaluated static conditions, while these skin contact pressure measurement systems commonly undergo dynamic pressure profiles with time. The effect on dynamic pressure application requires further investigation. Lastly, the pressure sensors were evaluated under the environmental conditions of a laboratory. Pressure sensors placed onto the human body may experience greater temperatures (e.g., body temperature) and humidity (e.g., from sweat) which could impact system performance.

3.5 Conclusion

The present study demonstrated that both absolute error and drift rate, while evaluated between 30–90 kPa on a flat and curved surface, depended on the system that captured pressure. Only Novel Pliance[®] exhibited no difference in absolute error between surface conditions; however, a difference in drift between surface conditions was revealed by all three systems. Only XSENSOR[™] X3 flat exhibited no effect on absolute error, while the remaining conditions of error (excluding Novel Pliance[®]) and drift exhibited a load dependency. Finally, time was identified to affect pressure measures per system, surface, and load, excluding both Novel Pliance[®] curved and XSENSOR[™] X3 flat at 30 kPa. This study indicated the importance of system selection to enhance confidence in measured pressures, reduce experimentally controlled parameters, and provide measurement stability over time. Novel Pliance[®] exhibited the greatest accuracy (4.51 ± 2.26 kPa), lowest drift (0.05 ± 0.06 kPa/min), and least time susceptibility; therefore, suggesting its validity in clinical and biomechanical research applications.

3.6 Funding

This work was supported by the Canadian Institute for Military and Veterans' Health Research contract #W7714-145967/ 001/SV/Task 49 for Defence Research and Development Canada.

3.7 Declaration of Competing Interest

The authors declare that they have no known competing financial interests or personal relationships that could have appeared to influence the work reported in this paper.

3.8 Supporting Information

Data files including metadata and results of statistical analyses are included in Appendix A.

Chapter 4

A comparative study of contact pressure measurement systems on the Dynamic Load Carriage Simulator

Adam Thompson^{a,*}, Michael Shepetycky^a, Jun-Tian Zhang^a, Tim Bryant^a, Evelyn Morin^a,
Adrienne Sy^b, Linda Bossi^b, and Qingguo Li^a

^a **Ergonomic Research Team, Queen's University**, Kingston, ON, Canada, K7L 3N6

^b **Defence Research and Development Canada**, North York, ON, Canada, M3K 2C9

* Corresponding author. Email: adam.thompson@queensu.ca (A.T.)

Manuscript in preparation for the journal of

Applied Ergonomics

(Elsevier, Amsterdam, Netherlands)

Highlights

- Comparison of three skin contact pressure measurement systems.
- The effect and agreement between systems and testing days were examined.
- Differences in system performance were identified.

Abstract

This study examined the effect and agreement of three commercially available skin contact pressure measurement systems on measuring average pressure, peak pressure, and contact area beneath the shoulder straps of a backpack loaded with three weight configurations. Three pressure sensor systems (Novel Pliance[®], Tekscan I-Scan[™], and XSENSOR[™] X3) were calibrated according to the manufacturer's protocol and placed on a Dynamic Load Carriage Simulator manikin. Each system exhibited different characteristics which non-uniformly impacted the evaluated parameters. Both Novel Pliance[®] and XSENSOR[™] X3 demonstrated more suitable load carriage characteristics than Tekscan I-Scan[™]. This study emphasized the need to evaluate pressure measurement systems within their specific application context, the utilization of caution when comparing the output of different pressure systems, and the careful selection of an appropriate pressure measurement system for future studies.

Keywords

Skin contact pressure, load carriage, and pressure measurement

4.1 Introduction

The mechanical interaction between a human and a supported load can lead to substantial levels of skin contact pressure. In addition to discomfort, exceeding safe limits of skin contact pressure can result in tissue deformation and long-term health complications (e.g., rucksack palsy) [1, 46, 47]. Injury and health complications are especially apparent for female load carriage individuals who experience twice the level of risk over males due to differences related to sex [13]. Skin contact pressure is a validated objective predictor of discomfort and injury, thus highly relevant for the assessment of human-load mechanics in diverse applications, including backpacks, exoskeletons, and biomechanical energy harvesters [3-7].

The mechanical loading beneath the shoulder strap appears to be a primary limiter of historical backpack design and functionality for load carriage [1, 9, 13, 36]. Mechanically loading the shoulder region can negatively impact blood flow and entrap sensitive nerves [1, 11, 40]. These challenges were partially addressed in advanced load carriage designs by incorporating rigid frames and hip belts to redistribute load from the shoulders to the hips [48, 69]. The hips were found to be more tolerable to static loading and skin contact pressure measured in the hip region can be used to predict perceived discomfort and injury [4]. Despite successful advances in backpack design, skin contact pressure from backpacks and other torso-borne systems (e.g., body armour) continues to impose substantial physiological strain and exceed critical thresholds to cause health complications [20, 29].

The study of human tolerance has established critical thresholds of skin contact pressure. These thresholds are particularly important beneath the shoulder strap, where a reduction in blood flow can lead to neurological dysfunction and loss of fine motor skills [21, 41, 79]. Classic investigations of hemodynamics revealed almost zero blood flow when skin contact pressure reaches 16 kPa [46], while others identify blood flow reduction from contact pressures ranging from 5.6 to 9.5 kPa based on the location of applied load [47]. More recent application-based scenarios found individuals carrying 12 kg for 10 minutes and 10 kg for 5 minutes showed reduced blood flow beneath the shoulder strap [41, 42]. Given that many individuals who carry heavy occupational loads (e.g., military soldiers and firefighters) are

willing to tolerate a certain degree of irritation, discomfort, and loss of sensory function, measured average and peak contact pressures have been suggested to remain below 20 and 45 kPa, respectively [20].

The distribution of skin contact pressure in load carriage applications has been examined using a combination of methods, including human participants and mechanical simulation techniques [4, 5, 11, 20, 21, 50, 69]. Despite participant-based studies providing valuable subjective insight, they can be labour-intensive and face participants' intra- and inter-variability. Mechanical load carriage simulation was consequently developed to provide a more direct and objective means for comparing the biomechanical properties of alternative load carriage systems [20, 52]. The combination of mechanical simulation and measuring skin contact pressure allows investigators to objectively assess perceived discomfort and risk of injury in an efficient manner [4, 20, 50]. Providing an objective and reliable measure enables a systematic approach to evaluate alternative load carriage designs, load configurations, and user adjustments on anthropometrically designed manikins in a way that is relevant to user safety and comfort [4, 20].

Previous load carriage assessments utilized the Tekscan F-ScanTM pressure measurement system (Tekscan Inc., Norwood, MA, United States) [4, 20, 22, 69]. This system faced challenges of measurement drift and hysteresis [15, 16], followed by sensitivity to surface hardness, loading speed, and operational temperature [17, 18]. These limitations impacted the performance of Tekscan F-ScanTM with measurement errors on a flat surface exceeding 30% and reliability dependent on sensor replacement [19, 58]. To address these limitations, careful calibration procedures [55, 57], experimental control [70, 80], and post-data collection processing [4], have been developed; however, these efforts may be negated by the basic performance of modern skin contact pressure measurement systems.

Newer systems have emerged, including Novel Pliance[®] (Novel GmbH, Munich, Germany), Tekscan I-ScanTM (Tekscan Inc., Norwood, MA, United States), and XSENSORTM X3 (XSENSORTM Technology Corp., Calgary, AB, Canada). These systems were recently evaluated for the effect of absolute error and measurement drift on a flat and semi-circular curved surface (demonstrated in Chapter 3). Results indicated that Novel Pliance[®] exhibited significantly greater accuracy, less measurement drift, and less

sensitivity to surface geometry than the other two systems. Moreover, all three systems experienced significantly less drift as time passed, emphasizing the importance of controlling the time of measure.

Beyond simple geometries, the newer skin contact pressure measurement systems lack the assessment in application. Therefore, this study aimed to assess the practicality and feasibility of using three skin contact pressure measurement systems (Novel Pliance[®], Tekscan I-Scan[™], and XSENSOR[™] X3) in the evaluation of contact pressure exerted beneath the shoulder strap of a common backpack loaded with three different weight configurations while placed onto the average male manikin of the Load Carriage Simulator. The study had two primary objectives:

1. **Between System Effect:** The first objective was to compare three skin contact pressure measurement systems using three backpack payloads to determine if the measured average pressure, peak pressure, and contact area depend on the evaluated system. Because the evaluated systems previously exhibited significantly different absolute errors (demonstrated in Chapter 3), a significant difference in measured average pressure and peak pressure is hypothesized. Because the evaluated systems exhibit a similar spatial resolution of pressure-sensing elements (see Table 4.1), no difference in the measured contact area is hypothesized.
2. **Between-Day Agreement:** The second objective was to determine the level of agreement within each pressure measurement system on different testing days for the same set-up. Based on previous findings of greater reliability exhibited by the systems from Novel and XSENSOR[™] over Tekscan I-Scan[™] [62, 63], it is hypothesized that Novel Pliance[®] and XSENSOR[™] X3 would exhibit stronger agreement between days.

4.2 Methodology

This study evaluated three skin contact pressure measurement systems in a repeated measure counter-balanced study design to determine the agreement in average pressure, peak pressure, and contact area measures across different measurement systems and test days. The evaluation was conducted using load magnitudes of 15, 25, and 35 kg, which were chosen based on the historical assessment of load carriage systems in literature [4, 20, 40].

4.2.1 Skin Contact Pressure Measurement Systems

The three evaluated skin contact pressure measurement systems (Novel Pliance[®], Tekscan I-Scan[™], and XSENSOR[™] X3) were marketed for load carriage applications by their manufacturers. Table 4.1 outlines their characteristics and specifications. Each system is comprised of a tactile sensor, an electronic hub, and computer software. The evaluated sensor models were the S2158 (Novel Pliance[®]; capacitive technology; 5–240 kPa measurable range), 9830 (Tekscan I-Scan[™]; resistive technology; 1–190 kPa measurable range), and LX210 (XSENSOR[™] X3; capacitive technology; 1–221 kPa measurable range); their spatial resolutions were 0.50, 0.46, and 0.62 elements/cm², respectively. Each evaluated sensor was rectangularly shaped with 240 (Novel Pliance[®]; 8 x 30), 176 (Tekscan I-Scan[™]; 16 x 11), and 140 (XSENSOR[™] X3; 10 x 14) elements. The pressure sensing hardware of Novel Pliance[®] and XSENSOR[™] X3 were enclosed with a sensor cover. The electronic units and associated operating software tested were the Pliance[®] XF box and Pliance-x 32 expert SD card v28.38.4 (Novel Pliance[®]), the VersaTek[™] high-speed hub and v7.6 (Tekscan I-Scan[™]), and the professional and v8 (XSENSOR[™] X3).

A Cartesian coordinate system of pressure-sensing elements initially captured the distribution of contact pressure in terms of digital outputs. Calibration of the sensors associates digital outputs with a standard unit of measure (e.g., kilopascals). Manufacturers recommend yearly re-calibration for Novel Pliance[®] and XSENSOR[™] X3, while Tekscan I-Scan[™] requires calibration before each set of experimental trials (e.g., one trial per 15, 25, and 35 kg load). The trublu[®] and PB100C calibration devices were purchased

for use with the Novel Pliance® and Tekscan I-Scan™, respectively. XSENSOR™ does not market a pneumatic device for the evaluated sensors, necessitating in-factory calibration.

Table 4.1 Evaluated pressure measurement system characteristics and specifications.

Characteristic	Skin Contact Pressure Measurement System		
	Novel Pliance®	Tekscan I-Scan™	XSENSOR™ X3
System Hub	Pliance® Box	High-Speed VersaTek™	X3 Pro
Sensor Technology	Capacitive	Resistive	Capacitive
Sensor Model	S2158	9830	LX210
Spatial Resolution	0.50 cm ²	0.46 cm ²	0.62 cm ²
Sensing Elements	8 x 30	16 x 11	10 x 14
Element Dimensions	1.41 x 1.41 cm	1.27 x 1.71 cm	1.27 x 1.27 cm
Analyzed Elements	8 x 13	9 x 10	9 x 14
Calibration Device	trublu®	PB100C	--
Calibration Frequency	Yearly	If idle > 3 hours	Yearly
Calibration Range	5–240 kPa	1–190 kPa	1–221 kPa

4.2.2 Data Collection

A single investigator familiarized themselves with the experimental setup and protocol before beginning data acquisition. Six independent trials were performed for each measurement system (Novel Pliance®, Tekscan I-Scan™, and XSENSOR™ X3) and load condition (15, 25, and 35 kg) while the Load Carriage Simulator operated dynamically. Data acquisition was randomized between systems and collected in a balanced load order. The balanced order consisted of each load (e.g., 15, 25, or 35 kg) collected in the first, second, and third positions twice, totalling six independently collected trials per system and load. Each

trial lasted 22 seconds and operated at a sampling frequency of 40 Hz. The experimental setup is described in the following sections.

4.2.2.1 Dynamic Load Carriage Simulator

The Dynamic Load Carriage Simulator is a specialized biomechanical evaluation tool developed and built by Queen's University (Kingston, ON, Canada) for Defence Research and Development Canada (Toronto, ON, Canada) [20]. This simulator is designed to enable objective, reliable, and efficient assessment of alternative torso-borne load carriage for its impact on the individual's comfort and safety. The simulator comprises a computer-controlled platform that oscillates an anthropometrically representative manikin. The design of the oscillatory motion aims to replicate the sinusoidal (wave-like) vertical movement of an individual's centre of mass during walking, with a range of approximately ± 2.5 cm. A custom program, called Overseer Mark II, controls both the motion of the simulator and the acquisition of data during the evaluation.

In this experiment, the Dynamic Load Carriage Simulator employed a third-generation manikin (Figure 4.1) designed to represent the average male in combat arms for the Canadian Army. The manikin's anthropometrics were derived from the 2012 Canadian Forces Anthropometric Survey [81]. The skin contact pressure measurement systems were evaluated using the average male to provide a baseline consistent with past research [3, 50], and establish the groundwork for examination and comparison with future manikins of the female population. The surface of all third-generation manikins is covered with a 4 mm thick skin analogue, called Bocklite™ (#617S1=H4, Ottobock, Duderstadt, Germany). Bocklite™ is a polyethylene closed-cell foam, that is characterized by a Shore A hardness rating of 30. The load carriage system, as discussed in Section 4.2.2.3, directly interfaced with the average male manikin's Bocklite™. The average male manikin remained unclothed to simplify experimental control and generate more relevant results for civilian backpacks.

4.2.2.2 Pressure Sensor Preparation and Placement

The Novel Pliance® and Tekscan I-Scan™ pressure sensors were prepared by a single investigator in a climate-controlled laboratory following guidelines found in the respective user manuals and calibration procedures [72, 73]. After sensor preparation, the sensors were placed symmetrically on the manikin to capture pressure beneath the backpack shoulder straps (Figure 4.1). Precise position and orientation of sensor placement were replicated between test sessions using identifiers on the manikin surface. To maintain placement during experimentation, each sensor was secured in place using 3M™ Micropore™ medical tape (1530S-1, Saint Paul, MN, United States). Where possible, tape was sparingly applied to non-active portions of the sensor to mitigate bi-directional bending during data collection.

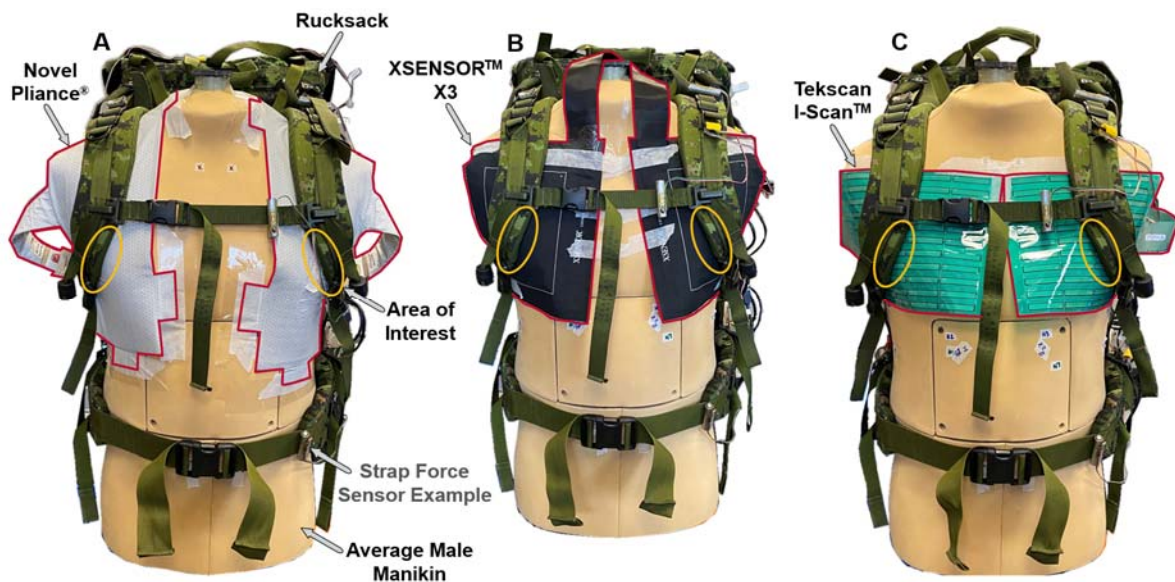


Figure 4.1 Experimental setup of pressure sensors. Sensor placement of Novel Pliance® (A), XSENSOR™ X3 (B), and Tekscan I-Scan™ (C) with the Canadian Army Cloth the Soldier rucksack placed onto the Load Carriage Simulator manikin.

4.2.2.3 Load Carriage System Setup

One backpack exerted pressure for the evaluation of skin contact pressure measurement systems: the Cloth the Soldier rucksack (National Stock Number [NSN]:8465-20-001-3172, FELLAB® Ltd.,

Hamilton, Canada) [82]. Selected according to the manikin anthropometrics was the medium-sized rucksack equipped with medium-sized shoulder straps (NSN: 8465-20-001-3187, FELLLAB[®] Ltd., Hamilton, Canada) and a medium-sized hip belt (NSN: 8465-20-001-3183, FELLLAB[®] Ltd., Hamilton, Canada). The backpack has a capacity of 85 litres. The main backpack compartment was loaded in three load configurations weighing 15, 25, or 35 kg, as shown in Figure 4.2. The load comprised a combination of light (polystyrene) and heavy (golf balls) elements to position the pack's centre of mass in the middle of the packable volume for each weight. Once loaded, the pack side compression straps were tightened. No additional loads were placed in pockets, pouches, fanny packs or detachable accessories to minimize experimental variability.

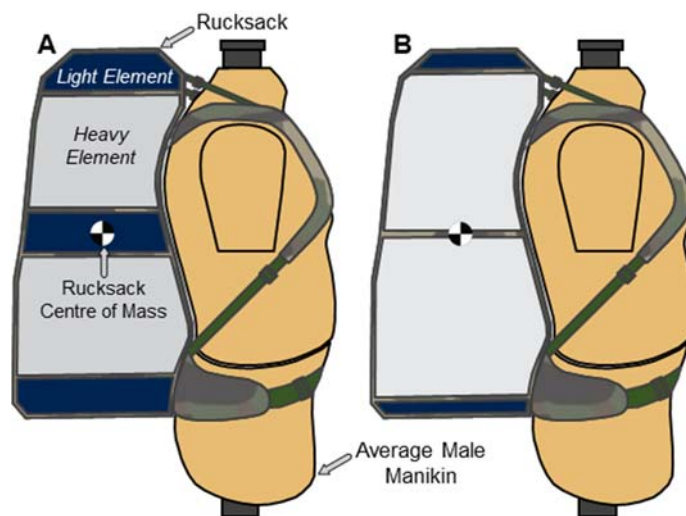


Figure 4.2 Load distribution. The 15 kg (A) and 35 kg (B) load distribution within the backpack, while placed on the average male manikin.

Consistency of backpack fit was executed through several steps. One of these steps included the adjustment of strap tension. Adjustable straps on the backpack included the shoulder straps, waist belt, chest strap, and load lifters. Fitted on these straps were tension-measuring sensors developed at Queen's University [83]. The tension-measuring sensors were calibrated up to 199 N in laboratory using an apparatus that simulated the experimental setup. A zero measurement was recorded upon sensor installation.

Placed at the head location of the manikin was a digital inclinometer (WR300-TY2, Barry Wixey Development, United States). The forward inclination of the manikin was set to $0^\circ \pm 0.2^\circ$ before the backpack was positioned. Using a hydraulic hoist, the backpack was lifted and became fully supported by the manikin through strap securement. The forward inclination of the manikin was adjusted to the experimental condition of $10^\circ \pm 0.2^\circ$ (Figure 4.3).

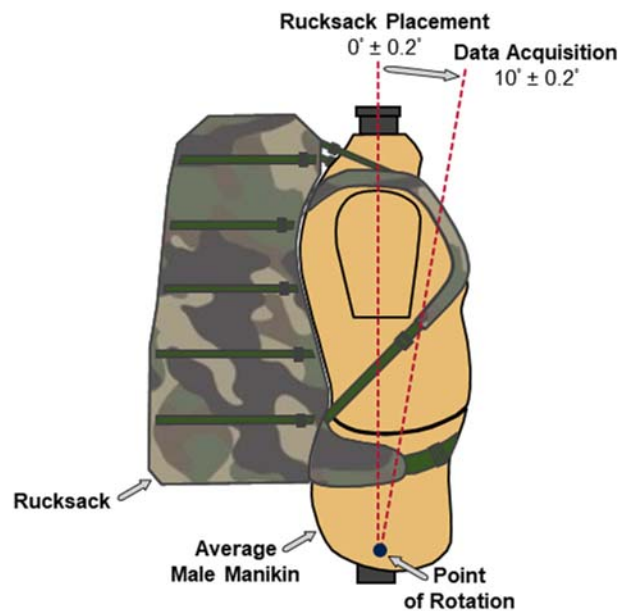


Figure 4.3 Experimental setup control. The backpack was placed onto the manikin at $0^\circ \pm 0.2^\circ$ and set to $10^\circ \pm 0.2^\circ$ for data acquisition.

An example strap force sensor is shown in Figure 4.1 and initial strap force tensions were defined per load magnitude in Figure 4.4. Initial tensions were derived from literature where possible (e.g., identical load configuration) [20] and adjusted linearly according to the carried load (e.g., 15, 25, or 35 kg). Straps were tensioned sequentially in the order of shoulders, waist, chest, and load lifters. The sequence was restarted in cases of initial tension deviation while adjusting succeeding straps. Acceptable tensions beyond desired were within ± 5 N, as drawn from the literature [20].

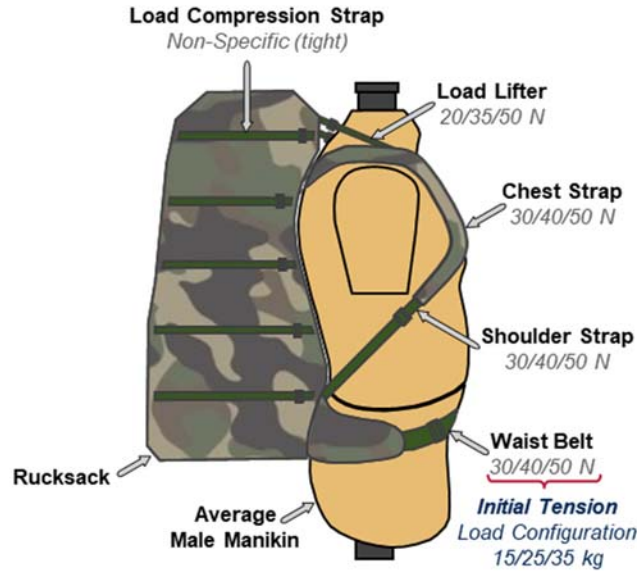


Figure 4.4 Location and tension of strap force sensor. Location and initial tension of strap force sensors attached to the backpack load lifters, chest strap, shoulder straps, and waist belt per load (15, 25, and 35 kg). Backpack compression straps were tensioned until tight.

To stabilize the generated load onto the pressure sensor, the Load Carriage Simulator was operated dynamically at a gait frequency of 1.8 Hz for a duration of 60 seconds. This action reduced frictional forces existing between the contacts of the backpack and the manikin. The strap tensions were reviewed and adjusted to the initial values, where necessary, upon return to the static state. Repeatable static and dynamic strap force measurements were achieved after an initial definition, dynamic operation and static check.

4.2.3 Data Analysis

The output data of each system were imported into a custom MATLAB (R2020B, The MathWorks Inc., Natick, Massachusetts, United States) script. In this script, the output data were structured into a matrix format with rows and columns representing physical pressure-sensing elements for each frame of data collected. To ensure consistency and comparability, a specific region of pressure-sensing elements was defined per system (see analyzed elements in Table 4.1), based on the sensor that individually limited the measurable area in terms of length (XSENSOR™ X3) and width (Novel Pliance®). Any pressure

measurements outside of this desired region were excluded from the analysis. The desired region was symmetric about the sagittal plane.

After extracting measurements from the defined region of each frame, the number of active elements and their corresponding numerical values were collected. An active element was defined as a measured pressure exceeding the highest activation threshold specified for the evaluated systems. While it was possible to reduce the activation threshold of Novel Pliance® using their calibration software, doing so would have contradicted the manufacturer's recommendation and the advertised measurable range.

The evaluation measures, including average pressure, peak pressure, and contact area, were computed for each data frame. Average pressure was calculated as the mean of the previously identified pressure-sensing elements (those with measurements greater than 5 kPa). Peak pressure represents the highest recorded pressure value from the identified elements. The contact area was calculated by multiplying the number of active elements for each frame by their corresponding element dimension, as specified in Table 4.1.

The calculated average pressure, peak pressure, and contact area for each frame were then divided into cycles per trial, based on the sinusoidal motion of the Dynamic Load Carriage Simulator. The 880 frames collected per trial were divided into 40 cycles of gait, corresponding to the 1.8 Hz frequency. An average pressure, overall peak pressure, and average contact area were calculated for each cycle. Finally, a grand average pressure, average peak pressure, and grand average contact area were computed.

4.2.4 Statistical Analysis

Mean and standard deviation were calculated for each system (Novel Pliance®, Tekscan I-Scan™, and XSENSOR™ X3) and load (15, 25, and 35 kg) condition. Average pressure, peak pressure, and contact area were individually compared per load using a one-way analysis of variance (ANOVA). If the omnibus ANOVA revealed a significant effect, the difference between conditions was compared using Tukey's honest significant difference (HSD) or Games-Howell as *post hoc* analyses. The Shapiro-Wilks (S-W) test verified the assumption of normality; however, violations remained uncorrected as an ANOVA is robust to

this violation [74]. Moreover, Levene's test verified the assumption of homogeneity of variance, where violations were corrected using the Satterthwaite adjustment for degrees of freedom [75], and the Cochran-Cox adjustment for the standard error estimate [76], as Welch's correction.

A combination of statistical analyses was used to assess the between-day agreement (day #1–2) for average pressure, peak pressure, and contact area. Normality was assessed using the S-W test. For normally distributed data, a one-sample two-tailed t-test with a comparator of zero was conducted to determine the agreement. In cases of normality violation, a one-sample two-tailed Wilcoxon Signed-Ranks test was conducted, with a comparator of zero. The Bland-Altman method was conducted to assess between-day agreement, providing 95% limits of agreement (LoA) as a measure of variability [84]. Bias between days was reported as fixed, where the means of one day give constantly higher measures than the other, or proportional, where a difference between days resulted in an increase or decrease in proportion to the average value [85]. All statistical analyses were performed using SPSS (V28, IBM Corp., USA), with a significance criterion set to $\alpha = 0.05$.

4.3 Results

Figure 4.5A illustrates the average pressure per system (mean \pm standard deviation). The one-way ANOVA conducted on average pressure revealed a significant effect for all load conditions (at 15 and 35 kg: all $F_{(2.00,15.00)}$ -values > 4.736 , all p -values < 0.025 ; at 25 kg: Welch's $F_{(2.00,7.98)} = 14.461$, p -value = 0.002). *Post hoc* tests revealed significant differences between XSENSOR™ X3 and Novel Pliance® (mean difference \pm standard error: 2.5 ± 0.7 kPa), as well as XSENSOR™ X3 and Tekscan I-Scan™ (3.0 ± 0.7 kPa) at 15 kg load. Similarly, Novel Pliance® and XSENSOR™ X3 differed significantly at 25 kg load (3.7 ± 0.7 kPa) and Novel Pliance® and Tekscan I-Scan™ at 35 kg load (2.7 ± 1.0 kPa). Furthermore, Figure 4.5B illustrates the peak pressure per system, where no effect was revealed by the one-way ANOVA.

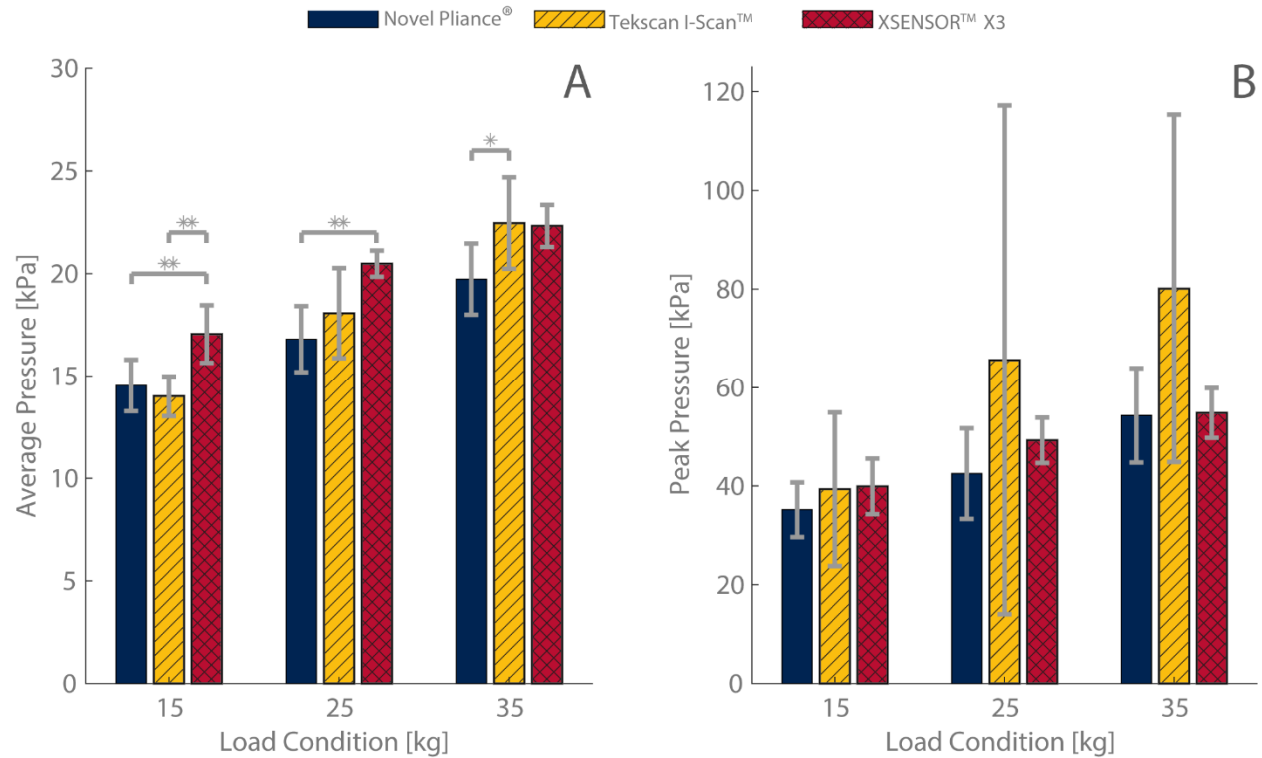


Figure 4.5 Measured average and peak pressure. Mean and standard deviation of average (A) and peak (B) pressure per system (Novel Pliance®, Tekscan I-Scan™, and XSENSOR™ X3) and load (15, 25, and 35 kg).

The area of contact is illustrated in Figure 4.6. The one-way ANOVA conducted on the contact area revealed a significant effect at 25 and 35 kg load (*all* $F_{(2,00,15,00)}$ -values > 7.771 , *all* p -values < 0.005), while no difference at 15 kg load ($F_{(2,00,15,00)} = 2.897$, $p = 0.086$). *Post hoc* analysis of conditions with significant effects revealed a significant difference between Novel Pliance® and Tekscan I-Scan™ at 25 kg (mean difference \pm standard error: 18.5 ± 4.7 cm²) and 35 kg (18.1 ± 4.1 cm²) load.

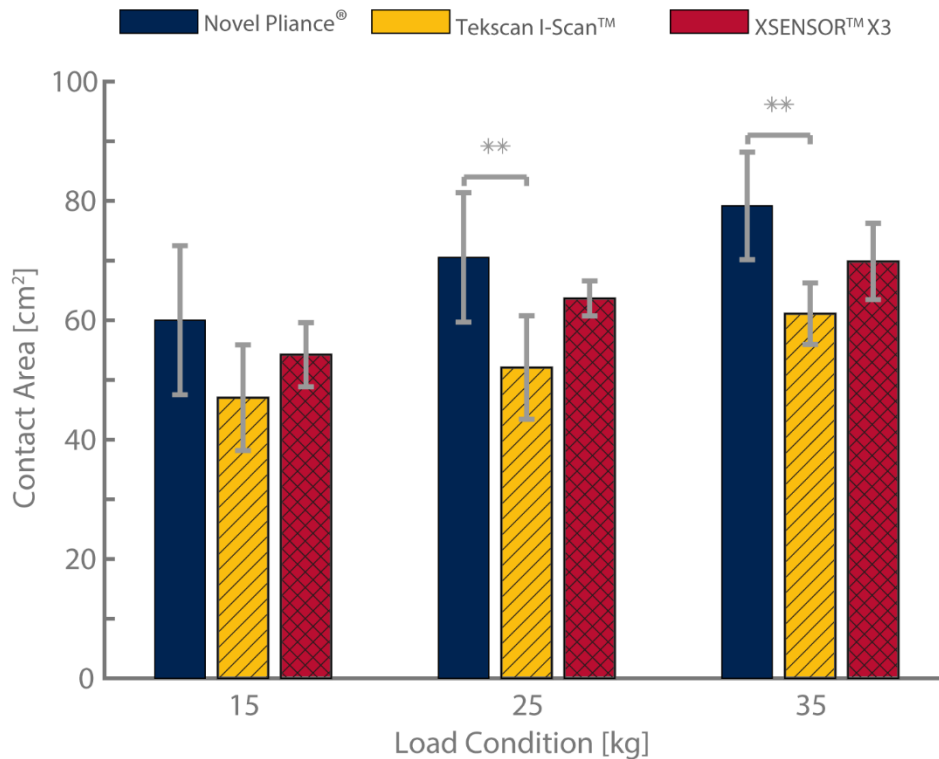


Figure 4.6 Measured contact area. Mean and standard deviation of measured contact area per system (Novel Pliance®, Tekscan I-Scan™, and XSENSOR™ X3) and load (15, 25, and 35 kg).

4.3.1 Between Day Agreement

Illustrated in Figure 4.7 is the mean and standard deviation of average pressure, peak pressure, and contact area differences (day #1-2) measured by Novel Pliance®, Tekscan I-Scan™, and XSENSOR™ X3. One-sample two-tailed t-tests revealed that Novel Pliance® measured a significant difference in average pressure at the 15 kg load between days (t -test: $t_{(2,00)} = 6.189$, $p = 0.025$; Figure 4.7A), while there was no significant difference in average pressure at 25 and 35 kg (t -test: all $t_{(2,00)}$ -values < 1.465 , all p -values > 0.280 ; Figure 4.7A). Additionally, there was no significant difference in peak pressure at all loads (t -test: all $t_{(2,00)}$ -values < 3.417 , all p -values > 0.076 ; Figure 4.7D), and no significant difference in contact area at all loads (t -test: all $t_{(2,00)}$ -values < 1.070 , all p -values > 0.397 ; Figure 4.7G). There was a significant proportional bias in average pressure by Novel Pliance® (t -test: $t_{(8,00)} = 2.841$, $p = 0.022$, slope: -0.3, intercept: 6.1; Figure 4.8A), while a non-significant proportional bias in peak pressure (t -test: $t_{(8,00)} = -1.587$,

$p = 0.151$, slope: -0.4, intercept: 11.8; Figure 4.8D) and contact area (t -test: $t_{(8,00)} = 1.175$, $p = 0.274$, slope: 0.3, intercept: -14.0; Figure 4.8G). The upper and lower limits were 5.1 and -1.8 kPa, 17.0 and -29.5 kPa, and 41.6 and -27.7 cm² for average pressure, peak pressure, and contact area, respectively.

One-sample statistical analyses revealed a significant difference in contact area measured by Tekscan I-Scan™ for all load conditions (t -test: all $t_{(2,00)}$ -values > 8.348 , all p -values < 0.014 ; Figure 4.7H), while there was no significant difference in average (t -test: all $t_{(2,00)}$ -values < 0.418 , all p -values > 0.717 ; Figure 4.7B) and peak (t -test at 15 and 25 kg: all $t_{(2,00)}$ -values < 2.148 , all p -values > 0.165 ; Wilcoxon Signed-Ranks test at 35 kg: $Z = -1.604$, $p = 0.109$; Figure 4.7E) pressure at all load conditions. Tekscan I-Scan exhibited a significant proportional bias for contact area (t -test: $t_{(8,00)} = 9.774$, $p < 0.001$, slope: -0.4, intercept: -34.6; Figure 4.8H), while there was a non-significant proportional bias for average (t -test: $t_{(8,00)} = -0.222$, $p = 0.830$, slope: -0.2, intercept: 3.3; Figure 4.8B) and peak (Wilcoxon Signed-Ranked test: $Z = -1.718$, $p = 0.086$, slope: -0.8, intercept: 23.9; Figure 4.8E) pressure. The upper and lower limits were 4.5 and -4.9 kPa, 59.5 and -104.5 kPa, and 19.6 and 4.9 cm² for average pressure, peak pressure, and contact area, respectively.

One-sample statistical analyses revealed no significant difference in average pressure (t -test: all $t_{(2,00)}$ -values < 2.857 , all p -values > 0.104 ; Figure 4.7C), peak pressure (Wilcoxon Signed-Ranks test at 15 kg: $Z = 1.069$, $p = 0.285$; t -test at 25 and 35 kg: all $t_{(2,00)}$ -values < 0.673 , all p -values > 0.570 ; Figure 4.7F), and contact area (t -test: all $t_{(2,00)}$ -values < 1.171 , all p -values > 0.362 ; Figure 4.7I) measured by XSENSOR™ X3. XSENSOR™ X3 exhibited a significant proportional bias in average pressure (t -test: $t_{(8,00)} = 3.035$, $p = 0.016$, slope: -0.1, intercept: 2.6; Figure 4.8C), while there was a non-significant proportional bias in peak pressure (Wilcoxon Signed-Ranks test: $Z = 1.125$, $p = 0.260$, slope: -0.3, intercept: 15.7; Figure 4.8F) and non-significant fixed bias in contact area (t -test: $t_{(8,00)} = 1.183$, $p = 0.271$, slope: 0.0, intercept: 0.0; Figure 4.8I). The upper and lower limits were 2.8 and -0.9 kPa, 18.7 and -11.7 kPa, and 18.1 and -12.1 cm² for average pressure, peak pressure, and contact area, respectively.

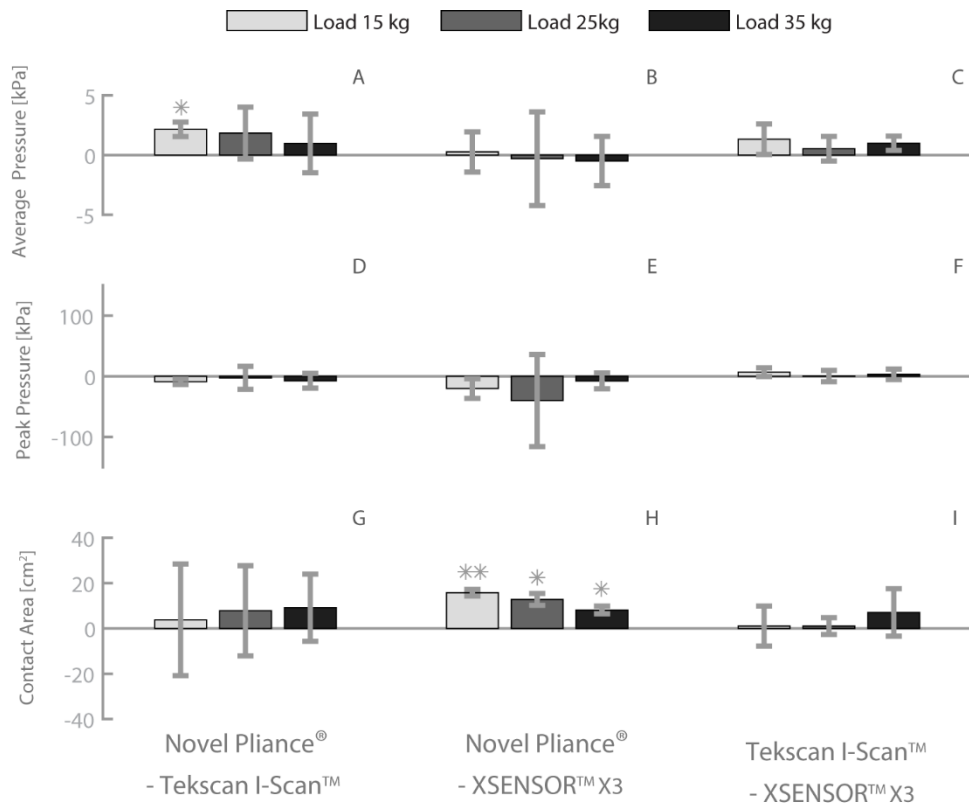


Figure 4.7 Between-Day Differences. The between-day differences of average pressure (A-C), peak pressure (D-F), and area of contact (G-I) as measured by Novel Pliance® (A, D, G), Tekscan I-Scan™ (B, E, H), and XSENSOR™ X3 (C, F, I) when measured at backpack external loads of 15, 25, and 35 kg. * *p*-value < 0.05, ** *p*-value < 0.01.

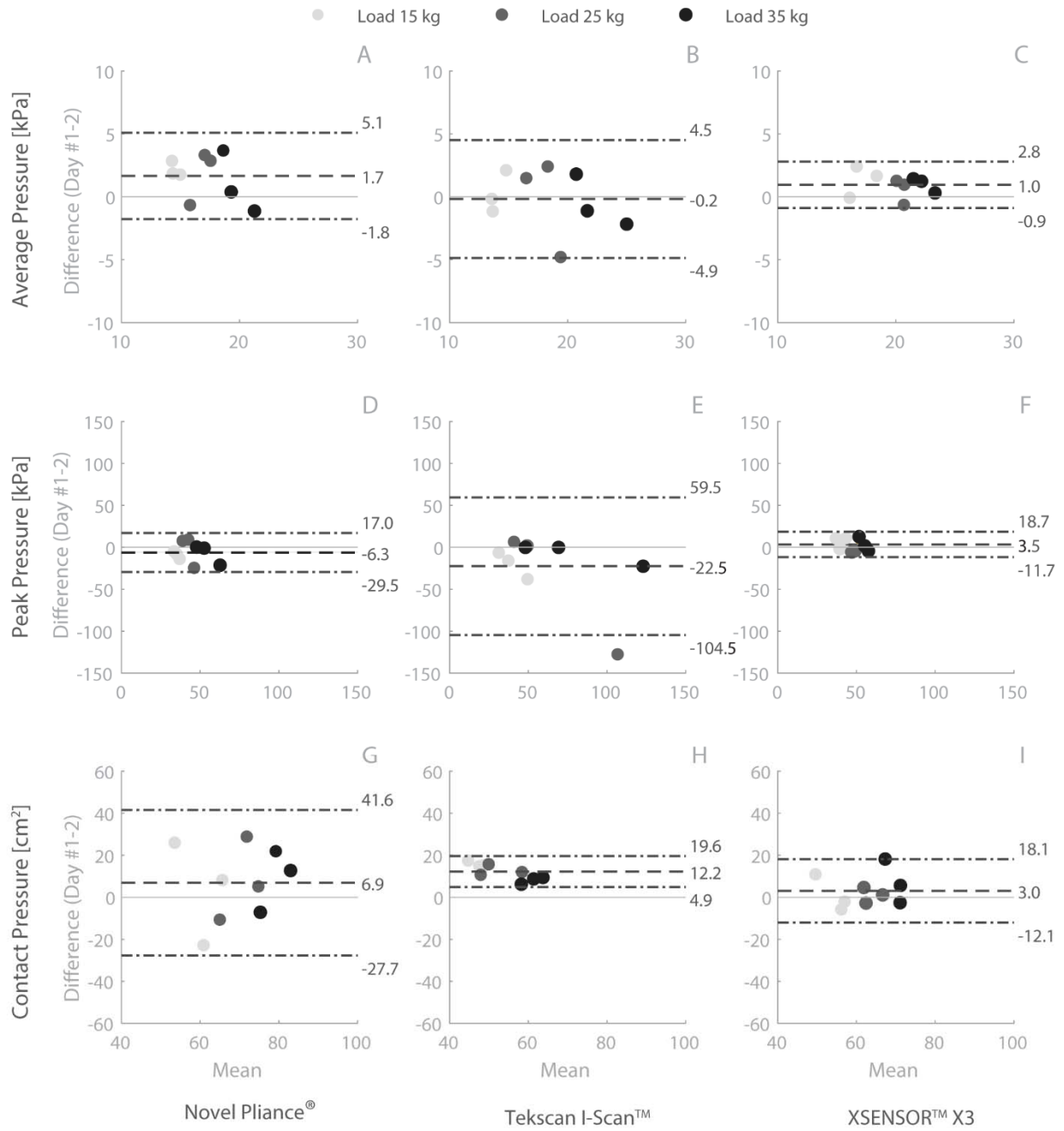


Figure 4.8 Between day Bland-Altman. Bland Altman plot comparing days of average pressure (A-C), peak pressure (D-F), and contact area (G-I) for Novel Pliance® (A, D, and G), Tekscan I-Scan™ (B, E, and H), and XSENSOR™ X3 (C, F, and I). Dashed grey line: mean difference, and dashed-dot grey line: 95% upper and lower limits of agreement.

4.4 Discussion

This study assessed the effect of system (Novel Pliance[®], Tekscan I-Scan[™], and XSENSOR[™] X3) on average pressure, peak pressure, and contact area with three backpack loads (15, 25, and 35 kg). In the field of load carriage, average and peak pressure hold particular significance since they assist in identifying human tolerances and help determine the risk of ischemia [3, 4, 21]. Moreover, the contact area is an important criterion while evaluating skin contact pressure measurement systems, as contact pressure can be defined as the force applied over a given area. This study aimed to provide researchers with valuable performance insight into the three skin contact pressure measurement systems. By comparing average pressure, peak pressure and contact area across different systems, backpack loads, and measurement days, this research aims to enhance the understanding of system capabilities and limitations in a real-world application.

Figure 4.5A illustrates no between-system performance consistency for average pressure. Although a significant effect was observed across load conditions, only a limited number of between-system comparisons reached significance. Since the performance of absolute error was significantly different between the evaluated systems (demonstrated in Chapter 3), the number of significant between-system comparisons was fewer than anticipated in the current study. Under the application conditions, this finding suggests that the evaluation of average pressure is not uniformly impacted by the selection of a single system. Moreover, each system demonstrated clinical significance by operating approximately within the recommended average pressure threshold to alleviate irritation, discomfort, and pain [20].

Among the significant average pressure differences, it was unsurprising that measurements between Novel Pliance[®] and XSENSOR[™] X3 exhibited more significant differences due to their absolute error performance (demonstrated in Chapter 3). The least difference was observed with Tekscan I-Scan[™], consistent with its absolute error falling between Novel Pliance[®] and XSENSOR[™] X3 (demonstrated in Chapter 3). These outcomes suggest that factors beyond the calculation of average pressure, such as sensing

technology, calibration processes, and sensor material properties, may also influence system selection in a particular application.

In contrast to average pressure, peak pressure demonstrated consistent performance across the evaluated systems. This would suggest that the selection of a single system is clinically insignificant in terms of peak pressure under the evaluated conditions. Despite Novel Pliance[®] consistently measuring smaller peak pressures than both Tekscan I-Scan[™] and XSENSOR[™] X3, statistical analyses revealed no significant difference. Figure 4.5B illustrates the lack of difference between the two capacitive-based systems, while Tekscan I-Scan[™] exhibited elevated deviation and greater peak measures. These characteristics suggest that Tekscan I-Scan[™] was application-challenged, as in agreement with previous load carriage studies [58]. Given potential wear-related challenges arising from dynamic repetitive loading, frequent and careful sensor calibration was undertaken for Tekscan I-Scan[™] to account for the loss of sensitivity [55, 57, 80]. Nevertheless, these precautions were illustrated as ineffective. Future investigations may consider frequent sensor replacement along with calibration if using Tekscan I-Scan[™].

Contact area revealed a similar outcome to average pressure, with a between-system effect at 25 and 35 kg load and few significant pairwise comparisons (Figure 4.6). Despite the hypothesis of no difference between systems based on the element spatial resolution (see Table 2.1), Novel Pliance[®] and Tekscan I-Scan[™] were significantly different at both 25 and 35 kg load. This finding is likely attributed to the design of the 9830 sensor, which can be characterized by large inactive areas encasing a small region that measures load per element. Given this large inactivity, the sensor may become less sensitive to partial loading as the inactive area assumes constant load with the small active region. In contrast, the elements of both Novel Pliance[®] and XSENSOR[™] X3 consist entirely of an active area, providing an advantage in measuring contact area.

Between-day differences per system and load are illustrated in Figure 4.7. Of these differences, Novel Pliance[®] was notable for a significant difference in average pressure at 15 kg. This difference may be a combination of many factors that affect pressure systems, encompassing dynamic load sensitivity,

measurement noise susceptibility, and non-linear behaviour recorded at lighter load conditions. Beyond pressure system-related factors, potential uncertainty can be attributed to the setup and placement of the sensor, strap force tensioning conditions, and the packing of load within the backpack. All these factors emphasize the importance of application-based evaluation across diverse conditions. Furthermore, Tekscan I-Scan™ displayed significant differences in contact area across the load conditions, indicating a change in sensor behaviour between measurement days. A positive bias in Figure 4.8H suggests reduced sensitivity on day #2 for Tekscan I-Scan™, thereby emphasizing the necessity for frequent sensor calibration and limiting the number of collected trials per sensor to maintain performance. It further highlights the importance of quality control measures in real-world applications, such as clinical assessments and research studies.

Contrary to the initial hypothesis based on literature [62, 63], Tekscan I-Scan™ exhibited the smallest proportional bias and greater LoA for between-day average pressure. Moreover, Novel Pliance® and XSENSOR™ X3 demonstrated stronger agreement on peak pressure and contact area based on the magnitude of proportional bias. These findings highlight the complexity of pressure system evaluation and emphasize the necessity to thoroughly assess system performance to understand its output in real-world scenarios. Future investigations may consider the collection of additional trials to strengthen the shown results.

4.4.1 Limitations

Differences in calibration processes can influence the overall performance and agreement of skin contact pressure measurement systems. Novel Pliance® employs pressure as an input parameter (measured in kilopascals), while Tekscan I-Scan™ relies on force (measured in Newtons). Additionally, Tekscan I-Scan™ applies a single calibration curve that assumes the uniformity of element characteristics, whereas Novel Pliance® captures unique element differences through individual curves per pressure-sensing element. Furthermore, recorded pressures in the current study spanned less than the measurable ranges.

Given the quantity limitation of digital outputs, reducing the maximum measurable pressure would enhance measurable resolution. As previously recommended, the preparation of pressure sensors should closely resemble the experimental conditions [17, 55]. In contrast, limited calibration information is provided by the manufacturer of XSENSOR™ X3 since they perform in-factory calibration.

The outcome measures in this study were influenced by several factors, encompassing manikin anthropometrics and sex, the equipment carried by the load carriage individual, gait frequency, and the degree of forward lean exhibited by the manikin. These variables had no gold standard associated with pressure system evaluation. Additionally, the study exclusively focused on pressures induced within the axilla region. To comprehensively enhance the understanding of system performance in load carriage scenarios, further investigations may expand the evaluated conditions to incorporate different contact sites, populations, activities, and load carriage styles. Another consideration recognizes that the manikin offers a simplified approximation of human tissue compliance, conducting experiments alongside human participants could improve manikin validity. Lastly, evaluating skin contact pressure measurement systems in real-world applications introduces inherent uncertainty in terms of the repeatability of experimental conditions. Despite undertaking comprehensive experimental control, uncertainty regarding the experimental setup and evaluation may potentially exist.

4.5 Conclusion

The effect and agreement of pressure systems on average pressure, peak pressure, and contact area measurements in the load carriage context were investigated. The selection of a single system was non-uniformly impacted by the evaluated parameters. While each system exhibited unique characteristics, Novel Pliance® and XSENSOR™ X3 demonstrated more suitable performance. Tekscan I-Scan™ remained challenged in the load carriage application. This study highlights several important considerations: (a) the need to evaluate skin contact pressure measurement systems with the specific context of their application to understand their response and characteristics; (b) the reiteration of caution when comparing output

measures from different skin contact pressure measurement systems; and (c) the importance of careful considerations in selecting an appropriate pressure system for future studies.

4.6 Funding

This work was supported by the Canadian Institute for Military and Veterans' Health Research contract #W7714-145967/ 001/SV/Task 49 for Defence Research and Development Canada.

4.7 Declaration of Competing Interest

The authors declare that they have no known competing financial interests or personal relationships that could have appeared to influence the work reported in this paper.

4.8 Supporting Information

Data files including metadata and results of statistical analyses are included in Appendix A.

Chapter 5

Conclusions and Future Work

The biomechanical evaluation of skin contact pressure has been widely adopted in the assessment of load carriage design and performance [4, 20, 68]. Objective skin contact pressure measurements are captured in load carriage studies as the carried load directly interfaces with the individual's trunk and measures can be related to limits of human tolerance [4, 21, 22]. While different limits of human tolerance exist based on the location of loading, magnitude of pressure, and duration of application, all investigations suggest the reduction of contact pressure to mitigate health complications [41, 42, 46, 47]. With understanding the importance of capturing skin contact pressure, the optimization of load carriage systems is possible with the use of a skin contact pressure measurement system.

The interface of contact pressure in the application of load carriage has been extensively measured using the Tekscan F-Scan™ skin pressure measurement system in both human participant and mechanical simulation-based studies [4, 20-22, 50]. Despite the longstanding standard of using Tekscan F-Scan™ in load carriage investigations, the system faced challenges to its validity and reliability [19, 57]. Evaluations of Tekscan F-Scan™ exhibited measurement errors as high as 30% in simplistic geometric conditions [19].

The challenges of Tekscan F-Scan™ were addressed with the development of newer skin contact pressure measurement systems (Novel Pliance®, Tekscan I-Scan™, and XSENSOR™ X3). Despite Tekscan F-Scan™ being extensively evaluated [17-19, 58], limited literature is available on the evaluation of the new skin contact pressure measurement systems to confidently extend their findings into the load carriage application [59-61]. Therefore, this work aimed to evaluate three modern skin contact pressure measurement systems across two surface geometries and five applied loads. This work further aimed to evaluate the same three skin contact pressure measurement systems for effect between systems and agreement between testing days while implemented into a realistic condition of load carriage research. The

technical specifications and information gained from these studies assist in the selection of a system for its use in subsequent load carriage investigations.

5.1 Effect of System, Surface Geometry, and Load on the Measure of Contact Pressure

The skin contact pressure measurement systems of Novel Pliance[®], Tekscan I-Scan[™], and XSENSOR[™] X3 were evaluated to determine the effect of system, surface geometry, and applied load on the measure of absolute error and drift rate. The five applied loads were 30, 45, 60, 75 and 90 kPa and the two surface geometries were flat and semi-circular curved.

Without the division of surface or load, absolute error depended on the specific system which captured the contact pressure. The significant difference suggests that these systems are non-interchangeable, particularly when absolute error is considered. A ranking of absolute error performance was established from least to greatest magnitude: Novel Pliance[®], Tekscan I-Scan[™], and XSENSOR[™] X3. Next, without the division of load, only Novel Pliance[®] showed no difference in absolute error between surface conditions, indicating minimal impact on absolute error performance. Among systems exhibiting surface significance, XSENSOR[™] X3 showed greater susceptibility to surface geometry compared to Tekscan I-Scan[™], as indicated by the magnitude of the mean difference between surface conditions. Moreover, both Tekscan I-Scan[™] and XSENSOR[™] X3 measured significantly less absolute error on a flat than curved surface. Lastly, XSENSOR[™] X3 on a flat surface measured no difference in absolute error, while significant differences were discovered between load conditions of XSENSOR[™] X3 on a curved surface and Tekscan I-Scan[™] on a flat and curved surface. Given that Novel Pliance[®] revealed no difference in surface geometry, further statistical analysis of load was unnecessary.

Without the division of surface or load, the drift rate also depended on the specific system which captured the contact pressure. Similarly to absolute error, the evaluated systems proved to be non-interchangeable as indicated by the statistically different drift rates. A performance ranking of drift rate from least to the greatest rate of change is as follows: Novel Pliance[®], XSENSOR[™] X3, and Tekscan I-

ScanTM. Next, without the division of load, the drift rate of each system depended on the surface condition. The difference between surface conditions for each system indicates that significantly less drift was measured on a flat than semi-circular curved surface. Novel Pliance[®] demonstrated the least impact of surface on drift rate based on the mean differences for the rate of change. Lastly, the drift rate exhibited a significant effect on each system and surface condition across the evaluated loads. Interestingly, Tekscan I-ScanTM showed the least impact of drift on the load conditions despite demonstrating the greatest magnitudes. Additionally, Novel Pliance[®] exhibited a negative drift rate at 30 kPa for both surface conditions, whereas all other system, surface and load conditions exhibited a positive drift rate.

Without the division of surface or load condition, the drift rate differed significantly between the time intervals of 3–12, 12–21, and 21–30 minutes for all systems. Additionally, all systems recorded drift rates that significantly lessened over time. Next, without the division of load, drift rates per system and surface differed across the time intervals of 3–12, 12–21, and 21–30 minutes, with all systems on both a flat and semi-circular curved surface significantly lessened over time. Lastly, drift rate significantly differed across the time intervals of 3–12, 12–21, and 21–30 minutes except for Novel Pliance[®] on a curved surface and XSENSORTM X3 on a flat surface at 30 kPa load. All other systems, surfaces and load conditions exhibited a significant effect of time on drift rate. This difference over time emphasizes the importance of controlling time in load carriage investigations.

5.2 Contact pressure on the Dynamic Load Carriage Simulator

This comparative study aimed to investigate the practicality and feasibility of three skin contact pressure measurement systems (Novel Pliance[®], Tekscan I-ScanTM, and XSENSORTM X3) while implemented onto the Dynamic Load Carriage Simulator. This study assessed the agreement in average pressure, peak pressure, and contact area measures across different skin contact pressure measurement systems and evaluation days. The evaluation was conducted using load magnitudes of 15, 25, and 35 kg within the backpack.

The selection of a single pressure measurement system was non-uniformly impacted by the evaluated parameters of average pressure, peak pressure, and contact area. These parameters were extracted from a total of six trials per system and payload. The outcome revealed distinct characteristics per pressure measurement system when applied to the load carriage application on the Dynamic Load Carriage Simulator. Among the three evaluated systems, Novel Pliance[®] and XSENSOR[™] X3 demonstrated more suitable performance than Tekscan I-Scan[™]. While significant differences were observed between the two capacitive-based systems (Novel Pliance[®] and XSENSOR[™] X3), Tekscan I-Scan[™] exhibited greater variability in outcome measures. Despite precautions taken to address the challenges to resistive-based sensors (e.g., sensitivity loss) [55, 57, 80], Tekscan I-Scan[™] exhibited greater variability in data over multiple trials. Furthermore, Novel Pliance[®] and Tekscan I-Scan[™] demonstrated differences in the measured contact area. This outcome was likely influenced by the active region of each pressure sensing element, where Novel Pliance[®] and Tekscan I-Scan[™] would exhibit the most different spatial resolution.

Few significant between-day differences in average pressure, peak pressure, and contact area were observed among the evaluated skin contact pressure measurement systems. Greater measures of average pressure at 15 kg load by Novel Pliance[®] on day #1 could be influenced by numerous system-related factors, including non-linear behaviour at low pressures, susceptibility to noise in an application, and dynamic sensitivity. Furthermore, Tekscan I-Scan[™] measured greater contact area on day #1 for all load conditions, indicating that reduced sensitivity could have occurred on day #2. This outcome emphasizes the necessity for frequent sensor preparation and replacement of Tekscan I-Scan[™] sensors if implemented into load carriage applications.

5.3 Limitations and Outlook

The evaluated pressure sensors were recommended by their respective manufacturer for the load carriage application. Although the surface and simulator evaluations focused on a single sensor type per manufacturer, numerous other commercially available sensor types exist. The chosen sensor type per

manufacturer was selected based on its suitability for measuring skin contact pressure across the shoulder region. Future investigations may explore alternative sensor types for their application in different sex and anatomical regions, such as the hips or upper back of women.

Each pressure sensor was evaluated when it was less than one year in age. Common to pressure sensors of capacitive-based technology is their employment in numerous investigations spanning several years. Alternatively, pressure sensors of resistive-based technology may only be employed for several days. Future studies may examine the long-term performance of the evaluated pressure sensors (e.g., accuracy over weeks or months). Future studies may also characterize the sensor-to-sensor performance when examining pressure sensors of the same model type.

The preparation and calibration of pressure sensors are approached differently by each manufacturer of skin contact pressure measurement systems. While Tekscan I-Scan™ employs a single curve of calibration across the entirety of sensing elements, Novel Pliance® captures the element-to-element variation through individual calibration curves. Future studies may explore the relative advantage of a single sensor calibration against individual element calibration in terms of setup time, hardware, and computation power. Future investigations may also employ the methodology of load application onto a curved surface via the apparatus highlighted in Chapter 3 to account for curved surface geometry.

The pressure sensors were evaluated within controlled laboratory conditions. Future investigations may implement these pressure sensors in participant-based studies, which may experience a dynamic profile of operating temperature and humidity with varying levels of exercise intensity. A possible next step is to examine the implications of temperature and humidity and how environmental factors may influence the performance of the evaluated pressure sensors. Furthermore, the surfaces on which the pressure sensors were evaluated were seamlessly contoured. Pressure sensors implemented in participant-based studies may experience surfaces with multi-faceted contours. Studies in the future may investigate the effects of more complex surfaces and their association with output performance.

A limitation of the simulator study is the exclusive assessment using the average male manikin. The purpose of developing the methodology of pressure measurement system evaluation on the Dynamic Load Carriage Simulator was to improve the design and evaluation of suitable equipment for all individuals who use a load carriage system. Future investigations may examine manikins representing the female Canadian military population, which were recently developed. As such, the interpretation of specific manikin-related results from the current study must await future investigations.

5.4 Conclusion

The results described in this thesis provided insight into the effect of system, surface geometry, and load on the measure of contact pressure. Furthermore, the results outline the effect between systems and agreement between testing days on the measure of contact pressure within the Dynamic Load Carriage Simulator application. This work contributes to the understanding of modern pressure measurement system performance when integrated into load carriage applications. In addition to revealing system performance under simplistic conditions, the present work offers important insight into practical application performance in real-world scenarios. The findings suggest the adoption of a modern pressure system containing measurement confidence, reduced requirements of experimental control, and ensuring measurement stability over time. The system of Novel Pliance[®] demonstrated opportunistic characteristics for future research and development of load carriage system designs.

References

- [1] S. A. Birrell and R. H. Hooper, "Initial subjective load carriage injury data collected with interviews and questionnaires," *Military Medicine*, vol. 172, no. 3, pp. 306-311, 2007, doi: <https://doi.org/10.7205/milmed.172.3.306>.
- [2] S. Golriz and B. Walker, "Can load carriage system weight, design and placement affect pain and discomfort? A systematic review," *Journal of Back and Musculoskeletal Rehabilitation*, vol. 24, no. 1, pp. 1-16, 2011, doi: <https://doi.org/10.3233/BMR-2011-0275>.
- [3] J. M. Stevenson, J. T. Bryant, R. P. Pelot, E. L. Morin, S. A. Reid, and J. B. Doan, "Research and development of an advanced personal load carriage system phases II and III. Section D: Development of acceptance criteria for physical tests of load carriage systems," PWGSC Contract No. W7711-5-7273/001/TOS 1997.
- [4] P. D. Wettenschwiler, S. Lorenzetti, R. Stämpfli, R. M. Rossi, S. J. Ferguson, and S. Annaheim, "Mechanical predictors of discomfort during load carriage," *PLOS One*, vol. 10, no. 11, p. e0142004, 2015, doi: <https://doi.org/10.1371/journal.pone.0142004>.
- [5] G. R. Jones and R. H. Hooper, "The effect of single- or multiple-layered garments on interface pressure measured at the backpack-shoulder interface," *Applied Ergonomics*, vol. 36, no. 1, pp. 79-83, 2005, doi: <https://doi.org/10.1016/j.apergo.2004.07.001>.
- [6] M. Shepertycky, S. Burton, A. Dickson, Y. F. Liu, and Q. Li, "Removing energy with an exoskeleton reduces the metabolic cost of walking," *Science*, vol. 372, no. 6545, pp. 957-960, 2021, doi: <https://doi.org/10.1126/science.aba9947>.

- [7] L. C. Rome, L. Flynn, E. M. Goldman, and T. D. Yoo, "Generating electricity while walking with loads," *Science*, vol. 309, no. 5741, pp. 1725-1728, 2005, doi: <https://doi.org/10.1126/science.1111063>.
- [8] K. M. Simpson, B. J. Munro, and J. R. Steele, "Effect of load mass on posture, heart rate and subjective responses of recreational female hikers to prolonged load carriage," *Applied Ergonomics*, vol. 42, no. 3, pp. 403-410, 2011, doi: <https://doi.org/10.1016/j.apergo.2010.08.018>.
- [9] J. J. Knapik, K. L. Reynolds, and E. Harman, "Soldier load carriage: historical, physiological, biomechanical, and medical aspects," *Military Medicine*, vol. 169, no. 1, pp. 45-56, 2004, doi: <https://doi.org/10.7205/milmed.169.1.45>.
- [10] M. Perrone, R. Orr, W. Hing, N. Milne, and R. Pope, "The impact of backpack loads on school children: a critical narrative review," *International Journal of Environmental Research and Public Health*, vol. 15, no. 11, p. 2529, 2018, doi: <https://doi.org/10.3390/ijerph15112529>.
- [11] M. Holewijn, "Physiological strain due to load carrying," *European Journal of Applied Physiology and Occupational Physiology*, vol. 61, pp. 237-245, 1990, doi: <https://doi.org/10.1007/bf00357606>.
- [12] J. Martin and R. H. Hooper, "Military load carriage: a novel method of interface pressure analysis," Defence Technical Information Center, ADP011005, 2001.
- [13] R. M. Orr and R. Pope, "Gender differences in load carriage injuries of Australian army soldiers," *BMC Musculoskeletal Disorders*, vol. 17, no. 488, 2016, doi: <https://doi.org/10.1186/s12891-016-1340-0>.

- [14] R. Wendland, L. Bossi, and M. Oliver, "Biomechanical and physiological effects of female soldier load carriage: A scoping review," *Applied Ergonomics*, vol. 105, p. 103837, 2022, doi: <https://doi.org/10.1016/j.apergo.2022.103837>.
- [15] A. A. Polliack, R. C. Sieh, D. D. Craig, S. Landsberger, D. R. McNeil, and E. Ayyappa, "Scientific validation of two commercial pressure sensor systems for prosthetic socket fit," *Prosthetics and Orthotics International*, vol. 24, no. 1, pp. 63-73, 2000, doi: <https://doi.org/10.1080/03093640008726523>.
- [16] J. Woodburn and P. S. Helliwell, "Observations on the F-Scan in-shoe pressure measuring system," *Clinical Biomechanics*, vol. 11, no. 5, pp. 301-304, 1996, doi: [https://doi.org/10.1016/0268-0033\(95\)00071-2](https://doi.org/10.1016/0268-0033(95)00071-2).
- [17] Z. P. Luo, L. J. Berglund, and K. N. An, "Validation of F-Scan pressure sensor system: a technical note," *Journal of Rehabilitation Research and Development*, vol. 35, no. 2, pp. 186-91, 1998.
- [18] T. Sumiya, Y. Suzuki, T. Kasahara, and H. Ogata, "Sensing stability and dynamic response of the F-Scan in-shoe sensing system: A technical note," *Journal of Rehabilitation Research and Development*, vol. 35, 2, pp. 192-200, 1998.
- [19] H. Hsiao, J. Guan, and M. Weatherly, "Accuracy and precision of two in-shoe pressure measurement systems," *Ergonomics*, vol. 45, no. 8, pp. 537-555, 2002, doi: <https://doi.org/10.1080/00140130210136963>.
- [20] J. M. Stevenson, L. L. Bossi, J. T. Bryant, S. A. Reid, R. P. Pelot, and E. L. Morin, "A suite of objective biomechanical measurement tools for personal load carriage system assessment," *Ergonomics*, vol. 47, no. 11, pp. 1160-1179, 2004, doi: <https://doi.org/10.1080/00140130410001699119>.

- [21] B. R. Macias, G. Murthy, H. Chambers, and A. R. Hargens, "High contact pressure beneath backpack straps of children contributes to pain," *Archives of Pediatrics and Adolescent Medicine*, vol. 159, no. 12, pp. 1186 - 1188, 2005, doi: <https://doi.org/10.1001/archpedi.159.12.1186>.
- [22] B. R. Macias, G. Murthy, H. Chambers, and A. R. Hargens, "Asymmetric loads and pain associated with backpack carrying by children," *Journal of Pediatric Orthopaedics*, vol. 28, no. 5, pp. 512-517, 2008, doi: <https://doi.org/10.1097/bpo.0b013e31817d8143>.
- [23] S. Negrini, R. Carabalona, and P. Sibilla, "Backpack as a daily load for schoolchildren," *The Lancet*, vol. 354, no. 9194, p. 1974, 1999, doi: [https://doi.org/10.1016/S0140-6736\(99\)04520-1](https://doi.org/10.1016/S0140-6736(99)04520-1).
- [24] A. Pinedo-Jauregi, T. Quinn, A. Coca, G. Mejuto, and J. Cámara, "Physiological stress in flat and uphill walking with different backpack loads in professional mountain rescue crews," *Applied Ergonomics*, vol. 103, p. 103784, 2022, doi: <https://doi.org/10.1016/j.apergo.2022.103784>.
- [25] M. J. Angelini, R. M. Kesler, M. N. Petrucci, K. S. Rosengren, G. P. Horn, and E. T. Hsiao-Wecksler, "Effects of simulated firefighting and asymmetric load carriage on firefighter obstacle crossing performance," *Applied Ergonomics*, vol. 70, pp. 59-67, 2018, doi: <https://doi.org/10.1016/j.apergo.2018.02.006>.
- [26] B. R. Jewett, C. Tomes, K. Voigt, and G. M. Mokha, "The effects of equipment carriage on functional movement quality among law enforcement officers," *Ergonomics*, vol. 66, no. 12, pp. 2277-2287, 2023, doi: <https://doi.org/10.1080/00140139.2023.2199954>.
- [27] M. N. Sax van der Weyden, J. W. Kearney, N. Cortes, O. Fernandes, and J. R. Martin, "Common law enforcement load carriage systems have limited acute effects on postural

- stability and muscle activity," *Applied Ergonomics*, vol. 113, p. 104091, 2023, doi: <https://doi.org/10.1016/j.apergo.2023.104091>.
- [28] C. E. Dean, "The modern warrior's combat load, dismounted operations in Afghanistan," *Medicine and Science in Sports and Exercise*, vol. 40, no. 5, pp. 60-62, 2004, doi: <https://doi.org/10.1249/01.mss.0000321238.28174.55>.
- [29] A. Hadid, Y. Epstein, N. Shabshin, and A. Gefen, "Modeling mechanical strains and stresses in soft tissues of the shoulder during load carriage based on load-bearing open MRI," *Journal of Applied Physiology*, vol. 112, no. 4, pp. 597-606, 2012, doi: <https://doi.org/10.1152/jappphysiol.00990.2011>.
- [30] H. M. Brackley and J. M. Stevenson, "Are children's backpack weight limits enough? A critical review of the relevant literature," *Spine*, vol. 29, no. 19, pp. 2184-2190, 2004, doi: <https://doi.org/10.1097/01.brs.0000141183.20124.a9>.
- [31] J. Knapik and K. Reynolds, "Load Carriage in Military Operations: A Review of Historical, Physiological, Biomechanical, and Medical Aspects," Defence Technical Information Center, ADA330082, 1997.
- [32] T. C. Roy *et al.*, "Physical training risk factors for musculoskeletal injury in female soldiers," *Military Medicine*, vol. 179, no. 12, pp. 1432-1438, 2014, doi: <https://doi.org/10.7205/MILMED-D-14-00164>.
- [33] B. Liew, S. Morris, and K. Netto, "The effect of backpack carriage on the biomechanics of walking: a systematic review and preliminary meta-analysis," *Journal of Applied Biomechanics*, vol. 32, no. 6, pp. 614-629, 2016, doi: <https://doi.org/10.1123/jab.2015-0339>.

- [34] R. L. Attwells, S. A. Birrell, R. H. Hooper, and N. J. Mansfield, "Influence of carrying heavy loads on soldiers' posture, movements and gait," *Ergonomics*, vol. 49, no. 14, pp. 1527-1537, 2006, doi: <https://doi.org/10.1080/00140130600757237>.
- [35] J. H. Goh, A. Thambyah, and K. Bose, "Effects of varying backpack loads on peak forces in the lumbosacral spine during walking," *Clinical Biomechanics*, vol. 13, no. 1, Supplement 1, pp. S26-S31, 1998, doi: [https://doi.org/10.1016/S0268-0033\(97\)00071-5](https://doi.org/10.1016/S0268-0033(97)00071-5).
- [36] J. J. Vacheron, G. Poumarat, R. Chandezon, and G. Vanneuville, "Changes of contour of the spine caused by load carrying," *Surgical and Radiologic Anatomy*, vol. 21, no. 2, pp. 109-113, 1999, doi: <https://doi.org/10.1007/s00276-999-0109-7>.
- [37] P. N. Ainslie, I. T. Campbell, J. P. Lambert, D. P. M. Maclaren, and T. Reilly, "Physiological and metabolic aspects of very prolonged exercise with particular reference to hill walking," *Sports Medicine*, vol. 35, no. 7, pp. 619-647, 2005, doi: <https://doi.org/10.2165/00007256-200535070-00006>.
- [38] B. M. Bhatt, "'Top cover neuropathy' - transient brachial plexopathy due to body armour," *Journal of the Royal Army Medical Corps*, vol. 136, no. 1, pp. 53-54, 1990, doi: <https://doi.org/10.1136/jramc-136-01-09>.
- [39] A. J. De Luigi, P. Pasquina, and E. Dahl, "Rucksack-induced plexopathy mimicking a lateral antebrachial cutaneous neuropathy," *American Journal of Physical Medicine & Rehabilitation*, vol. 87, no. 9, pp. 773-775, 2008, doi: <https://doi.org/10.1097/phm.0b013e3181837b83>.
- [40] A. Hadid, N. Belzer, N. Shabshin, G. Zeilig, A. Gefen, and Y. Epstein, "The effect of mechanical strains in soft tissues of the shoulder during load carriage," *Journal of*

- Biomechanics*, vol. 48, no. 15, pp. 4160-4165, 2015, doi:
<https://doi.org/10.1016/j.jbiomech.2015.10.020>.
- [41] S. H. Kim, T. B. Neuschwander, B. R. Macias, L. Bachman Jr., and A. R. Hargens, "Upper extremity hemodynamics and sensation with backpack loads," *Applied Ergonomics*, vol. 45, no. 3, pp. 608-612, 2014, doi:
<https://doi.org/10.1016/j.apergo.2013.08.005>.
- [42] C. P. Mao, B. R. Macias, and A. R. Hargens, "Shoulder skin and muscle hemodynamics during backpack carriage," *Applied Ergonomics*, vol. 51, pp. 80-84, 2015, doi:
<https://doi.org/10.1016/j.apergo.2015.04.006>.
- [43] J. P. Mäkelä, R. Ramstad, V. Mattila, and H. Pihlajamäki, "Brachial Plexus lesions after backpack carriage in young adults," *Clinical Orthopaedics and Related Research*, vol. 452, pp. 205-209, 2006, doi: <https://doi.org/10.1097/01.blo.0000229338.29277.29>.
- [44] J. T. Bryant, J. B. Doan, J. M. Stevenson, R. P. Pelot, and S. A. Reid, "Validation of objective based measures and development of a performance-based ranking method for load carriage systems," Defence Technical Information Center, ADP010998, 2001.
- [45] T. Husain, "An experimental study of some pressure effects on tissues, with reference to the bed-sore problem," *The Journal of Pathology and Bacteriology*, vol. 66, pp. 347-358, 1953, doi: <https://doi.org/10.1002/path.1700660203>.
- [46] G. A. Holloway, C. H. Daly, D. Kennedy, and J. Chimoskey, "Effect of external pressure loading on human skin blood flow measured by ¹³³Xe clearance," *Journal of Applied Physiology*, vol. 40, no. 4, pp. 597-600, 1976, doi:
<https://doi.org/10.1152/jappl.1976.40.4.597>.

- [47] B. J. Sangeorzan, R. M. Harrington, C. R. Wyss, J. M. Czerniecki, and F. A. Matsen III, "Circulatory and mechanical response of skin to loading," *Journal of Orthopaedic Research*, vol. 7, pp. 425-431, 1989, doi: <https://doi.org/10.1002/jor.1100070315>.
- [48] M. Lafiandra and E. Harman, "The distribution of forces between the upper and lower back during load carriage," *Medicine and Science in Sports and Exercise*, vol. 36, no. 3, pp. 460-467, 2004, doi: <https://doi.org/10.1249/01.mss.0000117113.77904.46>.
- [49] F. Scribano, M. Burns, and E. R. Barron, "Design, development and fabrication of a personnel armor load profile analyzer," Defence Technical Information Center, AD711876, 1970.
- [50] P. D. Wettenschwiler *et al.*, "Validation of an instrumented dummy to assess mechanical aspects of discomfort during load carriage," *PLoS ONE*, vol. 12, no. 6, p. e0180069, 2017, doi: <https://doi.org/10.1371/journal.pone.0180069>.
- [51] J. M. Stevenson, L. L. Bossi, J. T. Bryant, S. A. Reid, R. P. Pelot, and E. L. Morin, "Development of a suite of objective biomechanical measurement tools for personal load carriage system assessment," *Ergonomics*, vol. 47, pp. 1160-79, 2004, doi: <https://doi.org/10.1080/00140130410001699119>.
- [52] J. T. Bryant, J. M. Stevenson, L. L. Bossi, S. A. Reid, R. P. Pelot, and E. Morin, "Optimizing load carriage systems," *Ergonomics in Design: The Quarterly of Human Factors Applications*, vol. 12, no. 1, pp. 12-17, 2004, doi: <https://doi.org/10.1177/106480460401200105>.
- [53] M. Holewijn and T. Meeuwssen, "Physiological strain during load carrying: effects of mass and type of backpack," *Soldier Mobility: Innovations in Load Carriage System*

- Design and Evaluation, NATO-RTO Meeting Proceedings: MP*, vol. 56, no. 1, pp. 1-12, 2001.
- [54] K. N. Bachus, A. L. DeMarco, K. T. Judd, D. S. Horwitz, and D. S. Brodke, "Measuring contact area, force, and pressure for bioengineering applications: Using Fuji Film and TekScan systems," *Medical Engineering and Physics*, vol. 28, no. 5, pp. 483-488, 2006, doi: <https://doi.org/10.1016/j.medengphy.2005.07.022>.
- [55] E. L. Morin, J. T. Bryant, S. A. Reid, and R. A. Whiteside, "Calibration issues of Tekscan systems for human pressure assessment ", Defence Technical Information Center, ADP011007, 2000.
- [56] "I-Scan Equilibration and Calibration Practical Suggestions," Tekscan Inc., 2016.
- [57] J. M. Brimacombe, D. R. Wilson, A. J. Hodgson, K. C. T. Ho, and C. Anglin, "Effect of calibration method on Tekscan sensor accuracy," *Journal of Biomechanical Engineering*, vol. 131, no. 3, p. 034503, 2009, doi: <https://doi.org/10.1115/1.3005165>.
- [58] P. D. Wettenschwiler, R. Stämpfli, S. Lorenzetti, S. J. Ferguson, R. M. Rossi, and S. Annaheim, "How reliable are pressure measurements with Tekscan sensors on the body surface of human subjects wearing load carriage systems?," *International Journal of Industrial Ergonomics*, vol. 49, pp. 60-67, 2015, doi: <https://doi.org/10.1016/j.ergon.2015.06.003>.
- [59] L. Macintyre, "New calibration method for I-scan sensors to enable the precise measurement of pressures delivered by 'pressure garments'," *Burns*, vol. 37, no. 7, pp. 1174-1181, 2011, doi: <https://doi.org/10.1016/j.burns.2011.06.008>.

- [60] C. H. Y. Lai and C. W. P. Li-Tsang, "Validation of the Pliance X system in measuring interface pressure generated by pressure garment," *Burns*, vol. 35, no. 6, pp. 845-851, 2009, doi: <https://doi.org/10.1016/j.burns.2008.09.013>.
- [61] J. Wiseman, M. Simons, R. Kimble, and Z. Tyack, "Reliability and clinical utility of the Pliance X for measuring pressure at the interface of pressure garments and burn scars in children," *Burns*, vol. 44, no. 7, pp. 1820-1828, 2018, doi: <https://doi.org/10.1016/j.burns.2018.05.002>.
- [62] C. Price, D. Parker, and C. Nester, "Validity and repeatability of three in-shoe pressure measurement systems," *Gait & Posture*, vol. 46, pp. 69-74, 2016, doi: <https://doi.org/10.1016/j.gaitpost.2016.01.026>.
- [63] D. Parker, J. Andrews, and C. Price, "Validity and reliability of the XSENSOR in-shoe pressure measurement system," *PLoS ONE*, vol. 18, no. 1, p. e0277971, 2023, doi: <https://doi.org/10.1371/journal.pone.0277971>.
- [64] S. A. Reid, J. T. Bryant, J. M. Stevenson, and J. B. Doan, "Biomechanical assessment of rucksack shoulder strap attachment location: effect on load distribution to the torso," Defence Technical Information Center, ADP011003, 2001.
- [65] N. A. Taylor *et al.*, "Employment standards for Australian urban firefighters. Part 2: the physiological demands and the criterion tasks," *Journal of Occupational and Environmental Medicine*, vol. 57, no. 10, pp. 1072-1082, 2015, doi: <https://doi.org/10.1097/JOM.0000000000000526>.
- [66] B. C. Ruby, G. W. Leadbetter III, D. W. Armstrong, and S. E. Gaskill, "Wildland firefighter load carriage: effects on transit time and physiological responses during

- simulated escape to safety zone," *International Journal of Wildland Fire*, vol. 12, no. 1, pp. 111-116, 2003, doi: <https://doi.org/10.1071/wf02025>.
- [67] R. J. Bessen, V. W. Belcher, and R. J. Franklin, "Rucksack paralysis with and without rucksack frames," *Military Medicine*, vol. 152, no. 7, pp. 372-375, 1987, doi: <https://doi.org/10.1093/milmed/152.7.372>.
- [68] G. K. Lenton, T. L. A. Doyle, D. J. Saxby, D. Billing, J. Higgs, and D. G. Lloyd, "Integrating a hip belt with body armour reduces the magnitude and changes the location of shoulder pressure and perceived discomfort in soldiers," *Ergonomics*, vol. 61, no. 4, pp. 566 - 575, 2018, doi: <https://doi.org/10.1080/00140139.2017.1381278>.
- [69] H. W. Mackie, J. M. Stevenson, S. A. Reid, and S. J. Legg, "The effect of simulated school load carriage configurations on shoulder strap tension forces and shoulder interface pressure," *Applied Ergonomics*, vol. 36, no. 2, pp. 199-206, 2005, doi: <https://doi.org/10.1016/j.apergo.2004.10.007>.
- [70] C. J. Wolsley and P. D. Hill, "Review of interface pressure measurement to establish a protocol for their use in the assessment of patient support surfaces," *Journal of Tissue Viability*, vol. 10, no. 2, pp. 53-57, 2000, doi: [https://doi.org/10.1016/S0965-206X\(00\)80023-6](https://doi.org/10.1016/S0965-206X(00)80023-6).
- [71] O. Kokai, S. L. Kilbreath, P. McLaughlin, and E. S. Dylke, "The accuracy and precision of interface pressure measuring devices: A systematic review," *Phlebology*, vol. 36, no. 9, pp. 678-694, 2021, doi: <https://doi.org/10.1177/02683555211008061>.
- [72] "Pliance-X System Manual " Novel GmbH, 2014.
- [73] "Tekscan I-Scan & High Speed I-Scan User Manual " Tekscan Inc., 2012.

- [74] E. S. Pearson, "The Analysis of Variance in Cases of Non-Normal Variation," *Biometrika*, vol. 23, no. 1/2, pp. 114-133, 1931, doi: <https://doi.org/10.2307/2333631>.
- [75] F. E. Satterthwaite, "An approximate distribution of estimates of variance components," *Biometrics Bulletin*, vol. 2, no. 6, pp. 110-114, 1946, doi: <https://doi.org/10.2307/3002019>.
- [76] W. G. Cochran and G. M. Cox, *Experimental designs* New York: John Wiley and Sons Inc., 1957.
- [77] K. E. Muller and C. N. Barton, "Approximate power for repeated-measures ANOVA lacking sphericity," *Journal of the American Statistical Association*, vol. 84, no. 406, pp. 549-555, 1989, doi: <https://doi.org/10.1080/01621459.1989.10478802>.
- [78] A. J. Hayter, "The maximum familywise error rate of Fisher's least significant difference test," *Journal of the American Statistical Association*, vol. 81, no. 396, pp. 1000-1004, 1986, doi: <https://doi.org/10.1080/01621459.1986.10478364>.
- [79] A. Hadid *et al.*, "Effect of load carriage on upper limb performance," *Medicine and Science in Sports and Exercise*, vol. 49, no. 5, 2017, doi: <https://doi.org/10.1249/MSS.0000000000001192>.
- [80] E. R. Komi, J. R. Roberts, and S. J. Rothberg, "Evaluation of thin, flexible sensors for time-resolved grip force measurement," *Proceedings of the Institution of Mechanical Engineers, Part C: Journal of Mechanical Engineering Science*, vol. 221, no. 12, pp. 1687-1699, 2007, doi: <https://doi.org/10.1243/09544062JMES700>.
- [81] A. O'Keefe, "2012 Canadian Forces Anthropometric Survey (CFAS)," Defence Research and Development Canada, DRDC-RDDC-2015-R186, 2018.

- [82] J. M. Stevenson, S. A. Reid, J. T. Bryant, R. P. Pelot, and E. L. Morin, "Biomechanical assessment of the Canadian integrated load carriage system using objective assessment measures," Defense Technical Information Center, ADP011004, 2001.
- [83] S. A. Reid, G. A. B. Sanders, and J. A. Good, "Development of a dynamic biomechanical model for load carriage: phase II part A: initial development of a novel strap tension sensor," Defence Technical Information Center, ADA480772, 2005.
- [84] J. M. Bland and D. G. Altman, "Statistical methods for assessing agreement between two methods of clinical measurement," *The Lancet*, vol. 327, no. 8476, pp. 307-310, 1986, doi: [https://doi.org/10.1016/S0140-6736\(86\)90837-8](https://doi.org/10.1016/S0140-6736(86)90837-8).
- [85] J. Ludbrook, "Confidence in Altman–Bland plots: A critical review of the method of differences," *Clinical and Experimental Pharmacology and Physiology*, vol. 37, no. 2, pp. 143-149, 2010, doi: <https://doi.org/10.1111/j.1440-1681.2009.05288.x>.

Appendix A

Data Sharing and Statistics

This appendix provides essential measurements for data sharing and summarizes important findings of the statistical analysis regarding the surface and simulator evaluation.

A.1 Surface Evaluation

A.1.1 Analysis of Absolute Error

Table A.1 Absolute error of Novel. Absolute error (measured - applied load) of contact pressure measured by Novel Pliance® at 30 minutes of static pressure for ten independently collected trials per surface and load.

Trial	Absolute Error [kPa]									
	Flat Surface					Curved Surface				
	30 kPa	45 kPa	60 kPa	75 kPa	90 kPa	30 kPa	45 kPa	60 kPa	75 kPa	90 kPa
1	6.56	6.05	6.49	9.45	7.26	0.92	1.17	2.66	3.30	1.50
2	3.32	4.52	5.49	7.71	7.74	6.46	8.10	8.75	7.48	7.72
3	1.98	6.52	4.54	7.26	10.42	3.59	5.75	6.62	4.75	6.39
4	2.79	3.19	4.15	7.27	7.95	3.30	5.57	7.25	7.35	4.85
5	2.69	4.23	3.88	3.75	6.49	2.70	2.66	2.43	4.40	5.49
6	2.87	1.11	1.82	1.69	1.45	3.15	5.19	5.23	5.69	6.81
7	3.70	3.70	2.87	5.30	2.21	1.36	2.78	4.00	4.51	3.57
8	1.69	1.03	1.12	2.24	1.22	3.43	5.13	5.47	4.60	7.78
9	1.10	2.42	3.46	6.20	1.39	2.47	4.68	6.24	6.64	6.37
10	2.07	1.66	4.64	1.94	3.70	3.66	5.38	6.75	7.09	7.88
Mean	2.88	3.44	3.84	5.28	4.98	3.10	4.64	5.54	5.58	5.84
S.D.	1.51	1.93	1.62	2.74	3.37	1.50	1.96	2.02	1.48	2.06

Table A.2 Absolute error of Tekscan. Absolute error (measured - applied load) of contact pressure measured by Tekscan I-Scan™ at 30 minutes of static pressure for ten independently collected trials per surface and load.

Trial	Absolute Error [kPa]									
	Flat Surface					Curved Surface				
	30 kPa	45 kPa	60 kPa	75 kPa	90 kPa	30 kPa	45 kPa	60 kPa	75 kPa	90 kPa
1	0.09	4.40	9.37	11.95	12.08	2.92	6.78	10.74	18.51	18.67
2	0.22	3.81	3.12	8.78	14.04	2.62	5.81	10.46	14.41	17.70
3	0.11	1.41	5.71	8.17	9.27	1.05	2.67	6.65	7.51	12.82
4	1.14	3.37	3.64	8.42	9.06	2.89	6.01	8.59	10.70	13.10
5	2.48	2.24	7.22	9.08	11.87	1.51	6.72	11.03	13.35	16.42
6	1.80	2.10	3.41	9.11	10.18	0.86	3.35	5.69	6.53	10.94
7	0.19	1.11	6.50	8.85	11.33	2.83	6.36	9.24	13.12	14.33
8	1.96	2.27	5.96	8.42	12.17	0.78	4.08	10.06	12.42	15.74
9	2.56	3.30	5.58	10.03	10.99	1.83	4.90	4.82	8.56	10.33
10	1.49	2.21	5.23	9.27	8.91	2.97	5.16	8.45	11.04	15.68
Mean	1.20	2.62	5.57	9.21	10.99	2.03	5.18	8.57	11.62	14.57
S.D.	1.00	1.06	1.91	1.10	1.65	0.92	1.43	2.19	3.57	2.77

Table A.3 Absolute error of XSENSOR™. Absolute error (measured - applied load) of contact pressure measured by XSENSOR™ X3 at 30 minutes of static pressure for ten independently collected trials per surface and load.

Trial	Absolute Error [kPa]									
	Flat Surface					Curved Surface				
	30 kPa	45 kPa	60 kPa	75 kPa	90 kPa	30 kPa	45 kPa	60 kPa	75 kPa	90 kPa
1	2.36	9.02	12.03	0.96	6.69	6.31	7.38	10.18	13.50	15.07
2	14.49	16.23	4.21	12.75	2.05	7.78	6.60	7.64	9.27	13.61
3	13.92	6.02	14.14	3.50	16.03	9.08	9.15	10.52	11.42	17.02
4	6.24	2.95	6.55	3.41	7.39	9.30	9.54	10.85	15.36	20.40
5	9.99	15.87	5.72	9.41	3.71	7.59	8.60	9.66	17.48	17.75
6	3.17	8.19	11.39	0.59	5.77	9.67	10.07	11.09	12.38	16.91
7	14.40	2.46	12.83	0.82	12.62	8.89	8.90	9.21	12.09	16.37
8	8.16	5.58	8.71	1.11	2.98	7.25	8.66	10.24	12.14	16.87
9	2.32	9.77	0.31	2.76	4.37	9.84	10.31	11.43	13.44	19.41
10	6.68	11.32	0.26	2.10	1.13	10.09	10.70	12.32	14.54	19.49
Mean	8.17	8.74	7.62	3.74	6.27	8.58	8.99	10.31	13.16	17.29
S.D.	4.88	4.78	5.04	4.09	4.74	1.27	1.28	1.29	2.27	2.08

Table A.4 Descriptive statistics and assumption significance of absolute error. Mean, standard deviation, and significance of normality (Shapiro-Wilks Test) and homogeneity of variance (Levene’s Test) for absolute error per system, surface, and load.

Evaluated Condition			Mean ± S.D. [kPa]	S-W Test <i>p</i>	Levene’s Test <i>p</i>
System Comparison			6.99 ± 4.56	< 0.001	< 0.001
	Novel Pliance®	Surface Comparison	4.51 ± 2.26	0.010	0.175
	Tekscan I-Scan™	Surface Comparison	7.16 ± 4.70	0.003	0.118
	XSENSOR™ X3	Surface Comparison	9.29 ± 4.90	0.142	0.012
Tekscan I-Scan™	Flat Surface	Load Comparison	5.92 ± 4.00	0.006	0.296
	Curved Surface	Load Comparison	8.39 ± 5.05	0.069	0.011
XSENSOR™ X3	Flat Surface	Load Comparison	6.91 ± 4.86	0.005	0.845
	Curved Surface	Load Comparison	11.67 ± 3.65	0.002	0.290

Table A.5 Main effect of measurement drift. Results of the t-test and ANOVA for absolute error per system, surface, and load.

Evaluated Condition			t-test		ANOVA	
			<i>t</i>	<i>p</i>	<i>F</i>	<i>p</i>
System Comparison					45.148	< 0.001
	Novel Pliance®	Surface Comparison	-1.913	0.059		
	Tekscan I-Scan™	Surface Comparison	-2.717	0.008		
	XSENSOR™ X3	Surface Comparison	-5.532	< 0.001		
Tekscan I-Scan™	Flat Surface	Load Comparison			90.165	< 0.001
	Curved Surface	Load Comparison			64.319	< 0.001
XSENSOR™ X3	Flat Surface	Load Comparison			1.788	0.148
	Curved Surface	Load Comparison			45.393	< 0.001

Table A.6 Post hoc of absolute error between systems. Mean difference (#1-2), standard error, and *post hoc* significance of absolute error between systems.

System (#1)	System (#2)	Mean Diff. \pm S.E. [kPa]	<i>p</i>
Novel Pliance®	Tekscan I-Scan™	-2.64 \pm 0.52	< 0.001
Novel Pliance®	XSENSOR™ X3	-4.78 \pm 0.54	< 0.001
Tekscan I-Scan™	XSENSOR™ X3	-2.13 \pm 0.68	0.006

Table A.7 Post hoc of absolute error between load conditions per system and surface. Mean difference (#1-2), standard error, and *post hoc* significance of absolute error between loads per system and surface.

System	Surface	Load (#1)	Load (#2)	Mean Diff. \pm S.E. [kPa]	<i>p</i>
Tekscan I-Scan™	Flat	30 kPa	45 kPa	-1.42 \pm 0.62	0.170
		30 kPa	60 kPa	-4.37 \pm 0.62	< 0.001
		30 kPa	75 kPa	-8.00 \pm 0.62	< 0.001
		30 kPa	90 kPa	-9.79 \pm 0.62	< 0.001
		45 kPa	60 kPa	-2.95 \pm 0.62	< 0.001
		45 kPa	75 kPa	-6.59 \pm 0.62	< 0.001
		45 kPa	90 kPa	-8.37 \pm 0.62	< 0.001
		60 kPa	75 kPa	-3.63 \pm 0.62	< 0.001
		60 kPa	90 kPa	-5.41 \pm 0.62	< 0.001
	75 kPa	90 kPa	-1.78 \pm 0.62	0.047	
	Curved	30 kPa	45 kPa	-3.16 \pm 0.54	< 0.001
		30 kPa	60 kPa	-6.55 \pm 0.75	< 0.001
		30 kPa	75 kPa	-9.59 \pm 1.16	< 0.001
		30 kPa	90 kPa	-12.55 \pm 0.92	< 0.001
		45 kPa	60 kPa	-3.39 \pm 0.83	0.007
		45 kPa	75 kPa	-6.43 \pm 1.21	0.002
		45 kPa	90 kPa	-9.39 \pm 0.99	< 0.001
		60 kPa	75 kPa	-3.04 \pm 1.32	0.199
60 kPa		90 kPa	-6.00 \pm 1.12	< 0.001	
75 kPa	90 kPa	-2.96 \pm 1.43	0.277		
XSENSOR™ X3	Curved	30 kPa	45 kPa	-0.41 \pm 0.76	0.983
		30 kPa	60 kPa	-1.73 \pm 0.76	0.170
		30 kPa	75 kPa	-4.58 \pm 0.76	< 0.001
		30 kPa	90 kPa	-8.71 \pm 0.76	< 0.001
		45 kPa	60 kPa	-1.32 \pm 0.76	0.420
		45 kPa	75 kPa	-4.17 \pm 0.76	< 0.001
		45 kPa	90 kPa	-8.30 \pm 0.76	< 0.001
		60 kPa	75 kPa	-2.85 \pm 0.76	0.004
		60 kPa	90 kPa	-6.98 \pm 0.76	< 0.001
75 kPa	90 kPa	-4.13 \pm 0.76	< 0.001		

A.1.2 Analysis of Measurement Drift

Table A.8 Measurement drift of Novel. Measurement drift (upper - lower time) of contact pressure measured by Novel Pliance® for ten independently collected trials per surface and load. Time intervals a, b, and c correspond to 3–12, 12–21, and 21–30 minutes.

Trial	Time Interval	Drift Rate [kPa·min ⁻¹]									
		Flat Surface					Curved Surface				
		30 kPa	45 kPa	60 kPa	75 kPa	90 kPa	30 kPa	45 kPa	60 kPa	75 kPa	90 kPa
1	a	0.02	0.05	0.11	0.10	0.13	-0.01	0.14	0.13	0.22	0.28
	b	-0.02	0.03	0.04	0.01	0.07	0.00	0.05	0.06	0.07	0.10
	c	-0.03	0.03	0.05	0.02	0.04	-0.02	0.03	0.04	0.04	0.07
2	a	-0.05	0.05	0.12	0.07	0.12	-0.02	0.04	0.10	0.19	0.14
	b	-0.06	0.01	0.05	0.05	0.03	-0.02	0.02	0.04	0.06	0.05
	c	-0.05	0.01	0.03	0.00	0.03	-0.01	0.01	0.02	0.05	0.05
3	a	-0.04	0.06	0.13	0.13	0.10	-0.03	0.06	0.09	0.25	0.16
	b	-0.03	0.00	0.05	0.04	0.03	-0.05	0.00	0.03	0.08	0.06
	c	-0.02	0.01	0.02	0.02	0.03	-0.05	0.01	0.01	-0.05	0.07
4	a	-0.02	0.05	0.16	0.12	0.09	-0.01	0.03	0.12	0.14	0.24
	b	-0.02	0.02	0.04	0.03	0.03	-0.01	0.00	0.02	0.08	0.07
	c	-0.01	0.01	0.04	0.02	0.01	-0.03	0.00	0.03	0.03	0.04
5	a	-0.06	0.04	0.09	0.09	0.17	0.09	0.10	0.13	0.13	0.13
	b	-0.03	0.04	0.01	0.03	0.09	0.03	0.04	0.04	0.04	0.02
	c	-0.01	0.03	0.01	0.02	0.03	0.02	0.03	0.04	0.01	0.04
6	a	-0.04	0.05	0.12	0.14	0.13	0.00	0.10	0.11	0.16	0.19
	b	-0.04	0.03	0.05	0.05	0.05	-0.02	0.01	0.08	0.05	0.08
	c	-0.01	0.01	0.02	0.03	0.02	-0.01	0.04	0.02	0.04	0.03
7	a	-0.02	0.07	0.09	0.13	0.13	-0.01	0.05	0.09	0.15	0.29
	b	-0.03	0.02	0.04	0.07	0.02	-0.01	0.02	0.02	0.05	0.10
	c	0.00	0.01	0.02	0.01	0.03	-0.01	0.00	0.01	0.03	0.04
8	a	-0.09	0.08	0.10	0.18	0.14	-0.02	0.04	0.14	0.15	0.13
	b	-0.07	0.04	0.03	0.07	0.03	-0.03	0.02	0.05	0.06	-0.03
	c	-0.03	0.00	0.02	0.04	0.02	0.00	0.01	0.03	0.01	-0.03
9	a	-0.05	0.07	0.12	0.18	0.16	-0.01	0.06	0.12	0.15	0.20
	b	-0.05	0.01	0.03	0.07	0.06	-0.02	0.03	0.03	0.04	0.08
	c	-0.02	-0.03	0.01	0.04	0.01	-0.02	0.01	0.03	0.05	0.05
10	a	-0.04	0.06	0.07	0.12	0.22	0.01	0.07	0.11	0.13	0.17
	b	-0.06	0.01	0.02	0.04	0.07	-0.01	0.02	0.04	0.06	0.04
	c	-0.01	0.01	0.02	0.01	0.02	0.00	0.02	0.03	0.05	0.04
Mean		-0.03	0.03	0.06	0.06	0.07	-0.01	0.04	0.06	0.08	0.10
S.D.		0.02	0.03	0.04	0.05	0.06	0.03	0.03	0.04	0.07	0.08

Table A.9 Measurement drift of Tekscan. Measurement drift (upper - lower time) of contact pressure measured by Tekscan I-Scan™ for ten independently collected trials per surface and load. Time intervals a, b, and c correspond to 3–12, 12–21, and 21–30 minutes.

Trial	Time Interval	Drift Rate [kPa·min ⁻¹]									
		Flat Surface					Curved Surface				
		30 kPa	45 kPa	60 kPa	75 kPa	90 kPa	30 kPa	45 kPa	60 kPa	75 kPa	90 kPa
1	a	0.17	0.26	0.31	0.36	0.36	0.21	0.25	0.35	0.41	0.53
	b	0.07	0.07	0.11	0.13	0.15	0.10	0.05	0.15	0.21	0.15
	c	0.05	0.06	0.10	0.08	0.09	0.03	0.05	0.14	0.04	0.04
2	a	0.14	0.21	0.34	0.45	0.36	0.18	0.22	0.34	0.32	0.51
	b	0.05	0.07	0.14	0.13	0.14	0.08	0.07	0.15	0.14	0.08
	c	0.02	0.04	0.08	0.08	0.08	0.05	0.04	0.07	0.09	0.15
3	a	0.10	0.23	0.24	0.24	0.33	0.17	0.18	0.34	0.37	0.44
	b	0.04	0.07	0.09	0.10	0.12	0.04	0.11	0.12	0.08	0.20
	c	0.04	0.08	0.09	0.07	0.08	0.06	0.04	0.08	0.10	0.02
4	a	0.12	0.22	0.33	0.33	0.31	0.23	0.26	0.31	0.43	0.45
	b	0.04	0.08	0.13	0.13	0.14	0.10	0.08	0.11	0.08	0.15
	c	0.02	0.03	0.08	0.07	0.09	0.06	0.05	0.01	0.15	0.10
5	a	0.13	0.21	0.25	0.28	0.42	0.18	0.16	0.30	0.27	0.44
	b	0.05	0.06	0.10	0.09	0.16	0.08	0.12	0.08	0.11	0.09
	c	0.04	0.04	0.06	0.07	0.11	0.02	0.09	0.09	0.08	0.18
6	a	0.09	0.23	0.24	0.27	0.31	0.21	0.23	0.29	0.32	0.42
	b	0.05	0.07	0.09	0.11	0.12	0.10	0.11	0.11	0.11	0.14
	c	0.04	0.06	0.05	0.07	0.06	0.05	0.05	0.11	0.11	0.11
7	a	0.12	0.19	0.30	0.30	0.35	0.21	0.32	0.34	0.38	0.38
	b	0.04	0.11	0.10	0.10	0.11	0.14	0.10	0.09	0.16	0.18
	c	0.02	0.04	0.06	0.08	0.07	0.12	0.09	0.11	0.08	0.12
8	a	0.11	0.20	0.26	0.35	0.36	0.15	0.23	0.29	0.34	0.41
	b	0.02	0.07	0.09	0.15	0.13	0.07	0.11	0.14	0.18	0.14
	c	0.03	0.03	0.07	0.09	0.08	0.05	0.10	0.05	0.09	0.19
9	a	0.12	0.23	0.26	0.33	0.38	0.18	0.23	0.23	0.33	0.39
	b	0.02	0.08	0.11	0.12	0.13	0.08	0.08	0.14	0.14	0.14
	c	0.03	0.03	0.04	0.08	0.08	0.06	0.05	0.06	0.06	0.14
10	a	0.10	0.21	0.25	0.30	0.42	0.20	0.22	0.43	0.39	0.41
	b	0.05	0.09	0.09	0.10	0.16	0.13	0.06	0.12	0.20	0.21
	c	0.02	0.02	0.07	0.08	0.12	0.12	0.08	0.08	0.06	0.14
Mean		0.06	0.11	0.15	0.17	0.19	0.12	0.13	0.17	0.20	0.23
S.D.		0.04	0.08	0.10	0.11	0.12	0.06	0.08	0.11	0.13	0.15

Table A.10 Measurement drift of XSENSOR™. Measurement drift (upper - lower time) of contact pressure measured by XSENSOR™ X3 for ten independently collected trials per surface and load. Time intervals a, b, and c correspond to 3–12, 12–21, and 21–30 minutes.

Trial	Time Interval	Drift Rate [kPa·min ⁻¹]									
		Flat Surface					Curved Surface				
		30 kPa	45 kPa	60 kPa	75 kPa	90 kPa	30 kPa	45 kPa	60 kPa	75 kPa	90 kPa
1	a	0.07	0.09	0.13	0.18	0.16	0.07	0.12	0.16	0.25	0.40
	b	0.02	0.04	0.06	0.07	0.07	0.03	0.05	0.07	0.11	0.13
	c	0.02	0.02	0.04	0.04	0.04	0.01	0.05	0.04	0.07	0.16
2	a	0.01	0.11	0.15	0.19	0.19	0.06	0.18	0.16	0.19	0.22
	b	0.01	0.05	0.05	0.06	0.05	0.02	0.08	0.06	0.06	0.09
	c	0.00	0.01	0.05	0.06	0.07	0.01	0.06	0.03	0.06	0.06
3	a	0.00	0.08	0.14	0.18	0.22	0.07	0.08	0.11	0.25	0.24
	b	-0.01	0.02	0.05	0.07	0.07	0.03	0.01	0.05	0.11	0.11
	c	0.00	0.01	0.03	0.03	0.06	0.01	0.01	0.03	0.08	0.06
4	a	0.10	0.08	0.16	0.16	0.20	0.06	0.09	0.14	0.33	0.29
	b	0.03	0.04	0.06	0.09	0.06	0.02	0.02	0.04	0.11	0.11
	c	0.02	0.02	0.05	0.03	0.05	0.01	0.02	0.02	0.05	0.07
5	a	0.00	0.11	0.08	0.15	0.17	0.07	0.11	0.14	0.30	0.25
	b	-0.01	0.04	0.02	0.05	0.08	0.03	0.03	0.05	0.12	0.10
	c	0.00	0.02	0.02	0.03	0.03	0.01	0.02	0.04	0.08	0.08
6	a	0.01	0.10	0.16	0.14	0.18	0.07	0.11	0.17	0.17	0.23
	b	0.00	0.03	0.06	0.06	0.07	0.03	0.03	0.06	0.05	0.08
	c	0.00	0.01	0.03	0.03	0.06	0.01	0.02	0.03	0.04	0.07
7	a	0.00	0.14	0.16	0.18	0.20	0.06	0.09	0.19	0.18	0.24
	b	0.00	0.05	0.06	0.07	0.08	0.02	0.03	0.08	0.06	0.08
	c	-0.02	0.04	0.05	0.04	0.04	0.02	0.02	0.04	0.04	0.05
8	a	0.01	0.10	0.12	0.17	0.23	0.12	0.12	0.15	0.19	0.20
	b	-0.01	0.03	0.05	0.05	0.07	0.05	0.04	0.06	0.06	0.10
	c	0.00	0.02	0.03	0.04	0.06	0.04	0.02	0.01	0.04	0.05
9	a	0.00	0.09	0.12	0.11	0.17	0.06	0.11	0.12	0.17	0.18
	b	0.00	0.02	0.06	0.06	0.06	0.02	0.04	0.05	0.06	0.08
	c	0.00	0.02	0.03	0.01	0.05	0.02	0.02	0.02	0.04	0.06
10	a	0.01	0.12	0.10	0.18	0.27	0.07	0.10	0.12	0.17	0.31
	b	0.01	0.01	0.05	0.08	0.13	0.03	0.03	0.05	0.06	0.11
	c	0.00	0.03	0.02	0.02	0.07	0.02	0.02	0.02	0.05	0.06
Mean		0.01	0.05	0.07	0.09	0.11	0.04	0.06	0.08	0.12	0.14
S.D.		0.02	0.04	0.05	0.06	0.07	0.03	0.04	0.05	0.08	0.09

Table A.11 Descriptive statistics and assumption significance of measurement drift. Mean, standard deviation, and significance of normality (Shapiro-Wilks Test) and homogeneity of variance (Levene's Test) for measurement drift per system, surface, and load.

Evaluated Condition			Mean \pm S.D. [kPa \cdot min ⁻¹]	S-W Test <i>p</i>	Levene's Test <i>p</i>
		System Comparison	0.09 \pm 0.10	< 0.001	< 0.001
	Novel Pliance®	Surface Comparison	0.05 \pm 0.06	< 0.001	0.131
	Tekscan I-Scan™	Surface Comparison	0.15 \pm 0.11	< 0.001	0.144
	XSENSOR™ X3	Surface Comparison	0.08 \pm 0.07	< 0.001	0.067
Novel Pliance®	Flat Surface	Load Comparison	0.04 \pm 0.06	0.001	< 0.001
	Curved Surface	Load Comparison	0.05 \pm 0.07	< 0.001	< 0.001
Tekscan I-Scan™	Flat Surface	Load Comparison	0.14 \pm 0.10	< 0.001	< 0.001
	Curved Surface	Load Comparison	0.17 \pm 0.12	< 0.001	< 0.001
XSENSOR™ X3	Flat Surface	Load Comparison	0.07 \pm 0.06	< 0.001	< 0.001
	Curved Surface	Load Comparison	0.09 \pm 0.07	< 0.001	< 0.001

Table A.12 Main effect of measurement drift. Results of the t-test and ANOVA for measurement drift per system, surface, and load.

Evaluated Condition			t-test		ANOVA	
			<i>t</i>	<i>p</i>	<i>F</i>	<i>p</i>
System Comparison					107.565	< 0.001
Novel Pliance®	Surface Comparison		-2.289	0.023		
	Surface Comparison		-2.367	0.019		
	Surface Comparison		-2.615	0.009		
Novel Pliance®	Flat Surface Load Comparison				53.557	< 0.001
	Curved Surface Load Comparison				30.452	< 0.001
Tekscan I-Scan™	Flat Surface Load Comparison				14.145	< 0.001
	Curved Surface Load Comparison				6.001	< 0.001
XSENSOR™ X3	Flat Surface Load Comparison				29.363	< 0.001
	Curved Surface Load Comparison				14.985	< 0.001

Table A.13 Post hoc of measurement drift between systems. Mean difference (#1-2), standard error, and post hoc significance of measurement drift between systems.

System (#1)	System (#2)	Mean Diff. ± S.E. [kPa·min ⁻¹]	<i>p</i>
Novel Pliance®	Tekscan I-Scan™	-0.11 ± 0.01	< 0.001
Novel Pliance®	XSENSOR™ X3	-0.03 ± 0.01	< 0.001
Tekscan I-Scan™	XSENSOR™ X3	0.08 ± 0.01	< 0.001

Table A.14 *Post hoc* of measurement drift by Novel between loads per surface. Mean difference (#1-2), standard error, and *post hoc* significance of measurement drift by Novel Pliance® between loads per surface.

Surface	Load (#1)	Load (#2)	Mean Diff. ± S.E. [kPa·min ⁻¹]	<i>p</i>
Flat	30 kPa	45 kPa	-0.06 ± 0.01	< 0.001
	30 kPa	60 kPa	-0.09 ± 0.01	< 0.001
	30 kPa	75 kPa	-0.10 ± 0.01	< 0.001
	30 kPa	90 kPa	-0.10 ± 0.01	< 0.001
	45 kPa	60 kPa	-0.03 ± 0.01	0.031
	45 kPa	75 kPa	-0.03 ± 0.01	0.019
	45 kPa	90 kPa	-0.04 ± 0.01	0.011
	60 kPa	75 kPa	-0.01 ± 0.01	0.977
	60 kPa	90 kPa	-0.01 ± 0.01	0.867
	75 kPa	90 kPa	-0.01 ± 0.01	0.995
Curved	30 kPa	45 kPa	-0.04 ± 0.01	< 0.001
	30 kPa	60 kPa	-0.07 ± 0.01	< 0.001
	30 kPa	75 kPa	-0.09 ± 0.01	< 0.001
	30 kPa	90 kPa	-0.11 ± 0.02	< 0.001
	45 kPa	60 kPa	-0.02 ± 0.01	0.096
	45 kPa	75 kPa	-0.05 ± 0.01	0.008
	45 kPa	90 kPa	-0.06 ± 0.02	0.004
	60 kPa	75 kPa	-0.02 ± 0.01	0.492
	60 kPa	90 kPa	-0.04 ± 0.02	0.208
	75 kPa	90 kPa	-0.01 ± 0.02	0.963

Table A.15 Post hoc of measurement drift by Tekscan between loads per surface. Mean difference (#1-2), standard error, and *post hoc* significance of measurement drift by Tekscan I-Scan™ between loads per surface.

Surface	Load (#1)	Load (#2)	Mean Diff. ± S.E. [kPa·min ⁻¹]	<i>p</i>
Flat	30 kPa	45 kPa	-0.05 ± 0.02	0.035
	30 kPa	60 kPa	-0.09 ± 0.02	< 0.001
	30 kPa	75 kPa	-0.11 ± 0.02	< 0.001
	30 kPa	90 kPa	-0.13 ± 0.02	< 0.001
	45 kPa	60 kPa	-0.04 ± 0.02	0.450
	45 kPa	75 kPa	-0.06 ± 0.03	0.167
	45 kPa	90 kPa	-0.08 ± 0.03	0.031
	60 kPa	75 kPa	-0.02 ± 0.03	0.950
	60 kPa	90 kPa	-0.04 ± 0.03	0.566
	75 kPa	90 kPa	-0.02 ± 0.03	0.943
Curved	30 kPa	45 kPa	-0.01 ± 0.02	0.968
	30 kPa	60 kPa	-0.06 ± 0.02	0.124
	30 kPa	75 kPa	-0.08 ± 0.03	0.027
	30 kPa	90 kPa	-0.12 ± 0.03	0.003
	45 kPa	60 kPa	-0.05 ± 0.03	0.378
	45 kPa	75 kPa	-0.07 ± 0.03	0.110
	45 kPa	90 kPa	-0.11 ± 0.03	0.013
	60 kPa	75 kPa	-0.02 ± 0.03	0.956
	60 kPa	90 kPa	-0.06 ± 0.03	0.416
	75 kPa	90 kPa	-0.04 ± 0.04	0.813

Table A.16 *Post hoc* of measurement drift by XSENSOR™ between loads per surface. Mean difference (#1-2), standard error, and *post hoc* significance of measurement drift by XSENSOR™ X3 between loads per surface.

Surface	Load (#1)	Load (#2)	Mean Diff. ± S.E. [kPa·min ⁻¹]	<i>p</i>
Flat	30 kPa	45 kPa	-0.04 ± 0.01	< 0.001
	30 kPa	60 kPa	-0.06 ± 0.01	< 0.001
	30 kPa	75 kPa	-0.08 ± 0.01	< 0.001
	30 kPa	90 kPa	-0.10 ± 0.01	< 0.001
	45 kPa	60 kPa	-0.02 ± 0.01	0.347
	45 kPa	75 kPa	-0.04 ± 0.01	0.047
	45 kPa	90 kPa	-0.06 ± 0.01	0.003
	60 kPa	75 kPa	-0.02 ± 0.01	0.763
	60 kPa	90 kPa	-0.04 ± 0.02	0.132
	75 kPa	90 kPa	-0.02 ± 0.02	0.733
Curved	30 kPa	45 kPa	-0.02 ± 0.01	0.272
	30 kPa	60 kPa	-0.04 ± 0.01	0.008
	30 kPa	75 kPa	-0.08 ± 0.02	< 0.001
	30 kPa	90 kPa	-0.10 ± 0.02	< 0.001
	45 kPa	60 kPa	-0.02 ± 0.01	0.520
	45 kPa	75 kPa	-0.06 ± 0.02	0.008
	45 kPa	90 kPa	-0.09 ± 0.02	< 0.001
	60 kPa	75 kPa	-0.04 ± 0.02	0.166
	60 kPa	90 kPa	-0.07 ± 0.02	0.011
	75 kPa	90 kPa	-0.03 ± 0.02	0.797

A.1.3 Analysis of Measurement Drift Over Time

Table A.17 Descriptive statistics and assumption significance of measurement drift over time. Mean, standard deviation, and significance of normality (Shapiro-Wilks Test) and sphericity (Mauchly's Test) for measurement drift over time per system, surface, and load.

Evaluated Condition		Mean \pm S.D. [kPa \cdot min ⁻¹]	S-W Test <i>p</i>	Mauchly's Test <i>p</i>	
	Novel Pliance®	0.05 \pm 0.06	< 0.001	< 0.001	
	Tekscan I-Scan™	0.15 \pm 0.11	< 0.001	< 0.001	
	XSENSOR™ X3	0.08 \pm 0.07	< 0.001	< 0.001	
Novel Pliance®	Flat Surface	0.04 \pm 0.06	0.001	< 0.001	
	Curved Surface	0.05 \pm 0.07	< 0.001	< 0.001	
Tekscan I-Scan™	Flat Surface	0.14 \pm 0.10	< 0.001	< 0.001	
	Curved Surface	0.17 \pm 0.12	< 0.001	0.001	
XSENSOR™ X3	Flat Surface	0.07 \pm 0.06	< 0.001	< 0.001	
	Curved Surface	0.09 \pm 0.07	< 0.001	< 0.001	
Novel Pliance®	Flat Surface	30 kPa	-0.03 \pm 0.02	0.786	0.125
		45 kPa	0.03 \pm 0.03	0.763	0.455
		60 kPa	0.06 \pm 0.04	0.003	0.385
		75 kPa	0.06 \pm 0.05	0.009	0.810
		90 kPa	0.07 \pm 0.06	0.001	0.109
	Curved Surface	30 kPa	-0.01 \pm 0.03	< 0.001	0.166
		45 kPa	0.04 \pm 0.03	0.002	0.234
		60 kPa	0.06 \pm 0.04	0.001	0.031
		75 kPa	0.08 \pm 0.07	0.044	0.016
		90 kPa	0.10 \pm 0.08	0.018	0.005
Tekscan I-Scan™	Flat Surface	30 kPa	0.06 \pm 0.04	0.002	0.395
		45 kPa	0.11 \pm 0.08	< 0.001	0.275
		60 kPa	0.15 \pm 0.10	< 0.001	0.131
		75 kPa	0.17 \pm 0.11	< 0.001	< 0.001
		90 kPa	0.19 \pm 0.12	< 0.001	0.002
	Curved Surface	30 kPa	0.12 \pm 0.06	0.049	0.140
		45 kPa	0.13 \pm 0.08	0.002	0.072
		60 kPa	0.17 \pm 0.11	0.002	0.643
		75 kPa	0.20 \pm 0.13	0.002	0.430
		90 kPa	0.23 \pm 0.15	0.001	0.933
XSENSOR™ X3	Flat Surface	30 kPa	0.01 \pm 0.02	< 0.001	0.002
		45 kPa	0.05 \pm 0.04	0.002	0.284
		60 kPa	0.07 \pm 0.05	< 0.001	0.025
		75 kPa	0.09 \pm 0.06	< 0.001	0.421
		90 kPa	0.11 \pm 0.07	< 0.001	0.868
	Curved Surface	30 kPa	0.04 \pm 0.03	< 0.001	0.033
		45 kPa	0.06 \pm 0.04	0.003	0.007
		60 kPa	0.08 \pm 0.05	0.002	0.057
		75 kPa	0.12 \pm 0.08	< 0.001	< 0.001
		90 kPa	0.14 \pm 0.09	0.001	0.060

Table A.18 Main effect of measurement drift over time. Results of the repeated measures ANOVA for measurement drift over time per system, surface, and load.

Evaluated Condition		Repeated ANOVA	
		<i>F</i>	<i>p</i>
	Novel Pliance®	156.847	< 0.001
	Tekscan I-Scan™	552.008	< 0.001
	XSENSOR™ X3	347.264	< 0.001
Novel Pliance®	Flat Surface	69.975	< 0.001
		90.323	< 0.001
	Tekscan I-Scan™	358.675	< 0.001
		242.524	< 0.001
	XSENSOR™ X3	164.473	< 0.001
		197.593	< 0.001
Novel Pliance®	Flat Surface	30 kPa	4.983
		45 kPa	33.079
		60 kPa	119.254
		75 kPa	104.205
		90 kPa	79.425
	Curved Surface	30 kPa	2.359
		45 kPa	35.441
		60 kPa	136.469
		75 kPa	49.152
		90 kPa	91.661
Tekscan I-Scan™	Flat Surface	30 kPa	122.068
		45 kPa	303.722
		60 kPa	387.623
		75 kPa	178.858
		90 kPa	738.727
	Curved Surface	30 kPa	127.322
		45 kPa	81.833
		60 kPa	121.975
		75 kPa	107.335
XSENSOR™ X3	Flat Surface	30 kPa	4.501
		45 kPa	166.811
		60 kPa	143.406
		75 kPa	244.508
		90 kPa	218.952
	Curved Surface	30 kPa	129.808
		45 kPa	288.944
		60 kPa	251.065
		75 kPa	111.431
		90 kPa	130.782

Table A.19 Post hoc of measurement drift per system over time. Mean difference (#1-2), standard error, and *post hoc* significance of measurement drift between time intervals per system.

System	Time (#1)	Time (#2)	Mean Diff. \pm S.E. [kPa·min ⁻¹]	<i>p</i>
Novel Pliance®	3–12 mins	12–21 mins	0.07 \pm 0.00	< 0.001
	3–12 mins	21–30 mins	0.08 \pm 0.01	< 0.001
	12–21 mins	21–30 mins	0.01 \pm 0.00	< 0.001
Tekscan I-Scan™	3–12 mins	12–21 mins	0.18 \pm 0.01	< 0.001
	3–12 mins	21–30 mins	0.21 \pm 0.01	< 0.001
	12–21 mins	21–30 mins	0.03 \pm 0.00	< 0.001
XSENSOR™ X3	3–12 mins	12–21 mins	0.09 \pm 0.00	< 0.001
	3–12 mins	21–30 mins	0.11 \pm 0.01	< 0.001
	12–21 mins	21–30 mins	0.02 \pm 0.00	< 0.001

Table A.20 Post hoc of measurement drift over time per system and surface. Mean difference (#1-2), standard error, and *post hoc* significance of measurement drift between time intervals per system and surface.

System	Surface	Time (#1)	Time (#2)	Mean Diff. \pm S.E. [kPa·min ⁻¹]	<i>p</i>
Novel Pliance®	Flat	3–12 mins	12–21 mins	0.06 \pm 0.01	< 0.001
		3–12 mins	21–30 mins	0.07 \pm 0.01	< 0.001
		12–21 mins	21–30 mins	0.01 \pm 0.00	0.004
	Curved	3–12 mins	12–21 mins	0.08 \pm 0.01	< 0.001
		3–12 mins	21–30 mins	0.09 \pm 0.01	< 0.001
		12–21 mins	21–30 mins	0.01 \pm 0.00	< 0.001
Tekscan I-Scan™	Flat	3–12 mins	12–21 mins	0.16 \pm 0.01	< 0.001
		3–12 mins	21–30 mins	0.20 \pm 0.01	< 0.001
		12–21 mins	21–30 mins	0.03 \pm 0.00	< 0.001
	Curved	3–12 mins	12–21 mins	0.19 \pm 0.01	< 0.001
		3–12 mins	21–30 mins	0.23 \pm 0.01	< 0.001
		12–21 mins	21–30 mins	0.04 \pm 0.01	< 0.001
XSENSOR™ X3	Flat	3–12 mins	12–21 mins	0.08 \pm 0.01	< 0.001
		3–12 mins	21–30 mins	0.09 \pm 0.01	< 0.001
		12–21 mins	21–30 mins	0.02 \pm 0.00	< 0.001
	Curved	3–12 mins	12–21 mins	0.10 \pm 0.01	< 0.001
		3–12 mins	21–30 mins	0.12 \pm 0.01	< 0.001
		12–21 mins	21–30 mins	0.02 \pm 0.00	< 0.001

Table A.21 *Post hoc* of measurement drift over time per surface and load for Novel. Mean difference (#1-2), standard error, and *post hoc* significance of measurement drift between time intervals per surface and load for Novel Pliance®.

Surface	Load	Time (#1)	Time (#2)	Mean Diff. \pm S.E. [kPa·min ⁻¹]	<i>p</i>
Flat	30 kPa	3–12 mins	12–21 mins	0.00 \pm 0.01	0.869
		3–12 mins	21–30 mins	-0.02 \pm 0.01	0.056
		12–21 mins	21–30 mins	-0.02 \pm 0.01	0.008
	45 kPa	3–12 mins	12–21 mins	0.04 \pm 0.01	< 0.001
		3–12 mins	21–30 mins	0.05 \pm 0.01	< 0.001
		12–21 mins	21–30 mins	0.01 \pm 0.01	0.070
	60 kPa	3–12 mins	12–21 mins	0.07 \pm 0.01	< 0.001
		3–12 mins	21–30 mins	0.08 \pm 0.01	< 0.001
		12–21 mins	21–30 mins	0.01 \pm 0.00	0.033
	75 kPa	3–12 mins	12–21 mins	0.08 \pm 0.01	< 0.001
		3–12 mins	21–30 mins	0.11 \pm 0.01	< 0.001
		12–21 mins	21–30 mins	0.03 \pm 0.01	0.004
	90 kPa	3–12 mins	12–21 mins	0.09 \pm 0.01	< 0.001
		3–12 mins	21–30 mins	0.12 \pm 0.01	< 0.001
		12–21 mins	21–30 mins	0.02 \pm 0.01	0.009
Curved	45 kPa	3–12 mins	12–21 mins	0.05 \pm 0.01	< 0.001
		3–12 mins	21–30 mins	0.05 \pm 0.01	< 0.001
		12–21 mins	21–30 mins	0.01 \pm 0.00	0.208
	60 kPa	3–12 mins	12–21 mins	0.07 \pm 0.01	< 0.001
		3–12 mins	21–30 mins	0.09 \pm 0.00	< 0.001
		12–21 mins	21–30 mins	0.01 \pm 0.01	0.047
	75 kPa	3–12 mins	12–21 mins	0.11 \pm 0.01	< 0.001
		3–12 mins	21–30 mins	0.14 \pm 0.02	< 0.001
		12–21 mins	21–30 mins	0.03 \pm 0.01	0.024
	90 kPa	3–12 mins	12–21 mins	0.14 \pm 0.01	< 0.001
		3–12 mins	21–30 mins	0.15 \pm 0.02	< 0.001
		12–21 mins	21–30 mins	0.02 \pm 0.01	0.057

Table A.22 *Post hoc* of measurement drift over time per surface and load for Tekscan. Mean difference (#1-2), standard error, and *post hoc* significance of measurement drift between time intervals per surface and load for Tekscan I-Scan™.

Surface	Load	Time (#1)	Time (#2)	Mean Diff. ± S.E. [kPa·min ⁻¹]	<i>p</i>
Flat	30 kPa	3–12 mins	12–21 mins	0.08 ± 0.01	< 0.001
		3–12 mins	21–30 mins	0.09 ± 0.01	< 0.001
		12–21 mins	21–30 mins	0.01 ± 0.01	0.035
	45 kPa	3–12 mins	12–21 mins	0.14 ± 0.01	< 0.001
		3–12 mins	21–30 mins	0.17 ± 0.01	< 0.001
		12–21 mins	21–30 mins	0.03 ± 0.01	0.004
	60 kPa	3–12 mins	12–21 mins	0.17 ± 0.01	< 0.001
		3–12 mins	21–30 mins	0.21 ± 0.01	< 0.001
		12–21 mins	21–30 mins	0.04 ± 0.01	< 0.001
	75 kPa	3–12 mins	12–21 mins	0.21 ± 0.02	< 0.001
		3–12 mins	21–30 mins	0.24 ± 0.02	< 0.001
		12–21 mins	21–30 mins	0.04 ± 0.00	< 0.001
	90 kPa	3–12 mins	12–21 mins	0.23 ± 0.01	< 0.001
		3–12 mins	21–30 mins	0.27 ± 0.01	< 0.001
		12–21 mins	21–30 mins	0.05 ± 0.00	< 0.001
Curved	30 kPa	3–12 mins	12–21 mins	0.10 ± 0.01	< 0.001
		3–12 mins	21–30 mins	0.13 ± 0.01	< 0.001
		12–21 mins	21–30 mins	0.03 ± 0.01	0.006
	45 kPa	3–12 mins	12–21 mins	0.14 ± 0.02	< 0.001
		3–12 mins	21–30 mins	0.17 ± 0.01	< 0.001
		12–21 mins	21–30 mins	0.02 ± 0.01	0.017
	60 kPa	3–12 mins	12–21 mins	0.20 ± 0.02	< 0.001
		3–12 mins	21–30 mins	0.24 ± 0.02	< 0.001
		12–21 mins	21–30 mins	0.04 ± 0.01	0.015
	75 kPa	3–12 mins	12–21 mins	0.22 ± 0.02	< 0.001
		3–12 mins	21–30 mins	0.27 ± 0.02	< 0.001
		12–21 mins	21–30 mins	0.05 ± 0.02	0.045
	90 kPa	3–12 mins	12–21 mins	0.29 ± 0.03	< 0.001
		3–12 mins	21–30 mins	0.32 ± 0.03	< 0.001
		12–21 mins	21–30 mins	0.03 ± 0.03	0.323

Table A.23 *Post hoc* of measurement drift over time per surface and load for XSENSOR™. Mean difference (#1-2), standard error, and *post hoc* significance of measurement drift between time intervals per surface and load for XSENSOR™ X3.

Surface	Load	Time (#1)	Time (#2)	Mean Diff. ± S.E. [kPa·min ⁻¹]	<i>p</i>
Flat	45 kPa	3–12 mins	12–21 mins	0.07 ± 0.01	< 0.001
		3–12 mins	21–30 mins	0.08 ± 0.00	< 0.001
		12–21 mins	21–30 mins	0.01 ± 0.00	0.008
	60 kPa	3–12 mins	12–21 mins	0.08 ± 0.01	< 0.001
		3–12 mins	21–30 mins	0.10 ± 0.01	< 0.001
		12–21 mins	21–30 mins	0.02 ± 0.00	< 0.001
	75 kPa	3–12 mins	12–21 mins	0.10 ± 0.01	< 0.001
		3–12 mins	21–30 mins	0.13 ± 0.01	< 0.001
		12–21 mins	21–30 mins	0.03 ± 0.01	< 0.001
	90 kPa	3–12 mins	12–21 mins	0.13 ± 0.01	< 0.001
		3–12 mins	21–30 mins	0.15 ± 0.01	< 0.001
		12–21 mins	21–30 mins	0.02 ± 0.01	0.030
Curved	30 kPa	3–12 mins	12–21 mins	0.04 ± 0.00	< 0.001
		3–12 mins	21–30 mins	0.05 ± 0.00	< 0.001
		12–21 mins	21–30 mins	0.01 ± 0.00	< 0.001
	45 kPa	3–12 mins	12–21 mins	0.07 ± 0.00	< 0.001
		3–12 mins	21–30 mins	0.08 ± 0.00	< 0.001
		12–21 mins	21–30 mins	0.01 ± 0.00	< 0.001
	60 kPa	3–12 mins	12–21 mins	0.09 ± 0.01	< 0.001
		3–12 mins	21–30 mins	0.12 ± 0.01	< 0.001
		12–21 mins	21–30 mins	0.03 ± 0.00	< 0.001
	75 kPa	3–12 mins	12–21 mins	0.14 ± 0.01	< 0.001
		3–12 mins	21–30 mins	0.16 ± 0.02	< 0.001
		12–21 mins	21–30 mins	0.03 ± 0.01	0.002
	90 kPa	3–12 mins	12–21 mins	0.15 ± 0.02	< 0.001
		3–12 mins	21–30 mins	0.18 ± 0.01	< 0.001
		12–21 mins	21–30 mins	0.03 ± 0.01	0.004

A.2 Simulator Evaluation

A.2.1 Analysis Between Systems

Table A.24 Average pressure, peak pressure, and contact area measured by Novel. Measurements of average pressure, peak pressure, and contact area by Novel Pliance® for six independently collected trials per load.

Trial	Average Pressure [kPa]			Peak Pressure [kPa]			Contact Area [cm ²]		
	15 kg	25 kg	35 kg	15 kg	25 kg	35 kg	15 kg	25 kg	35 kg
1	15.28	18.98	20.70	30.03	42.80	52.00	49.46	59.67	71.73
2	15.86	18.71	19.49	31.03	47.00	52.05	69.74	77.38	89.35
3	15.70	15.48	20.46	31.05	33.95	47.95	66.51	86.27	90.18
4	13.43	16.11	21.83	43.88	35.03	73.33	72.27	70.30	78.86
5	14.09	15.39	19.10	35.85	37.88	53.03	61.56	72.20	76.61
6	12.85	16.14	16.78	39.33	58.40	47.65	40.54	57.40	68.26
Mean	14.54	16.80	19.73	35.19	42.51	54.33	60.01	70.54	79.16
S.D.	1.26	1.61	1.73	5.55	9.20	9.58	12.49	10.84	9.01

Table A.25 Average pressure, peak pressure, and contact area measured by Tekscan. Measurements of average pressure, peak pressure, and contact area by Tekscan I-Scan™ for six independently collected trials per load.

Trial	Average Pressure [kPa]			Peak Pressure [kPa]			Contact Area [cm ²]		
	15 kg	25 kg	35 kg	15 kg	25 kg	35 kg	15 kg	25 kg	35 kg
1	13.08	19.51	21.10	30.47	49.92	69.18	56.28	57.81	65.73
2	15.84	17.24	21.63	28.05	44.16	48.05	54.99	64.39	68.42
3	13.49	17.01	23.91	29.34	42.91	111.65	53.43	53.25	61.33
4	14.23	17.10	22.22	68.51	48.37	69.29	41.27	42.07	56.98
5	13.73	15.75	19.83	34.45	37.67	48.17	40.16	52.40	59.01
6	13.66	21.80	26.08	45.28	170.5	134.22	35.98	42.56	55.12
Mean	14.01	18.07	22.46	39.35	65.59	80.09	47.02	52.08	61.10
S.D.	0.97	2.20	2.23	15.60	51.58	35.23	8.86	8.68	5.14

Table A.26 Average pressure, peak pressure, and contact area measured by XSENSOR™. Measurements of average pressure, peak pressure, and contact area by XSENSOR™ X3 for six independently collected trials per load.

Trial	Average Pressure [kPa]			Peak Pressure [kPa]			Contact Area [cm ²]		
	15 kg	25 kg	35 kg	15 kg	25 kg	35 kg	15 kg	25 kg	35 kg
1	17.89	20.69	22.20	48.77	44.19	58.01	55.97	61.04	76.39
2	16.05	21.19	22.79	42.29	46.95	56.09	55.05	64.21	73.98
3	19.21	20.36	23.47	38.79	57.17	55.37	53.23	67.22	69.79
4	15.47	19.42	20.77	37.79	49.84	45.29	58.02	63.81	58.19
5	16.13	20.23	21.56	31.57	51.13	54.29	44.11	59.54	68.36
6	17.55	21.00	23.16	40.26	46.22	59.78	59.03	66.09	72.38
Mean	17.05	20.48	22.33	39.91	49.25	54.81	54.23	63.65	69.85
S.D.	1.41	0.64	1.02	5.65	4.62	5.06	5.38	2.92	6.39

Table A.27 Descriptive statistics and assumption significance between systems. Mean, standard deviation, and significance of normality (Shapiro-Wilks Test) and homogeneity of variance (Levene's Test) between systems per load and evaluated parameter.

Load	Evaluated Parameter	Mean ± S.D.	S-W Test	Levene's Test
			<i>p</i>	<i>p</i>
15 kg	Average Pressure	15.20 ± 1.79 kPa	0.203	0.316
	Peak Pressure	38.15 ± 9.73 kPa	0.004	0.060
	Contact Area	53.76 ± 10.36 cm ²	0.604	0.055
25 kg	Average Pressure	18.45 ± 2.18 kPa	0.115	0.036
	Peak Pressure	52.45 ± 30.22 kPa	< 0.001	0.032
	Contact Area	62.09 ± 10.99 cm ²	0.842	0.117
35 kg	Average Pressure	21.51 ± 2.08 kPa	0.985	0.326
	Peak Pressure	63.08 ± 23.51 kPa	< 0.001	0.001
	Contact Area	70.04 ± 10.07 cm ²	0.405	0.367

Table A.28 Main effect between systems. Results of the ANOVA between systems per load and evaluated parameter.

Load	Evaluated Parameter	ANOVA	
		<i>F</i>	<i>p</i>
15 kg	Average Pressure	10.538	0.001
	Peak Pressure	0.390	0.683
	Contact Area	2.897	0.086
25 kg	Average Pressure	14.461	0.002
	Peak Pressure	1.510	0.278
	Contact Area	7.771	0.005
35 kg	Average Pressure	4.736	0.025
	Peak Pressure	1.422	0.295
	Contact Area	9.891	0.002

Table A.29 Post hoc between systems at 15 kg. Mean difference (#1-2), standard error, and *post hoc* significance of evaluated parameters between systems at the 15 kg load configuration.

Evaluated Parameter	System (#1)	System (#2)	Mean Diff. ± S.E.	<i>p</i>
Average Pressure	Novel Pliance®	Tekscan I-Scan™	0.53 ± 0.71 kPa	0.739
	Novel Pliance®	XSENSOR™ X3	-2.51 ± 0.71 kPa	0.008
	Tekscan I-Scan™	XSENSOR™ X3	-3.05 ± 0.71 kPa	0.002
Peak Pressure	Novel Pliance®	Tekscan I-Scan™	-4.15 ± 5.83 kPa	0.760
	Novel Pliance®	XSENSOR™ X3	-4.72 ± 5.83 kPa	0.703
	Tekscan I-Scan™	XSENSOR™ X3	-0.56 ± 5.83 kPa	0.995
Contact Area	Novel Pliance®	Tekscan I-Scan™	12.99 ± 5.41 cm ²	0.072
	Novel Pliance®	XSENSOR™ X3	5.78 ± 5.41 cm ²	0.547
	Tekscan I-Scan™	XSENSOR™ X3	-7.21 ± 5.41 cm ²	0.399

Table A.30 Post hoc between systems at 25 kg. Mean difference (#1-2), standard error, and *post hoc* significance of evaluated parameters between systems at the 25 kg load configuration.

Evaluated Parameter	System (#1)	System (#2)	Mean Diff. \pm S.E.	<i>p</i>
Average Pressure	Novel Pliance®	Tekscan I-Scan™	-1.27 \pm 1.11 kPa	0.516
	Novel Pliance®	XSENSOR™ X3	-3.68 \pm 0.71 kPa	0.004
	Tekscan I-Scan™	XSENSOR™ X3	-2.42 \pm 0.93 kPa	0.093
Peak Pressure	Novel Pliance®	Tekscan I-Scan™	-23.08 \pm 21.39 kPa	0.564
	Novel Pliance®	XSENSOR™ X3	-6.74 \pm 4.20 kPa	0.303
	Tekscan I-Scan™	XSENSOR™ X3	16.34 \pm 21.14 kPa	0.734
Contact Area	Novel Pliance®	Tekscan I-Scan™	18.46 \pm 4.73 cm ²	0.004
	Novel Pliance®	XSENSOR™ X3	6.89 \pm 4.73 cm ²	0.339
	Tekscan I-Scan™	XSENSOR™ X3	-11.57 \pm 4.73 cm ²	0.066

Table A.31 Post hoc between systems at 35 kg. Mean difference (#1-2), standard error, and *post hoc* significance of evaluated parameters between systems at the 35 kg load configuration.

Evaluated Parameter	System (#1)	System (#2)	Mean Diff. \pm S.E.	<i>p</i>
Average Pressure	Novel Pliance®	Tekscan I-Scan™	-2.73 \pm 1.00 kPa	0.039
	Novel Pliance®	XSENSOR™ X3	-2.60 \pm 1.00 kPa	0.050
	Tekscan I-Scan™	XSENSOR™ X3	0.14 \pm 1.00 kPa	0.990
Peak Pressure	Novel Pliance®	Tekscan I-Scan™	-25.76 \pm 14.91 kPa	0.274
	Novel Pliance®	XSENSOR™ X3	-0.47 \pm 4.42 kPa	0.994
	Tekscan I-Scan™	XSENSOR™ X3	25.29 \pm 14.53 kPa	0.277
Contact Area	Novel Pliance®	Tekscan I-Scan™	18.07 \pm 4.06 cm ²	0.001
	Novel Pliance®	XSENSOR™ X3	9.32 \pm 4.06 cm ²	0.088
	Tekscan I-Scan™	XSENSOR™ X3	-8.75 \pm 4.06 cm ²	0.112

A.2.2 Analysis Between Testing Days

Table A.32 Between testing day difference of average pressure, peak pressure, and contact area measured by Novel. Between testing day difference (#1-2) of average pressure, peak pressure, and contact area by Novel Pliance® for three independently collected trials per load configuration.

Trial	Average Pressure [kPa]			Peak Pressure [kPa]			Contact Area [cm ²]		
	15 kg	25 kg	35 kg	15 kg	25 kg	35 kg	15 kg	25 kg	35 kg
1	1.85	2.86	-1.13	-13.85	7.78	-21.33	-22.81	-10.64	-7.14
2	1.76	3.32	0.39	-4.83	9.13	-0.98	8.18	5.18	12.74
3	2.85	-0.66	3.68	-8.28	-24.45	0.30	25.97	28.87	21.93
Mean	2.16	1.84	0.98	-8.98	-2.52	-7.33	3.78	7.80	9.18
S.D.	0.60	2.18	2.46	4.55	19.01	12.13	24.69	19.88	14.86

Table A.33 Between testing day difference of average pressure, peak pressure, and contact area measured by Tekscan. Between testing day difference (#1-2) of average pressure, peak pressure, and contact area by Tekscan I-Scan™ for three independently collected trials per load configuration.

Trial	Average Pressure [kPa]			Peak Pressure [kPa]			Contact Area [cm ²]		
	15 kg	25 kg	35 kg	15 kg	25 kg	35 kg	15 kg	25 kg	35 kg
1	-1.16	2.41	-1.12	-38.03	1.55	-0.11	15.01	15.75	8.74
2	2.11	1.48	1.80	-6.40	6.49	-0.12	14.82	12.00	9.41
3	-0.16	-4.79	-2.17	-15.94	-127.59	-22.57	17.45	10.70	6.21
Mean	0.26	-0.30	-0.50	-20.12	-39.85	-7.60	15.76	12.81	8.12
S.D.	1.68	3.92	2.06	16.23	76.03	12.96	1.47	2.62	1.69

Table A.34 Between testing day difference of average pressure, peak pressure, and contact area measured by XSENSOR™. Between testing day difference (#1-2) of average pressure, peak pressure, and contact area by XSENSOR™ X3 for three independently collected trials per load configuration.

Trial	Average Pressure [kPa]			Peak Pressure [kPa]			Contact Area [cm ²]		
	15 kg	25 kg	35 kg	15 kg	25 kg	35 kg	15 kg	25 kg	35 kg
1	2.41	1.27	1.43	10.98	-5.65	12.72	-2.06	-2.77	18.20
2	-0.08	0.96	1.23	10.72	-4.18	1.80	10.94	4.67	5.62
3	1.66	-0.64	0.31	-1.47	10.95	-4.41	-5.80	1.13	-2.59
Mean	1.33	0.53	0.99	6.74	0.38	3.37	1.03	1.01	7.08
S.D.	1.28	1.03	0.60	7.12	9.19	8.67	8.79	3.72	10.47

Table A.35 Descriptive statistics and normality significance between testing days per parameter and system. Mean, standard deviation, and significance of normality (Shapiro-Wilks Test) between testing days per evaluated parameter and system.

Evaluated Parameter	System	Mean \pm S.D.	S-W Test p
Average Pressure	Novel Pliance®	1.66 \pm 1.75 kPa	0.292
	Tekscan I-Scan™	-0.18 \pm 2.39 kPa	0.339
	XSENSOR™ X3	0.95 \pm 0.94 kPa	0.871
Peak Pressure	Novel Pliance®	-6.28 \pm 11.86 kPa	0.684
	Tekscan I-Scan™	-22.52 \pm 41.85 kPa	< 0.001
	XSENSOR™ X3	3.50 \pm 7.76 kPa	0.042
Contact Area	Novel Pliance®	6.92 \pm 17.67 cm ²	0.714
	Tekscan I-Scan™	12.23 \pm 3.75 cm ²	0.764
	XSENSOR™ X3	3.04 \pm 7.70 cm ²	0.352

Table A.36 Main effect between testing days per parameter and system. The one-sample two-tailed t-test, Wilcoxon Signed-Ranks test, and Bland-Altman slope and bias results between testing days per evaluated parameter and system.

Evaluated Parameter	System	t-Test		Wilcoxon Signed-Ranks Test		Bland-Altman	
		t	p	Z	p	Slope	Bias
Average Pressure	Novel Pliance®	2.841	0.022			-0.26	6.08
	Tekscan I-Scan™	-0.222	0.830			-0.19	3.29
	XSENSOR™ X3	3.035	0.016			-0.08	2.55
Peak Pressure	Novel Pliance®	-1.587	0.151			-0.41	11.76
	Tekscan I-Scan™			-1.718	0.086	-0.75	23.93
	XSENSOR™ X3			1.125	0.260	-0.25	15.69
Contact Area	Novel Pliance®	1.175	0.274			0.30	-14.02
	Tekscan I-Scan™	9.774	< 0.001			-0.42	34.65
	XSENSOR™ X3	1.183	0.271			0.05	0.02

Table A.37 Descriptive statistics and normality significance between testing days per parameter, system and load. Mean, standard deviation, and significance of normality (Shapiro-Wilks Test) between testing days per evaluated parameter, system, and load.

Evaluated Parameter	System	Load	Mean \pm S.D.	S-W Test <i>p</i>
Average Pressure	Novel Pliance®	15 kg	2.16 \pm 0.60 kPa	0.143
		25 kg	1.84 \pm 2.18 kPa	0.201
		35 kg	0.98 \pm 2.46 kPa	0.599
	Tekscan I-Scan™	15 kg	0.26 \pm 1.68 kPa	0.576
		25 kg	-0.30 \pm 3.92 kPa	0.226
		35 kg	-0.50 \pm 2.06 kPa	0.496
	XSENSOR™ X3	15 kg	1.33 \pm 1.28 kPa	0.569
		25 kg	0.53 \pm 1.03 kPa	0.286
		35 kg	0.99 \pm 0.60 kPa	0.320
Peak Pressure	Novel Pliance®	15 kg	-8.98 \pm 4.55 kPa	0.742
		25 kg	-2.52 \pm 19.01 kPa	0.068
		35 kg	-7.33 \pm 12.13 kPa	0.100
	Tekscan I-Scan™	15 kg	-20.12 \pm 16.23 kPa	0.570
		25 kg	-39.85 \pm 76.03 kPa	0.062
		35 kg	-7.60 \pm 12.96 kPa	< 0.001
	XSENSOR™ X3	15 kg	6.74 \pm 7.12 kPa	0.035
		25 kg	0.38 \pm 9.19 kPa	0.153
		35 kg	3.37 \pm 8.67 kPa	0.700
Contact Area	Novel Pliance®	15 kg	3.78 \pm 24.69 cm ²	0.704
		25 kg	7.80 \pm 19.88 cm ²	0.781
		35 kg	9.18 \pm 14.86 cm ²	0.600
	Tekscan I-Scan™	15 kg	15.76 \pm 1.47 cm ²	0.121
		25 kg	12.81 \pm 2.62 cm ²	0.478
		35 kg	8.12 \pm 1.69 cm ²	0.379
	XSENSOR™ X3	15 kg	1.03 \pm 8.79 cm ²	0.410
		25 kg	1.01 \pm 3.72 cm ²	0.945
		35 kg	7.08 \pm 10.47 cm ²	0.770

Table A.38 Main effect between testing days per parameter and system. The one-sample two-tailed t-test, Wilcoxon Signed-Ranks test, and Bland-Altman slope and bias results between testing days per evaluated parameter, system, and load configuration.

Evaluated Parameter	System	Load	t-Test		Wilcoxon Signed-Ranks Test	
			<i>t</i>	<i>p</i>	<i>Z</i>	<i>p</i>
Average Pressure	Novel Pliance®	15 kg	6.189	0.025		
		25 kg	1.465	0.280		
		35 kg	0.689	0.562		
	Tekscan I-Scan™	15 kg	0.274	0.810		
		25 kg	-0.132	0.907		
		35 kg	-0.418	0.717		
	XSENSOR™ X3	15 kg	1.804	0.213		
		25 kg	0.895	0.465		
		35 kg	2.857	0.104		
Peak Pressure	Novel Pliance®	15 kg	-3.417	0.076		
		25 kg	-0.229	0.840		
		35 kg	-1.047	0.405		
	Tekscan I-Scan™	15 kg	-2.148	0.165		
		25 kg	-0.908	0.460		
		35 kg			-1.604	0.109
	XSENSOR™ X3	15 kg			1.069	0.285
		25 kg	0.071	0.950		
		35 kg	0.673	0.570		
Contact Area	Novel Pliance®	15 kg	0.265	0.816		
		25 kg	0.680	0.567		
		35 kg	1.070	0.397		
	Tekscan I-Scan™	15 kg	18.608	0.003		
		25 kg	8.465	0.014		
		35 kg	8.348	0.014		
	XSENSOR™ X3	15 kg	0.202	0.859		
		25 kg	0.471	0.684		
		35 kg	1.171	0.362		